INFORMATION TO USERS

This manuscript has been reproduced from the microfilm master. UMI films the text directly from the original or copy submitted. Thus, some thesis and dissertation copies are in typewriter face, while others may be from any type of computer printer.

The quality of this reproduction is dependent upon the quality of the copy submitted. Broken or indistinct print, colored or poor quality illustrations and photographs, print bleedthrough, substandard margins, and improper alignment can adversely affect reproduction.

In the unlikely event that the author did not send UMI a complete manuscript and there are missing pages, these will be noted. Also, if unauthorized copyright material had to be removed, a note will indicate the deletion.

Oversize materials (e.g., maps, drawings, charts) are reproduced by sectioning the original, beginning at the upper left-hand corner and continuing from left to right in equal sections with small overlaps.

ProQuest Information and Learning
300 North Zeeb Road, Ann Arbor, MI 48106-1346 USA
800-521-0600

PROSAPOSIN: A GLYCOPROTEIN WITH MULTIPLE FUNCTIONS AND DUAL DESTINATIONS

Qing Zhao

Department of Anatomy and Cell Biology

McGill University

A thesis submitted to the Faculty of Graduate Studies and Research

in partial fulfillment of the requirements for the degree of

Doctor of Philosophy

ABSTRACT

Prosaposin is a multifunctional glycoprotein with different molecular masses and dual destinations. A 65 kDa form of prosaposin is targeted to lysosomes and converted by partial proteolysis, into four smaller non-enzymatic saposin A-D required for the hydrolysis of glycosphingolipids. However, the 65 kDa protein may be further glycosylated to a 70 kDa secretory form that is found in various biological fluids and suspected to have a trophic activity. Mutations of the prosaposin gene are linked to several lysosomal disorders. This thesis examines various aspects of the synthesis, targeting and function of prosaposin, and for practical purposes, the results and discussion were divided in three main sections. The first part deals with the cloning of the mouse prosaposin gene, the analysis of its transcribed mRNA and translation products. The second section examines the mechanism of targeting of the 65 kDa protein to lysosomes using mutagenic analyses. The third part deals with the effect of the inactivation of the prosaposin gene on the development of the male reproductive system. Sequence analysis revealed that the mouse prosaposin gene is over 20 kb in length and composed of 15 exons and 14 introns. Two forms of alternatively spliced mRNA (including or excluding exon 8) were found by RT-PCR in a tissue specific manner. Structure analysis and secondary structure predictions among mouse, rat and human prosaposins illustrated a common framework of amino acids forming amphiphatic helices enclosing an internal hydrophobic core implicated on their interaction with lipids. Mutagenic deletions of functional domains of

prosaposin demonstrated that its C-terminus was required for the lysosomal targeting of this protein. Further evidence from chimeric constructs of albumin attached to various functional domains of prosaposin, suggested that the C-terminus plus at least one saposin domain are necessary for the targeting of albumin to lysosomes. Investigation of the effect of prosaposin gene inactivation (-/-) demonstrated that this protein is involved in the development and maintenance of the testis, efferent ducts, epididymis, seminal vesicles and prostate gland. In the prostate, prosaposin appears to be involved in the activation of the mitogen activated protein kinase (MAPK) pathway.

Résumé

La prosaposine est une glycoprotéine de poids moléculaires variés et de fonctions multiples. La molécule de 65 kDa est destinée aux lysosomes où elle est fractionnée en quatre fragments non-enzymatiques, les saposines A-D qui agissent sur l'hydrolyse des glycosphingolipides. Par ailleurs, cette prosaposine-65 kDa peut-être glycolysée en une molécule de 70 kDa sécrétée dans certains liquides tissulaires qui semblent posséder des actions trophiques. Des mutations du gène de la prosaposine sont responsables de nombreuses anomalies du système lysosomial. Le présent mémoire, qui concernent la synthèse, le ciblage et les fonctions de cette protéine, est divisé en trois chapitres composés d'une introduction, des résultats et d'une discussion. Le premier chapitre concerne le clonage du gène prosaposine de souris, l'analyse de la transcription du mRNA et le transfert des produits qui en dérivent. Le second chapitre étudie le mécanisme de ciblage de la prosaposine-65 kDa vers les lysosomes, en utilisant des mutations expérimentales. Enfin le troisième chapitre aborde le sujet des conséquences des gènes de la prosaposine sur le système reproducteur mâle. L'analyse du gène prosaposine démontre l'existence d'une séquence de molécules dépassanr 20kb possédant 15 exons et 14 introns. Deux formes d'épissages alternatifs du mRNA (i.e.incluant ou excluant l'exon 8) ont été obtenues par le PCR-RT qui produisent des actions tissulaires sélectives. L'analyse structurale des prosaposines de souris, de rats, et d'hommes révèlent

des structures hélicoïdales internes hydrophobes, ce qui suggère une interaction de ces protéines avec les lipides. La suppression de segments de prosaposines démontre que l'existence des domaines terminaux-C de ces protéines sont requis pour leur ciblage intracellulaire. D'autres données, obtenues par la construction d'albumines chimériques liées à diverses fractions de la saposine, montrent que les terminaisons-C sont nécessaires au ciblage de ces albumines aux lysosomes. Finalement, une étude de l'inactivation de gène prosaposine(-/-) démontre que cette protéine est impliquée dans le développement et le maintient fonctionne des testicules, canaux efférents, épipidymes, vesicules séminales et prostate. Dans le cas de la prostate, la prosaposine semble impliquée dans la voie mitogen activated protein kinase (MAPK).

To my husband haijiang, my son christopher,

my mother, and the loving memory of my father.

ACKNOWLEDGEMENTS

I would like to express my deep sense of gratitude and appreciation to my supervisor Dr. Carlos Morales, for his exceptional generosity, kindness, expert guidance, patience and continued support throughout my Ph.D studies. I would also extend my special thanks to Mrs. Morales for her continual encouragement, caring and enthusiasm during my studies.

I would like gratefully to acknowledge Drs.Yves Clermont and Richard Oko for their constant interests and enthusiasm towards science, informative advice and persistent encouragement and support during the course of my work. Special thanks to Dr. Clermont for his excellent French translation of the abstract.

I would like to extend my appreciation to the people in Polypeptide Laboratory, especially to Dr. Simon Wing, Nathalie Bedard, for their instant help whenever I need, and thank to Dr. Wing for helping to make the antibody.

I wish to thank Dr. Mohammed EL Alfy who helped me for immunostaining presented in this thesis, and for his utmost kindness and consideration, and his unforgettable friendship.

I thank Ms. Matilda Cheung, Ms. Jeannie Mui and Ms. Emma Ressurections for their technical assistance.

I also thank to the secretaries of the department, particularly, Mrs Audrey Innes, Ann Silkauskas, Karen Halse for their kindly assistance.

Many thanks would go to Farkhondeh Pouresmaeily, Demetra Moshonas, Stephane Lefrancois, and to the memory of Jana Fuska, who shared wonderful time with

me during the course of my studies. Special thanks to Stephane, who is always there whenever I struggled with a computer problem.

Thanks to Dr. Suleiman Igdoura, for his continual encouragement and interest in my work, I would never forget for his warm help when I first arrived in Canada.

I thank to Dr. Alexander Bell for his interest and good advice in my work and especially, for his expert help in protein sequence analysis.

I would like to thank to Drs. Micheal Griswold, Marilyn Farquhar, John Mort for providing antibodies. Thanks to Dr. K Suzuki for providing prosaposin heterozygous mice.

My most sincere thanks go to my family for their great love, continual support, and lots of patience, especially to the loving memory of my father, who passed away just before I was ready to hand in this thesis. I would like also to express my thanks to my husband, Haijiang Lin, without him I wouldn't be able to accomplish my studies, he is always there to support, encourage and help me.

Finally, I would like to thank to the Faculty of the Graduate Studies at McGill University for their financial support in the last two years of my studies, awarding me the McGill Major Scholarship.

Abbreviations and Amino Acids Codes

BFA: brefeldin A

bp: base pair

cDNA: complementary DNA

ChAT: choline acetyltransferase

CPY: carboxypeptidase

D609: tricyclodecan-9-yl xanthate potassium

EGF: epidermal growth factor

EM: electronic microscope

Endo H: endoglycosidase H

ER: endoplasmic reticulum

ERK: extracellular signal regulated kinase

FGF: fibroblast growth factor

FITC: fluorescein isothiocyanate

Galβ1: β1 Galactoside

GlcNAc: N-acetyl-D-glucosamine

G_{M2}: ganglioside G_{M2}

GSL: glycosphingolipid

HEXA: hexosaminidase A

IGF: insulin-like growth factor

IGF II: insulin-like growth factor II

IgG: immunoglobulin

Kb: kilobase pair

kDa: kilodalton

Lamp: lysosomal associated membrane protein

LAP: lysosomal acid phosphatase

LEP 100: lysosome-endosome plasma membrane protein

Limp: lysosomal integral membrane protein

LRP: low-density lipoprotein receptor related protein

MAPK: mitogen activated protein kinase

ML-II:mucolipidosis II

ML-III:mucolipidosis III

MLD: metachromatic leukodystrophy

MPR: mannose 6-phosphate receptor

MVB: multivesicular body

M6P: mannose 6-phosphate

NK-lysin: natural killer cell lysin

PCR: polymerase chain reaction

PDMP: DL-threo-1-phenyl-2-decanoyl-amino-3-morpholino-1-propanol-HCL

RT-PCR: reverse transcriptase polymerase chain reaction

SAPLIP: saposin-like protein

SGP-1: sulfated glycoprotein-1

SP-A: surfactant protein A

SP-B: surfactant protein B

SP-D: surfactant protein D

TGFβ1: tumor growth factor β1

TGFβ2: tumor growth factor β2

TGN: trans-Golgi network

TLC: thin layer chromatography

TRITC: tetramethylrhodamine isothiocyanate

UGM: urogenital sinus mesenchyme

WT: wild type

Amino Acid Codes

Alanine	(Ala, A)
Arginine	(Arg, R)
Asparagine	(Asn, N)
Aspartate	(Asp, D)
Cysteine	(Cys, C)
Glutamine	(Gln, Q)
Glycine	(Gly, G)
Histidine	(His, H)
Isoleucine	(ILE, I)
Leucine	(Leu, L)

Lysine	(lys, K)
Methionine	(Met, M)
Phenylanine	(Phe, F)
Proline	(Pro, P)
Serine	(Ser, S)
Threonine	(Thr, T)
Tryptophan	(Tyr, Y)
Tyrosine	(Tyr, Y)
Valine	(Val, V)

Table of Contents

LIST OF FIGURES

Figure Number

LIST OF TABLES

Table Number

CHAPTER ONE

Literature Review

1.1 Introduction

Prosaposin, also known as sulfated glycoprotein-1 (SGP-1) is an intriguing, ubiquitous, and highly conserved protein believed to be involved in a variety of biological processes, including lipid transport, sperm maturation and sphingolipid degradation [1]. Two existing forms of prosaposin have been identified. Both derive from the same gene and their different oligosaccharide side chains account for their distinct molecular weights. A 70 kDa secretory form, is present in several body fluids, such as in milk [2], cerebrospinal fluid [3], seminiferous tubule fluid [4] as well as in the secretion of the prostate gland [5]. However, little or no information is available on the function of this secretory prosaposin. Another existing form is a 65 kDa protein, considered the lysosomal precursor of four smaller proteins. Thus, after partial proteolysis, prosaposin gives rise to four smaller activator proteins in the lysosomes, designated as saposin A, B, C and D. The function of lysosomal saposins is either to solubilize certain membrane glycolipids or to form complexes with lysosomal enzymes and/or their glycolipid substrates to promote their degradation [6]. The physiological significance of saposins as glycosphingolipid activators has been linked to two known lysosomal storage diseases. Deficiency of saposin C causes a variant form of Gaucher's disease [7] and lack of saposin B gives rise to metachromatic leukodystrophy [8]. No deficiencies of saposin A or D have yet been reported. However, a genetic disease caused by the complete absence of prosaposin in human [9] and a genetic deficiency caused by the inactivation of the prosaposin gene in mutant homozygous mice [10] resulted in multiple glycolipid elevation, including

lactosylceramidosis with normal sphingomyelinase activity.

The existence of two forms of prosaposin suggests that there are at least two different trafficking pathways for prosaposin: a direct delivery of prosaposin from the Golgi apparatus to the lysosomes and a secretory routing from the Golgi apparatus to the extracellular compartment [11]. Existing evidence also suggests that there may be a delivery pathway of prosaposin to the lysosomes via receptor-mediated endocytosis [12]. In summary, the elucidation of the mechanisms of transport of prosaposin to the lysosomes or to the extracellular space is still compelling.

Recently, prosaposin was found in the nervous system and proposed to be a neurotrophic factor stimulating neurite outgrowth in murine cells and choline acetyltransferase (ChAT) activity in human neuroblastoma cells [3]. Prosaposin was also found to protect hippocampal neurons from lethal ischemic damage [13]. Furthermore, prosaposin and an internal sequence called the neurotrophic peptide were demonstrated to activate the MAPK pathway by a G-protein dependent mechanism in Schwann cells [14]. As a matter of fact, prosaposin is expressed in high levels in the brain as well as in the testis and other organs of the male reproductive system. Therefore, it would be important to determine if the secretory form of prosaposin present in seminal fluids has a trophic function in the male reproductive organs as well.

To answer these questions, and eventually to develop strategies for therapeutic intervention in Gaucher's and metachromatic leukodystrophy associated to prosaposin genetic defects, it is important to obtain information on

the gene encoding for this protein. Therefore, the following objectives are pursued in the present study:

I. To characterize the structure of the mouse prosaposin (SGP-1) gene

II. To study the conservation of prosaposin among different species

III. To determine the targeting signal responsible for delivering prosaposin to lysosomes

IV. To assess the role of prosaposin in the development of male reproductive organs by examining the effects of inactivation of prosaposin gene

1.1.1 Objectives

Since prosaposin is a lysosomal resident protein, the first objective of this review is to discuss the structure, function and biogenesis of lysosomes. In addition, other functions of lysosomes will be addressed such as information on lysosomal resident proteins, relationship between the endosomal and lysosomal compartments, targeting pathways of lysosomal proteins including soluble hydrolases and lysosomal membrane proteins.

In addition to saposin A-D, the G_{M2} activator is another lysosomal glycosphingolipid activator protein involved in the degradation of glycosphingolipids. Its function and medical relevance will also be discussed.

Finally, the focus will shift to prosaposin and saposins, the main subject of this thesis. This part will include a summary on the biosynthesis and intracellular processing of prosaposin, tissue distribution, and possible roles of the secreted

prosaposin. The structure and function of saposins, mechanisms of action of saposins, prosaposin/saposin related diseases, interaction of prosaposin/saposin with lipids will also be reviewed.

1.2 Structure and Function of Lysosomes

Lysosomes are intracytoplasmic acidic organelles containing more than 60 hydrolases and involved in the degradation of extracellular and intracellular materials [15-17]. Lysosomes are also implicated in a range of other cellular processes, including antigen presentation [18], bone remodeling [19], and regulation of growth factors and hormones [20]. Under the electron microscope, lysosomes are extraordinarily diverse in shape and size but can be easily identified morphologically, histochemically and immunocytochemically [21]. Lysosomes are formed by four mechanisms: 1) bulk and receptor-mediated pinocytosis involving plasma membrane flow by means of pinocytotic vesicles, endosomes and multivesicular bodies (MVBs) [22]; 2) phagocytosis of particulate matters, bacteria, erythrocytes, cellular debris, apoptotic cell, etc. [15, 21, 23]. 3) autophagy involving ER membrane flow through autophagosomes [24]. While pinocytosis exists in most cells [15], phagocytosis occurs mainly in professional phagocytes such as macrophages and Sertoli cells [15, 23]. Autophagy occurs in most cells although formation of lysosomes by this process is not always evident.

During endocytic flow, lysosomes acquire transmembrane proteins with specific functions such as proton pump ATPases [25], protective membrane glycoproteins [26-28], and integral membrane hydrolases [29]. In addition,

lysosomes receive from the Golgi apparatus, intraluminal activator proteins such as the G_{M2} activator protein and prosaposin which promote the degradation of glycosphingolipids by specific hydrolases [30] [31]. In summary, like all other intracellular organelles, the lysosomes not only contain a unique collection of enzymes but also have activator proteins that promote the degradation of macromolecules such as glycosphingolipids. Moreover, lysosomes have a unique surrounding membrane. This membrane contains transport proteins that allow the final products of hydrolysis to diffuse to the cytoplasm [32-35]. The lysosomal membrane also contains a H^+ pump that utilizes ATP to pump H^+ into the lysosome, thereby, maintaining a pH of about 5 [25]. Most lysosome membrane proteins are heavily glycosylated, to provide protection and maintain the integrity of the lysosomal membrane [31]. Overall, lysosome is the destination point of materials acquired during endocytosis, phagocytosis and autophagy.

1.3 Classification of Lysosomal Resident Proteins

According to their functions, lysosomal resident proteins can be divided into five groups as illustrated in Table I, which include lysosomal soluble hydrolases (such as proteases, glycosidases and lipases, etc.), lysosomal membrane hydrolase (such as, lysosomal acid phosphatase), lysosomal activator proteins (including saposins A-D and G_{M2} activator), lysosomal membrane proteins (including lysosomal associated membrane proteins and lysosomal integral membrane proteins) and lysosomal hyrogen pump protein, the H^+ pump ATPase. Their functions are listed in Table I.

Table I: Classifications of Lysosomal Resident Proteins

Resident proteins	Examples	Functions
Soluble hydrolases	Nucleases Proteases Glycosidases Lipases Phosphatases Sulfatases	Degradation of nucleic acids, proteins, carbohydrates, and lipids and other macromolecules. Hydrolysis of esters.
Membrane hydrolases	Lysosomal Acid Phosphatase (LAP)	Hydrolysis of phosphate groups.
Activator proteins	Prosaposin, Saposins A, B, C and D; G_{M2} activator;	Hydrolysis of glycosphingolipids with short oligonucleotide chain and G_{M2} gangliosides
Lysosomal membrane proteins	Lysosomal associated membrane proteins (lamps) Lysosomal integral membrane proteins (limps)	Protection of the membrane from degradation.
Hydrogen pumps	ATPase-H+ pump	Transport of protons to maintain the acidic pH

1.4 Relationship between the Endosomal and Lysosomal Compartments

Lysosomes are spherical structures of various sizes (0.2-0.4um in diameter), with electron-dense content [21], acidic pH [36] and enriched in acid phosphatases [15, 37-40]. Endosomes, on the other hand, are electron-lucent, acid-phosphatase negative elements [15, 39]. Multivesicular bodies (MVBs) are intermediate structures between endosomes and lysosomes [21]. MVBs are membrane bound structures containing numerous vesicles that pinch off from their delimiting membrane. A clear distinction between late endosomes and early MVBs is sometimes difficult. Treatment with NH_4Cl blocks the maturation of both endosomes and lysosomes. Treatment with leupeptin affects lysosomes but not endosomes. These agents are sometimes used to allow the structural and biochemical dissection of the endosomal and lysosomal compartments [41, 42].

1.5 Targeting Pathways of Lysosomal Proteins

Targeting of newly synthesized lysosomal proteins follows two routes: the mannose 6-phosphate (M6P) dependent pathway and the mannose 6-phosphate independent pathway.

In the M6P dependent pathway, newly synthesized soluble lysosomal enzymes leave the Golgi apparatus to late endosomes/lysosomes bound to the M6P receptor [43, 44]. This receptor recognizes proteins that acquired M6P residues while tranversing the cis-Golgi compartment. M6P residues function as high-affinity recognition signals for receptors that mediate the segregation and

targeting to the lysosomes of soluble lysosomal enzyme precursors. Subsequently, the lysosomal protein and receptor are transported in clathrin-coated vesicles [45-48]. These cargo vesicles fuse with endosomal membranes, where the receptors release the lysosomal enzymes due to the luminal acidic pH of this compartment [43, 49]. The physiologic importance of this pathway became evident with the finding of fibroblasts from patients with mucolipidosis II (ML-II or I-cell disease)[43] and mucolipidosis III (ML-III or pseudo-Hurler polydystrophy) [50], lacking or exhibiting low phosphotransferase activity, the key enzyme responsible for the synthesis of the mannose 6-phosphate signal on lysosomal enzymes. Fibroblasts from patients with mucolipidosis II and III secrete most of their lysosomal enzymes.

The mannose 6-phosphate independent pathway includes lysosomal membrane proteins, some lysosomal hydrolases, prosaposin and yeast vacuolar proteins. In the case of lysosomal membrane proteins, it is proposed that the signals essential for the M6P receptor-independent lysosomal targeting are localized in the cytoplasmic domain of the lysosomal membrane proteins. There are two known targeting routes: 1) Direct transport of lysosomal membrane proteins such as lamps (lysosomal associated membrane proteins) and limp II (lysosomal integral membrane protein II) [51] from the trans-Golgi network to endosomes and lysosomes. 2) Indirect transport of some lysosomal membrane proteins such as, LAP (lysosomal acid phosphatase), limp I (lysosomal integral membrane protein I), and lamp 1 (lysosomal membrane glycoprotein 1, also known as lgp-A, rat lgp, and chicken lysosome-endosome plasma membrane

protein 100, LEP 100) from the trans-Golgi network to the cell surface and subsequently to endosomes and lysosomes via endocytosis [26, 28, 29].

Some soluble hydrolases, such as glucocerebrosidase, are transported to the lysosomes in I-cell fibroblasts [52] [53] and others, such as cathepsin L, despite containing the mannose 6-phosphate tag, are secreted in certain cell types [54, 55]. Targeting of prosaposin, is not yet fully clarified. However, it was shown that prosaposin is targeted to the lysosomes in a M6P independent manner which does not require glycosylation [4, 11, 12, 44, 56]. Evidence from studies in I-cell disease suggested the existance of a M6P independent targeting pathway [57, 58]. In the yeast *S.cerevisiae*, proteins are transported to the vacuoles by a number of different pathways, which depends on motifs residing on specific domains of the vacuolar proteins.

1.5.1 Mannose 6-Phosphate Dependent Lysosomal Protein Transport

1.5.1.1 Mannose 6-Phosphate Receptors (MPRs)

Two distinct M6P receptors are involved in the targeting of lysosomal enzymes under the mannose 6-phosphate dependent pathway. According to their molecular mass, they are referred to as MPR 300 [59] and MPR 46 [60]. According to their binding properties, the MPR 300 is cation-independent (CI) and the MPR 46 is cation-dependent (CD). Thus, binding of certain ligands to bovine and murine MPR 46, is favored by the presence of divalent cations under in vitro condition, but not to the MPR 300 [60]. The MPR 300 is also referred to as mannose 6-phosphate/IGF II receptor, since it binds insulin-like growth factor II

(IGF II) in addition to mannose 6-phosphate containing ligands [61-63]. The physiological significance of IGF II-binding by MPR 300 has not been elucidated yet, and their putative functions are probably related to signal transduction and clearance of IGF II from the serum [64].

1.5.1.2 Roles of the M6P Receptors in the Transport of Hydrolases

The M6P dependent sorting and transport of lysosomal enzymes is involved in several pathways: (1) intracellular sorting of newly synthesized lysosomal enzymes, i.e. segregation from the secretory pathway and transport to the endosomal compartment, appears to be the major task of the M6P receptors; (2) a minor fraction of newly synthesized lysosomal enzymes are exported by M6P-mediated-transport into the secretions of the cell; and (3) exogenous M6P-containing ligands may be bound at the plasma membrane and internalized by M6P receptors. Both M6P receptors are involved in intracellular sorting, albeit with different efficiency. In contrast, export of newly synthesized lysosomal enzymes is a specific function of the MPR 46, and internalization of M6P-containing ligands is accompanied by the MPR 300 only.

1.5.1.2.1 M6P Dependent Intracellular Sorting of Newly Synthesized Lysosomal Enzymes

Investigations of cultured human fibroblasts from patients with I-cell disease (mucolipidosis II) and pseudo Hurler polydystrophy (mucolipidosis III) [50], unfolded the function of the M6P receptors in intracellular sorting of lysosomal

enzymes. In these patients, most of the newly synthesized soluble lysosomal enzymes are secreted due to an inherited deficiency of one of the enzymes involved in the synthesis of the M6P sorting signal. Residual sorting of soluble lysosomal enzymes in some tissues of I cell patients, like in liver, has been attributed to alternative sorting mechanisms [50].

In certain murine tumor cells which express MPR 46 but not MPR 300, 60-75% of the newly synthesized lysosomal enzymes are secreted [65]. Overexpression of MPR 300 in these cell lines efficiently corrected the sorting defect and decreased secretion of newly synthesized lysosomal enzymes to at best 3% [66-69]. In contrast, overexpression of high levels of MPR 46 only partly corrected the defect resulting in moderately reduced secretion of 30-35% of the newly synthesized lysosomal enzymes [69-73]. These independent observations suggested that the MPR 300 was more efficient in intracellular sorting of newly synthesized lysosomal enzymes than the MPR 46.

Sorting was also studied by loading cells with endocytosed antibodies that bind to the extracytoplasmic domain of M6P receptors, to interfere with ligand binding [72] [73]. In cell lines expressing both MPRs, blockage of MPR 300 by endocytosed antibodies caused missorting, whereas endocytosed antibodies against MPR 46 did not affect intracellular sorting of lysosomal enzymes. Missorting due to antibody blockage of MPR 46 was evident only when MPR 300 had also been blocked, or in cells deficient in MPR 300. These results suggest that MPR 300 can compensate a blockage of MPR 46, but not vice versa.

The dominant role of MPR 300 in intracellular sorting of lysosomal enzymes

in cultured cells raised considerable doubt about the physiological relevance of MPR 46 for intracellular sorting in vivo. This question has been addressed by the generation of transgenic mice that are deficient for MPR-46, but expressing normal levels of MPR 300. In one strain of homozygous MPR 46 deficient mice the intracellular levels of several lysosomal enzymes in situ as well as lysosomal enzyme activities in serum were indistinguishable from the normal mice [74]. In contrast, cultured cells (fibroblasts and cells from spleen and or thymus) from the same receptor deficient mice showed significantly increased secretion of newly synthesized M6P-containing ligands. The conclusion was that MPR 46 fulfills a critical function in sorting newly synthesized lysosomal enzymes, which is evident only in cultured cells, because secreted ligands are efficiently diluted into the culture medium. While in situ, secretion of newly synthesized lysosomal enzymes can be compensated by recapture and endocytosis which are mediated by MPR 300, and other carbohydrate-specific receptors such as, the mannose receptor and the asialoglycoprotein receptor [74]. In an independent study, Ludwig et al [75] observed increased levels of lysosomal enzymes in the serum and reduced intracellular levels in several tissues of MPR 46-deficient mice. The reason why the efficiency of lysosomal enzyme sorting in situ differed among the two strains of MPR 46-deficient mice are not yet understood. Nevertheless, partial missorting of lysosomal enzymes has been reported by both laboratories and suggests a critical function of MPR 46 in intracellular sorting of lysosomal enzymes.

Homozygous deficiency of MPR 300 turned out to be lethal due to the loss of MPR 300 as an IGF II binding receptor rather than due to the disturbed sorting

of lysosomal enzymes [76]. Very recently, M6P receptor deficient mice were generated by crossing mice carrying null alleles for IGF II, MPR 300 and MPR 46 [77]. Triple deficient mice surviving the first postnatal day had normal viability and developed a phenotype resembling human I-cell disease. The triple deficient mice were characterized by dwarfism, facial dysplasia, waddling gait, dysostosis multiplex, elevated lysosomal enzymes in serum and histological signs of lysosomal storage predominantly in fibroblasts, but also in parenchymal cells of brain and liver. Surprisingly, the ability of MPR-deficient cells to transport newly synthesized lysosomal enzymes to lysosomes were found to depend on the cell type [58]. MPR-deficient thymocytes target newly synthesized cathepsin D to lysosome via an intracellular route. In contrast, hepatocyte and fibroblasts secrete newly synthesized cathepsin D. The efficiency of recapture of secreted lysosomal enzymes via endocytosis is different in fibroblast and heptocyte in vivo and in vitro. Kasper et al [78] demonstrated in mouse embryonic fibroblasts deficient in both M6P receptors that neither MPR46 nor MPR 300 overexpression is sufficient for intracellular targeting of lysosomal proteins.

In summary, the data obtained in cultured cells and transgenic mice strongly suggest that both MPRs are involved in intracellular sorting of lysosomal enzymes. It remains an open question, whether the difference in their efficiency of sorting is a result of the reported differences in their ligand binding properties or in their intracellular trafficking.

1.5.1.2.2 Endocytosis of Mannose 6-Phosphate Containing Ligands

Exogenous M6P containing ligands undergo receptor-mediated endocytosis. This process is inhibited by antibodies against the luminal domain of MPR 300, but not MPR 46 [73]. MPR 46 has been shown to reach the cell surface and to be rapidly internalized [70, 73, 79, 80] via clathrin-coated pits [81]. Endocytosis of M6P containing ligands by MPR 46 at a low rate has been observed only when cells overexpresssing very high levels of this receptors were incubated at pH 6.5 [69]. Thus, under physiological conditions, endocytosis of M6P containing ligands most likely is mediated exclusively by MPR 300.

Several putative physiological functions have been attributed to the internalization of M6P containing ligands. In general, MPR 300 may recapture endogenous, newly synthesized lysosomal enzymes that have escaped sorting in the trans-Golgi network [82] or that have been actively exported by MPR 46 [83]. M6P dependent endocytosis may also contribute to the clearance of lysosomal enzymes from plasma by liver cells, as internalization of lysosomal enzymes by rat heptocytes is inhibited by mannose 6-phosphate [84, 85]. Another potential function of M6P dependent endocytosis may involve the transfer of lysosomal enzymes from one cell type to another [30]. In addition, MPR 300 may be involved in clearance and/or activation of polypeptide hormones [86-91].

M6P receptors at the cell surface may be part of the machinery required for virus attachment and viral infection, as Herpes simplex virus protein D has been shown to contain M6P residues and to bind to MPR 300 as well as MPR 46 [92].

Taken together, the function of MPR 300 at the cell surface probably is not

only restricted to binding IGF II but other polypeptide hormones and hydrolases as well.

1.5.1.3.2 M6P Dependent Export of Newly Synthesized Lysosomal Enzymes

Cells overexpressing human MPR 46 were shown to export increased levels of newly synthesized lysosomal enzymes [83], while the percentage of exported newly synthesized lysosomal enzymes was remarkedly reduced by simutaneous overexpression of MPR 300. Efficient MPR 46 mediated export of newly synthesized lysosomal enzymes depends on recycling of the receptor as shown by analysis of a C-terminal truncated mutant, which accumulates at the plasma membrane due to its reduced rate of endocytosis. These observations suggest that increased export of newly synthesized lysosomal enzymes from cells lacking MPR 300 [65] at least partly reflects an active function of MPR 46 in export rather than merely its lower efficiency in intracellular sorting. The physiological relevance of M6P dependent export of lysosomal enzymes has not been elucidated.

1.5.2 Mannose-6-Phosphate Independent Transport

As we know so far, MPRs play a major role in the intracellular transport of newly synthesized lysosomal enzymes. However, studies of patients with I-cell disease have provided evidence for MPR-independent transport of soluble acid hydrolases to lysosomes [93]. Recent characterization of a number of lysosomal membrane proteins has revealed that none of these proteins possess the M6P

recognition marker, indeed, they reach the lysosomes independent on M6P receptors but dependent on their own protein sequence determinants [26-29].

The mechanisms of lysosomal and secretory sorting and targeting of certain activator proteins for sphingolipid degradation such as prosaposin are not fully clarified. Recently, when subcellular Golgi fractions obtained from Sertoli cells of adult rat testis, were permeabilized with saponin, a mild detergent, the lysosomal prosaposin was not released, suggesting it is associated to the Golgi membrane. When the permeabilized Golgi fractions were further challenged with free mannose 6-phosphate, again the treatment did not result in the displacement of the lysosomal prosaposin, which remained attached to the Golgi membranes. Finally, the N-glycosylation inhibitor tunicamycin did not affect the transport of this prosaposin to its destination in lysosomes, suggesting an alternative transport pathway exists [4]. Together with other observations, prosaposin is believed to be targeted to the lysosomes by a mannose 6-phosphate independent mechanism that does not require glycosylation [12, 44, 56].

Some lysosomal enzymes and yeast vacuolar proteins are also included in the M6P independent transport pathway, such as, procathepsin D [44, 94, 95], procathepsin L [95], procathepsin B [96], yeast carboxypeptidase Y (CPY) [97], proteinase A (PrA) [98], aminopeptidase I (API) and α-mannosidase 1 (Ams1p) are transported to yeast vacuoles independent of such M6P transport pathway.

1.5.2.1 M6P Independent Transport of Lysosomal Membrane Proteins

There are several lysosomal membrane proteins (Figure 1-1) such as

Figure 1-1: Structure and membrane orientation of lysosomal membrane protein families. Disulfide-bounded loops and O-linked carboxyhydrates (open circles) are only depicted for lamp-1 and lamp-2. Filled circles represent N-linked poly-lactosaminoglycans and complex N-linked oligosaccharides (BioEssays, 18 (5) 1995, by Walter Hunziker and Hans J. Geuze).

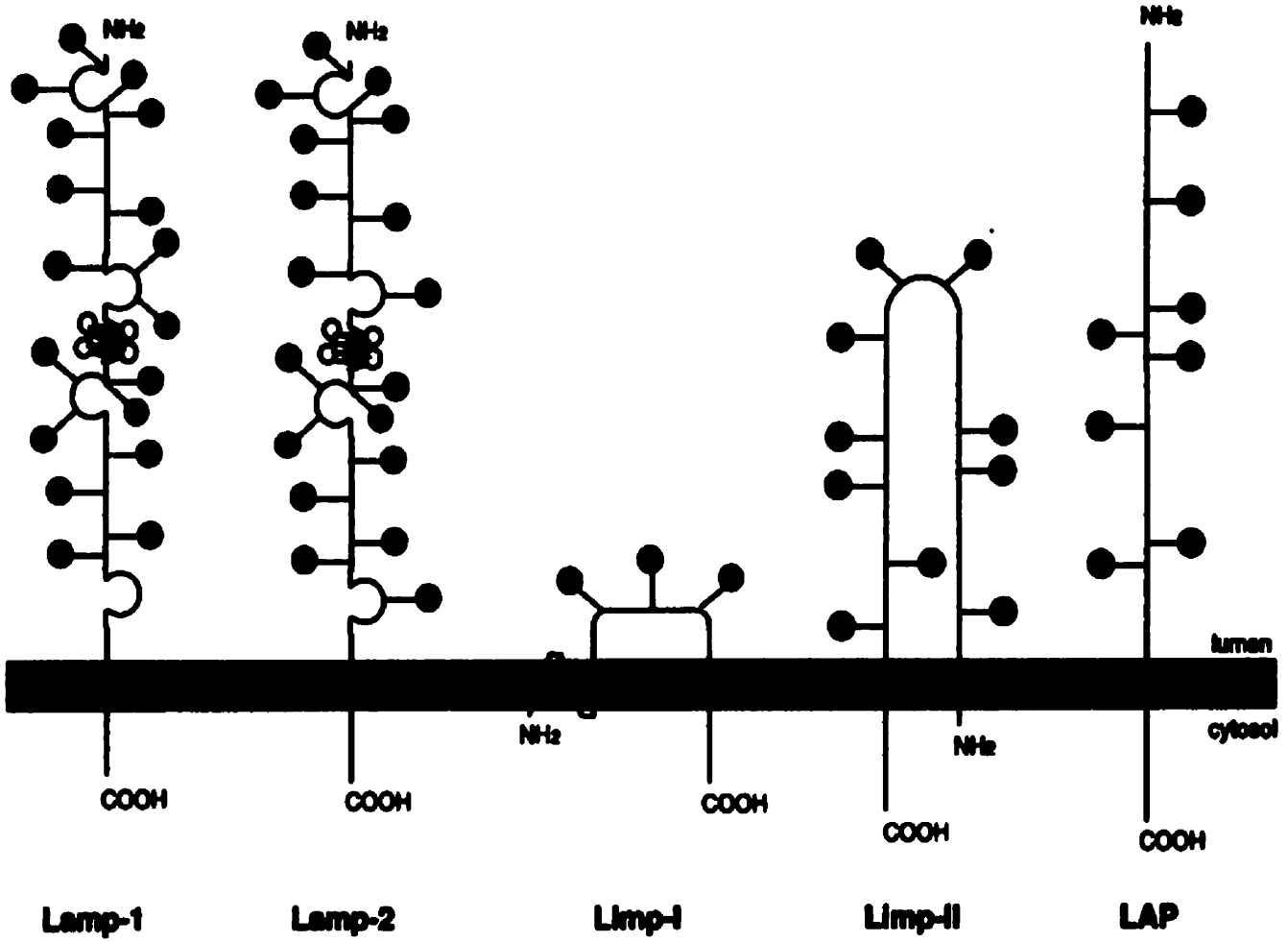
NH2
NH2
NH2
lumen
cytosol
NH2
NH2
COOH
COOH
COOH
COOH
COOH
Lamp-1
Lamp-2
Limp-I
Limp-II
LAP

lysosomal associated membrane proteins (lamps), including lamp-1 and lamp-2, lysosomal integral membrane proteins (limps), including limp-I and limp-II, as well as lysosomal membrane proteins with enzymatic activity such as lysosomal acid phosphatase (LAP).

1.5.2.1.1 Lysosomal Membrane Proteins

Lamp-1 and lamp-2 are two of the best-characterized lysosomal membrane proteins. The two proteins display strikingly conserved primary sequences and therefore have similar domain structures and biochemical properties. Both are type-I membrane proteins, with a large luminal ectodomain connected to a transmembrane region and a short cytosolic tail (Figure 1-1). The cytosolic domain of lamp-1 and lamp-2 composed of 11 residues and is highly conserved between the two proteins (Figure 1-1). Despite the high degree of overall similarity (65-70% identity irrespective of species), lamp-1 and lamp-2 represent separate proteins encoded by two distinct genes located in different chromosomes [99]. Lamp-2 have been shown to undergo alternative splicing, generating at least three lamp-2 isoforms [100, 101]. Common to lamp-1 and the different lamp-2 isoforms is a conserved C-terminal lysosomal targeting motif, G-Y-X-X-Z, Z represents a hydrophobic residue, where Z corresponds to I in lamp-1 [102-105], or to F, L or V in the different lamp-2 isoforms [103],.

Limp-I, displays no overall homology to lamp-1 or lamp-2 and probably traverses the lipid bilayer four times (Figure 1-1), thus belonging to the class of type-II membrane proteins. Limp-I posess an 11-residues short cytoplasmic

domain, which encodes a C-terminal lysosomal sorting motif (G-Y-X-X-M) [106], similar to lamp-1 and lamp-2.

Limp-II, however, only traverses the membrane twice. It displays no homology whatsoever to lamp-1, lamp-2 or limp-I, and also lacks the cytosolic G-Y-X-X-Z targeting motif characteristic of limp-I. Instead, lysosomal targeting of limp-II occurs via a di-leucine type LI signal [107] [108].

LAP, is a soluble lysosomal enzyme, it can be considered a lysosomal membrane protein since it is transiently associated with late endosomal and lysosomal membranes as an integral membrane protein. It belongs to a type I membrane protein with a large luminal domain, a single transmembrane region, and a cytosolic tail of 19 amino acids (Figure 1-1). The cytosolic domain of LAP, almost twice as long as that of lamp-1, lamp-2 or limp-I, encoded a G-Y-X-X-V motif [109], that is not exposed at the end of the cytosolic domain but lies within the tail (Figure 1-1).

Lysosomal membrane proteins can reach the endosome/lysosome compartments via two distinct pathways: 1) An indirect pathway through the secretory pathway to the plasma membrane and endocytosis, which corresponds to LAP [29] as well as to a minor portion of lamp-1 and lamp-2 [28]. 2) A direct transport from the TGN to endosome and lysosome via clathrin-coated vesicles, which includes limp-II [107] [108] and most of lamp-1 and lamp-2 [110, 111]. To date, two distinct classes of cytosolic signals able to mediate late endosome and lysosome targeting have been identified on lysosomal membrane proteins. One determinant, present in lamp-1 [102-105], lamp-2 [103], limp-I and LAP [106, 109],

is based on a G-Y-X-X-Z motif containing a critical tyrosine residue. The second signal, an (leu-Ile) LI found in limp-II [112], is related to the di-leucine motif. Although the role of these tyrosine and di-leucine based signals has been analysed in some detail for sorting at the level of trans-Golgi network and the plasma membrane, the role of these determinants in segregating proteins into different pathways from endosomes remains largely obscure.

Finally, lysosomal membrane proteins are heavily glycosylated proteins involved in a number of functions in late endosomes and lysosomes, including protection of the membrane from degradation, transport of amino acids or carbohydrates resulting from the hydrolytic degradation, transport of protons to maintain the acidic pH, or control of their specific interaction and fusion with other organelles. However, with the exception of the phosphatase activity of LAP, definitive functions assigned to each of the lysosomal membrane proteins are still unknown.

1.5.2.1.2 Protein Transport to the Yeast Vacuole: Independent on Mannose 6-phosphate Transport Pathway

The vacuole of yeast *Saccharomyces cerevisiae* is considered to be the mammalian equivalent to lysosomes. Transport of proteins to the yeast vacuole does not require a carbohydrate modification. Rather, peptide sequences are responsible for targeting. The sorting information for the vacuolar soluble protein, for example, caboxypeptidase Y (CPY) and proteinase A, resides in an N-terminal propeptide which is cleaved in the vacuole to yield mature form. Over forty yeast

mutants have been isolated which are defective in vacuolar protein sorting, and the identification of the disrupted genes in these mutants is leading to an understanding of the mechanisms involved in the sorting pathway. Recently, the *VPS10* gene was shown to encode a sorting receptor for CPY, which was not required for the sorting of any other vacuolar proteins tested [113]. Other *VPS* genes are required for the sorting of multiple vacuolar proteins. For example, Vps1p is an 80 kDa GTP-binding protein required for the sorting of both CPY and proteinase A [114]. Small GTP-binding proteins are involved in many transport steps throughout the cell, and *VPS21* encodes a member of this family which is homologous to the mammalian *RAB5* gene and is important for vacuolar transport [115]. Vps15p is a protein kinase which forms a complex with, and activates, Vps34p, a phophatidylinositol 3-kinase [116]. These proteins may thus be involved in the regulation of vesicle trafficking to the vacuole.

In addition to the better-characterized pathway of transport to the vacuole via the Golgi complex, an additional route of transport exists in yeast. Aminopeptidase I (API) and mannosidase I (Ams1p) are known to be delivered post-translationally to the vacuole, directly from the cytosol, by an alternative mechanism which is independent of the secretory pathway.

In summary, mannose 6-phosphate independent transport pathway is based primarily on the targeting signals localized in protein peptide sequences, and their transport is receptor-mediated. Information on protein transport mechanism in yeast vacuole will be useful to identify similar transport pathways in mammals.

1.6 Glycosphingolipids and Lysosomal Activator Proteins

1.6.1 Glycosphingolipids

1.6.1.1 Structure, Occurrence, and Function of Glycosphingolipids

Glycosphingolipids are important and ubiquitous components of eukaryotic cell membranes [117-119]. They are amphipathic molecules containing a hydrophilic oilgosaccharide chain linked to ceramide. Over 150 glycosphingolipids with different glycans have been isolated from mammalian tissues. They have been classified according to the structure of the core oligosaccharide (Figure 1-2). Glycosphingolipids with glycan chains containing sialic acid are called gangliosides, reflecting their abundance in nerve tissue [120].

There is a much higher concentration of glycosphingolipids in the plasma membrane than in the intracellular membrane of most cells. However, some cells have high intracellular concentrations of glycosphingolipids [121]. It has been suggested that some of the intracellular glycosphingolipids may be associated with cytoskeletal proteins [122]. Glycosphingolipids are located in the outer leaflet of plasma membranes, with the ceramide portion acting as an anchor and the oligosaccharide protruding from the cell surface (Figure 1-2). They are not distributed uniformly over the surface but aggregate in clusters [123]. The conformations of the glycans are probably determined by these interactions, expanding the repertoire of potential functions for a particular structure.

The glycosphingolipid composition of membranes varies markedly form one cell type to another, reflecting the diverse function of glycosphingolipids in cell growth, differentiation, transformation, adhesion, antigenicity, and interaction with

Figure 1-2: Schematic representation of the catabolic pathway of glycosphingolipids in human. Lipid substrates are in boxes, enzymes and activator proteins are in italics, and disorders associated to deficiencies of a given hydrolase and /or activator protein are in bold letters. In mouse, an alternative pathway exists whereby G_{M2} ganglioside is converted to G_{A2} ganglioside by the action of sialidase, which in turn is converted to lactosylceramide by hexB (Phaneuf et al., 1996).

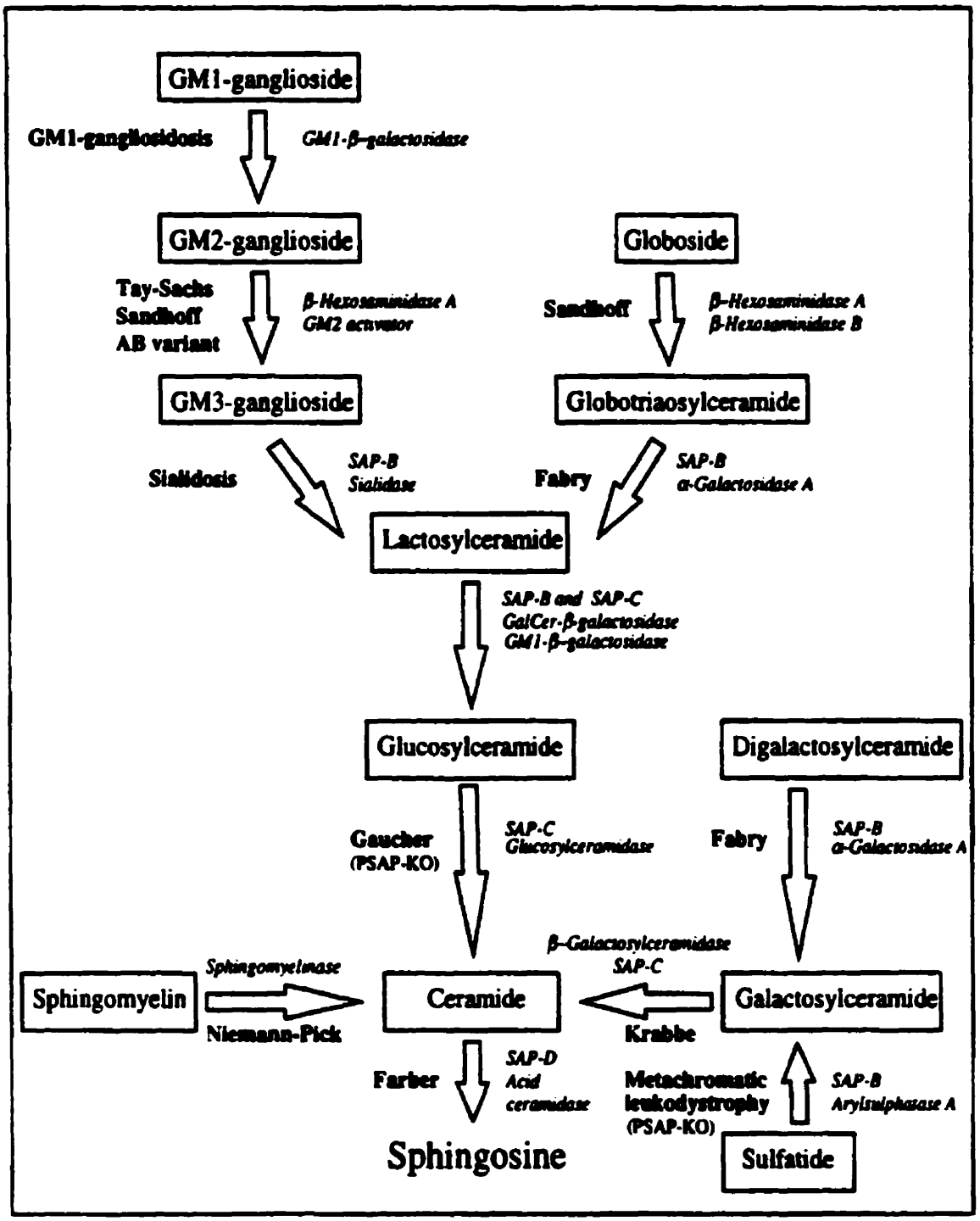
GM1-ganglioside
GM1-gangliosidosis
GM1-β-galactosidase
GM2-ganglioside
Globoside
Tay-Sachs
Sandhoff
AB variant
β-Hexosaminidase A
GM2 activator
Sandhoff
β-Hexosaminidase A
β-Hexosaminidase B
GM3-ganglioside
Globotriaosylceramide
Sialidosis
SAP-B
Sialidase
Fabry
SAP-B
α-Galactosidase A
Lactosylceramide
SAP-B and SAP-C
GalCer-β-galactosidase
GM1-β-galactosidase
Glucosylceramide
Digalactosylceramide
Gaucher
(PSAP-KO)
SAP-C
Glucosylceramidase
Fabry
SAP-B
α-Galactosidase A
β-Galactosylceramidase
SAP-C
Sphingomyelinase
Sphingomyelin
Ceramide
Galactosylceramide
Niemann-Pick
Krabbe
Farber
SAP-D
Acid
ceramidase
Metachromatic
leukodystrophy
(PSAP-KO)
SAP-B
Arylsulphatase A
Sphingosine
Sulfatide

hormones and tissues [119, 124]. In some instances, the function of the sphingolipid may be indirect by modulating the effect of a protein receptor.

1.6.1.2 Turnover of Glycosphingolipids

The plasma membrane is internalized continuously. The components destined for catabolism are delivered to the lysosomes via the endosome system [125], in which sorting takes place, with other components being returned to the plasma membrane or directed to the Golgi (Figure 1-3) [125, 126]. The precise route by which plasma membrane glycosphingolipids reach the lumen of the lysosomes is not fully understood. It has been suggested that during sorting they are sequestered into intraendosomal vesicles, which are delivered to the lumen of the lysosome by membrane fission and fusion [127] [128] [129]. In this way glycosphingolipids on the outer leaflet of the plasma membrane would be on the outer surface of intralysosomal vesicles and exposed to the catabolic hydrolases (Figure 1-3). Experimental evidence for this hypothesis is provided by the observation of MVBs in normal, early, and late endosomes [130] and especially of MVBs in Kupffer cells of patients with a deficiency of the sphingolipid activator precursor [131, 132]. Although the intracellular membrane glycosphingolipid content is low, some glycosphingolipid is delivered to lysosomes by autophagy. A major source of the glycosphingolipids that are degraded in lysosomes is the plasma membrane of senescent or damaged cells, which are phagocytosed by macrophages and neutrophils. Awareness of the relative importance of the catabolism of endogenous and exogenous glycosphingolipids in different cells is

Figure 1-3: Schematic representation of the endocytic pathways according to the "maturational "model. Endocytic vesicles (EV) fuse together to become endosomes (E). Enzymes (rhomboid) and activators (star) are targeted from the Golgi apparatus to the endosomes, which transform into multivesicular bodies (MVB) and which further mature into lysosomes (L) upon digestion of the vesicular content. Sphingolipids (triangles) reach the lysosomes by endocytic flow of the plasma membrane or from the Golgi apparatus bound to activator proteins such as prosaposin (star). The dashed arrow shows the recycling of receptors and membranes that normally takes place in endosomes. Note that in MVB sphingolipids are segregated into luminal vesicles and digested without compromising the integrity of the lysosomal membrane.

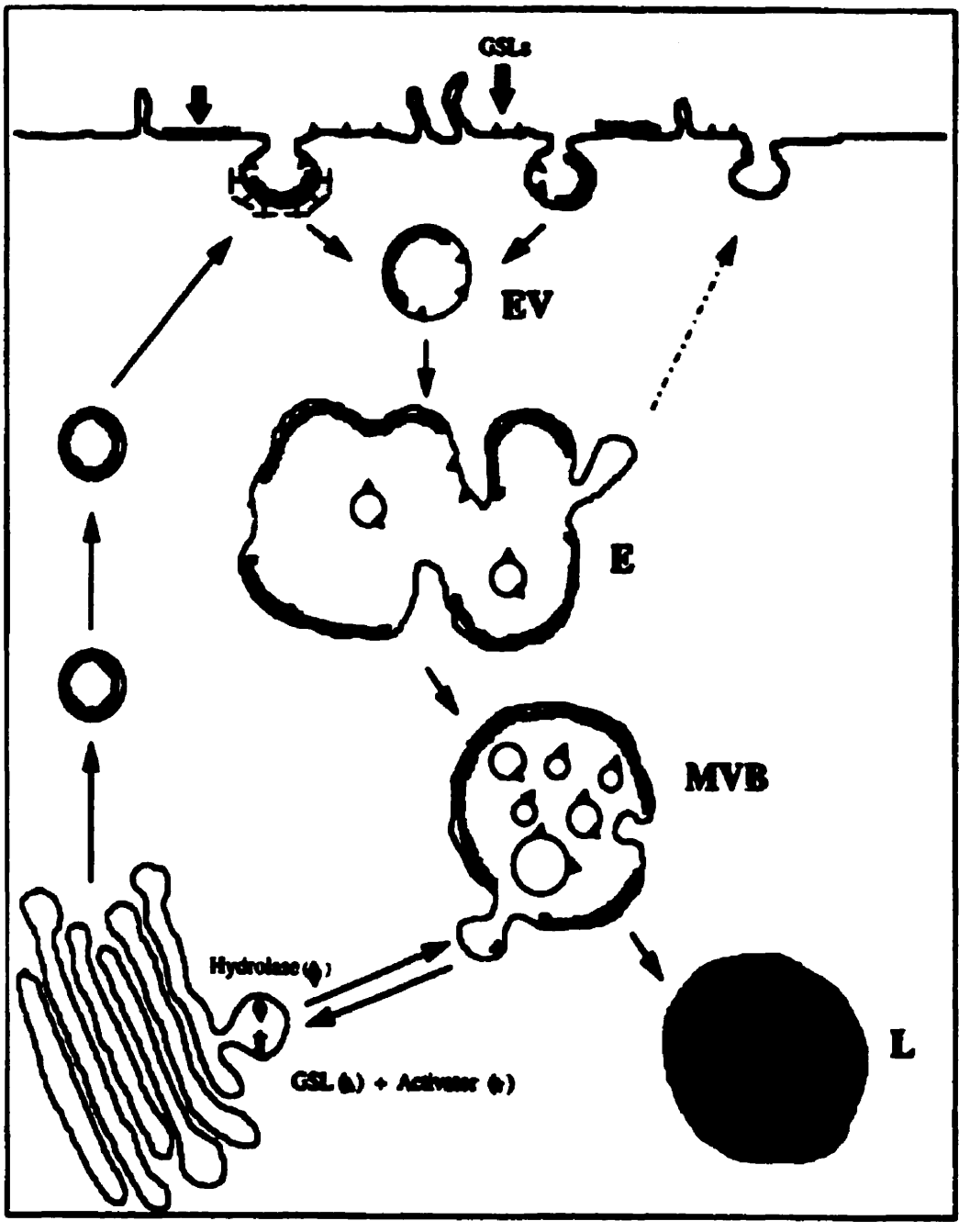
GSLs
EV
E
MVB
L
Hydrolase (ϕ)
GSL (λ) + Activator (ϕ)

extremely important for understanding the nature of the storage products, and the pathogenesis and progress of the sphingolipidoses, the lysosomal storage diseases resulting from defects in the catabolism of glycosphingolipids.

1.6.1.3 Lysosomal Catabolism of Glycosphingolipids' Glycans

The characterization of accumulating lipids in the sphingolipidosis was a great stimulus to the elucidation of the pathways for the catabolism of the glycan moieties of glycosphingolipids. As with the glycans in other glycoconjugates, the oligosaccharide chains of glycosphingolipids are degraded by the sequential action of exoglycosidases from the nonreducing end. For glycosphingolipids this takes place while the oligosaccharides are still conjugated to the lipid moiety, ceramide. Thus, the pathways for the different glycosphingolipids converge on ceramide. Figure 1-2 shows the pathways for the breakdown of common representatives of the major groups of glycosphingolipids. The glycosidases can hydrolyze the same linkage to several different sugar glycans in glycosphingolipids and often in other glycoconjugates. For example, acid β-galactosidase hydrolyzes Galβ1→3GalNAc linkages in glycosphingolipids and O-glycans in glycoproteins, Galβ1→ 3GlcNac and Galβ1→ 4Glc linkages in glycosphingolipids, and Galβ1→ 4GlcNAc linkages in glycosphingolipids, glycosaminoglycans, and N-glycans in glycoproteins.

A genetic deficiency of any of the enzymes in these pathways leads to a characteristic pattern of storage of glycosphigolipids in different cells and a specific sphingolipidosis (Figure 1-2). Most of the human enzymes have now

been cloned and mutation analysis carried out for patients. All of the disorders are genetically heterogeneous, although there are some common mutations in ethnic groups. The different mutations in a particular enzyme have provided important information about the relationship between the structure and specificity, stability, intracellular transport, and interaction with other proteins of the enzymes.

1.6.2 Lysosomal Activator Proteins

The breakdown of the glycans of glycosphingolipids while they are still linked to ceramide poses the problem of accessibility of the soluble lysosomal glycosidases to these amphipathic molecules. Studies on the hydrolysis of its natural substrate, cerebroside sulfate, by purified arylsulfatase A showed that it required an added detergent [133]. It was discovered that the detergent could be replaced by a nonenzymic protein, which was called sulfatide activator [133]. It is now known that several lysosomal hydrolases require the assistance of small nonenzymatic glycoproteins for the hydrolysis of glycosphingolipids (Table II). Today two genes are known to encode these sphingolipid activator proteins [128] [134]. One encodes the G_{M2} activator protein, which facilitates the action of hexosaminidase A on ganglioside G_{M2} [135] and cause the AB variant of G_{M2} gangliosidosis, such as, Tay-Sachs and Sandhoff diseases [136, 137], when it is genetically defective. The other gene encodes prosaposin [138], which is proteolytically processed sequentially in the lysosomes to four saposin A-D [139] with specificities with different sphingolipids (Table II). A deficiency of prosaposin leads to the accumulation of a range of glycosphingolipids [131].

Table II: Lysosomal Activator Proteins

Protein	Size (amino acids)	Function		
		Enzyme	Substrate(s)	Deficiency
GM2-activator	162	β-hexosaminidase	GM2 (GA2)	AB variant of GM2 gangliosidosis
Prosaposin	524	Unknown-lipid carrier?		Prosaposin deficiency
Saposin A	84	β-glucocerebrosidase	Glucocerebroside	Not known
		β-galactocerebrosidase	Galactocerebroside	
Saposin B	80	Arylsulfatase A	Sulfatide	MLD-like storage disorder
		α-Galactosidase	Globotriaosylceramide	
		Sphingomyelinase	Sphingomyelin	
Saposin C	80	β-glucocerebrosidase	Glucocerebroside	Variant of Gaucher's disease
		β-galactocerebrosidase	Galactocerebroside	
Saposin D	78	Acid sphingomyelinase	Sphingomyelin	Not known
		Ceremidase	Ceremide	

1.6.2.1 Functions of GM_2 Activator Proteins and its Related Diseases

The enzymatic degradation of G_{M2} ganglioside, the main accumulated material in G_{M2} gangliosidosis disease, requires β-hexosaminidase A and a lysosomal ganglioside-binding protein, the G_{M2} activator protein. Several mutations of the genes encoding hexosaminidase A and G_{M2} activator protein resulting in intralysosomal accumulation of ganglioside G_{M2} and related glycolipids, in neuronal cells have been identified. Hexosaminidase A is a heterodimer encoded by two different genes, HEXA gene [136] and HEXB gene [137] encoding the α subunit and β subunit of β-hexosaminidase A, respectively, i.e. αβ. Two other Hex isozymers, formed by αα subunit (Hex S) and ββ subunit (Hex B) are also present. Mutation of HEXA gene is associated with deficient activity of Hex A and S but normal level of Hex B, causing a B-variant of Tay-Sachs disease. Mutation of Hex B is associated with deficient activity of Hex A and B, resulting the o-variant of Sandhoff's disease. Mutations in the gene encoding the G_{M2} (G_{M2}A) activator protein [140] give rise to an AB-variant characterized by normal levels of Hex A and B.

1.6.2.1.1 G_{M2} Activator : Roles as a Co-factor in G_{M2} Hydrolysis

β-hexosaminidase A is a water-soluble enzyme which acts on substrates of the membrane surface only if they enter far enough into the aqueous lumen of the lysosome. However, those glycosphingolipid substrates with short oligosaccharide chains, which can not be reached by the active site of water-soluble β-

hexosaminidase A cannot be degraded. G_{M2} activator protein is required in such kind of degradation. The G_{M2} activator protein has a wide specificity [141], act by binding to G_{M2} ganglioside and other related gangliosides to bring them into aqueous solution and make them accessible to the soluble lysosomal glycosidase. The exact mode of action played by the G_{M2} activator protein in the hydrolysis of G_{M2} is still a matter of debate. However, unlike other lectin-like GSL-binding proteins, e.g. the β subunit of cholera toxin, that interacts only with the oligosaccharide portion of the molecules, the G_{M2} activator protein and the saposins also bind the ceramide moiety resulting in a soluble complex. Furthermore, TLC overlay analysis and Sephacryl S-200 gel filtration unveiled that the interaction of G_{M2} activator protein with GSLs required the presence of an acidic moiety on the GSL and the binding is not significantly affected by the sugar chain backbone [142]. The recognition sites on the GSLs for the binding by G_{M2} activator are the anionic residues [142].

Two models (Figure 1-4) have been suggested in the mechanism of action of G_{M2} activator protein. In model 1: The G_{M2} activator protein works as a 'liftase' by recognizing G_{M2} within the membrane, binding to and lifting the lipid out of the bilayer and by presenting it to the water-soluble β-hexosaminidase A. In model 2: The activator binds lipid forming an activator-lipid complex, which can be recognized by the water-soluble β-hexosaminidase A. The enzymatic reaction takes place in free solution. In addition, formation of the ternary complex presumably involves a protein-protein interaction between the G_{M2} activator and β-hexosaminidase A [143].

Figure 1-4: Mode for the G_{M2} activator-stimulated degradation of ganglioside G_{M2} by human β-hexosaminidase A. Water-soluble β-hexosaminidase A does not degrade membrane-bound ganglioside G_{M2}, which has a short carbohydrate chain, in the absence of G_{M2} activator or appropriate detergents. The G_{M2} activator binds one molecule of ganglioside G_{M2} and lifts it a few angstroms out of the membrane. In this position, this activator-lipid complex can be reached and recognized by water-soluble β-hexosaminidase A, which cleaves the substrates (mode 1). Alternatively, the water soluble activator-lipid complex may leave the membrane completely and the enzymatic reaction may take place in free solution (mode 2) (FEBS Letters, 346, 1994, by K Sandhoff and A Klein).

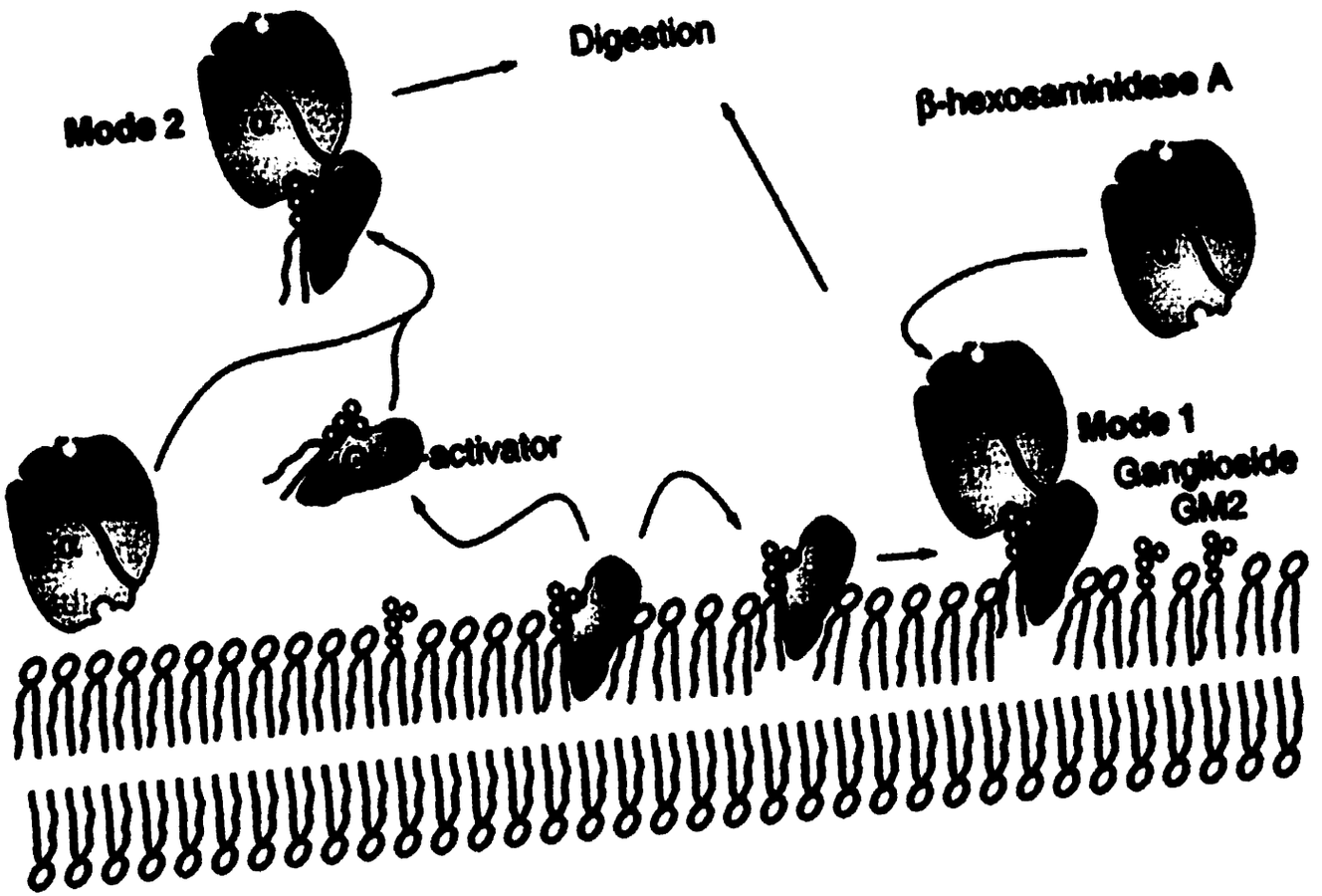
Digestion
Mode 2
β-hexosaminidase A
activator
Mode 1
Ganglioside
GM2

G_{M2} activator protein is unique in several aspect compared to saposin A-D. (a) It is encoded by an unrelated gene [144]. (b) It shares no significant deduced primary structure homologies with the saposins. (c) It functions as a monomer (saposins are probably dimers). (d) Its strength of binding is likely dependent on the structure of the GSL's oligosaccharide and its only 'activating' function is as a substrate-specific co-factor for Hex A in its degradation of G_{M2}, a role that cannot be filled by any of the other saposins.

1.6.2.1.2 G_{M2} Activator Protein: Roles as a General Transport Protein

GM_2 activator protein not only binds G_{M2} ganglioside specifically but also has a wide spectrum of binding capacities with other related gangliosides, such as, G_{M1}, GD_{1a}, G_{M3} and G_{A2}. The G_{M2} activator protein was found to transport glycosphingolipid between two membranes of preparation [143] and from the donor to acceptor liposomes [145]. This binding suggests that the GM_2 activator protein serves as a general glycosphingolipid transport protein. Early binding or transport studies using radiolabeled glycosphingolipid with G_{M2} activator alone, or mixed with differentially charged liposome, respectively, indicated that the G_{M2} binding affinity is in the following order: $G_{M2}>>G_{M1}=GD_{1a}>>G_{M3}=G_{A2}$ [128]. TLC overlay analysis, demonstrated that G_{M2} activator binds to various negatively charged glycosphingolipids without showing preference to any particular sugar composition [142]. Thus, G_{M2} activator protein does not behave like lectins, which display the recognition of a specific saccharide structure. As both G_{M2} activator protein and saposin B were shown to be able to transport GSLs from donor to

acceptor liposomes [145], G_{M2} activator protein may have a specific role, in vivo, in the transport of acidic GSLs.

In summary, the G_{M2} activator protein is considered as a biological detergent. The following roles has been assigned to the G_{M2} activator protein: 1) a non-specific hydrophobic binding to ceramide to produce a water soluble complex; 2) a more specific hydrophilic binding to oligosaccharides with both the non-reducing terminal GalNAc and NeuAc residues of G_{M2}; and 3) a strong, specific interaction with Hex A.

1.6.2.2 Functions of Saposins and Their Medical Implications

The first activator protein was identified in 1964 as a protein which was necessary for the hydrolytic degradation of glycosphingolipids carrying a sulfuric ester group (sulfatides) by lysosomal arylsufatase A [133]. This activator, SAP-B, now known as Saposin B, is a small lysosomal glycoprotein consisting of 80 amino acids, with a N-linked carbohydrate chain and three disulfide bonds [128]. Like G_{M2} activator protein, it binds glycosphingolipids, but with broader specificity and is also considered as a physiological detergent. In vitro, it behaves similarly to the G_{M2} activator protein in some aspects, i.e. it can recognize and bind several different GSLs on the surface of micelles by forming a stoichiometric complex and is then able to transfer the GSLs to the membranes of acceptor liposomes [31]. Thus, Saposin B solubilizes and presents glycosphingolipids to water-soluble hydrolases as substrates [146]. The inherited deficiency of saposin B leads to a lysosomal storage disease, which resembles metachromatic leukodystrophy.

However, unlike typical metachromatic leukodystrophy, not only sulfatide but also other glycolipids, e.g. globotriaosylceramide, accumulate owing to a blockage of degradation at several points in the catabolic pathway of glycosphingolipids [147].

Subsequently, saposin B, together with other three activator proteins, known as saposin A, C and D, were found to derive from a same precursor, prosaposin. The four saposins show some homology and conservation and have similar properties. However, they differ in their specificity and their mechanism of action. The physiological function of these sphingolipid activator proteins is only partially clarified to date. As indicated above, the inherited deficiency of saposin B leads to an atypical form of metachromatic leukodystrophy, and saposin C deficiency causes an atypical form of Gaucher's disease, charaterized by the accumulation of glucosylceramide [7, 132]. In one patient with a complete deficiency of the whole prosaposin precursor due to a homoallelic mutation within the start codon [132], there was multiple accumulation of undegraded sphingolipids, such as, ceramide, glucosylceramide, lactosylceramide, ganglioside G_{M3}, galactosylceramide, sulfatides, digalactosylceramide and globotriaosylceramide [9]. Diseases related to the deficiency of Saposin A and D are not yet characterized. The general mechanism of saposins appears to be similar to the G_{M2} activator protein, which act either as a liftase or by forming a water-soluble complex with the lipid and hence mobilizing the lipid out of the membrane. Details of how individual saposins act with their specific substrates are summarized below.

1.7 Prosaposin and Saposins

1.7.1 Biosynthesis and Intracellular Processing of Prosaposin

Human prosaposin is a 524 amino acid glycoprotein containing a 16-residue signal peptide sequence and five potential N-linked glycosylation sites [138]. Like all other glycoproteins, prosaposin employs the secretory pathway to accomplish the intracellular delivery to its final destinations. The N-terminal signal sequence directs it into the lumen of the endoplasmic reticulum (ER) first, where it receives high mannose, asparagine-linked oligosaccharides. Disulfide bridges are subsequently followed by its proper folding and assembly into oligomeric structures [148]. Prosaposin is then transported to the Golgi apparatus, where the oligosaccharide chains are probably trimmed and remodeled like most glycoproteins [149], and also within the Golgi apparatus where prosaposin is sorted to different destinations. As a matter of fact, two forms of prosaposin with slightly different molecular weights exist due to different post-translational modifications: a 70 kDa form secreted extracellularly or retained as an integral membrane protein and a 65 kDa form targeted to lysosomes. Prosaposin is also widely distributed as a neuronal cell surface membrane component in human adult and fetal brain [150] and in rat brain [151], suggesting it has a role in neuronal function and development. In lysosomes, prosaposin is proteolytically processed into four smaller peptides known as saposin A, B, C and D. Saposins, acting as activator proteins for specific lysosomal enzymes, are required for hydrolysis of different glycosphingolipids (GSLs) within the lysosomes. The rat homologue of human prosaposin is known as sulfated glycoprotein-1 (SGP-1), which has about

80% amino acid identity when aligned with human prosaposin [152]. SGP-1 is a major glycoprotein secreted by rat Sertoli cells [153]. It was initially thought to be exclusively secreted by Sertoli cells; however, immunocytochemical studies demonstrated that this protein is also present in lysosomes of Sertoli cells [153, 154].

Biosynthesis of prosaposin has been studied in vitro by pulse-chase experiments in cultured human fibroblasts [44, 155]. Immunoprecipitation of whole cell lysates by anti-saposin B antibody demonstrated that the precursor of Saposin B was first synthesized as a 65 kDa glycoprotein and then converted to a 70 kDa polypeptide by co-translational glycosylation. The 65 kDa precursor was rapidly processed into mature 8-13 kDa saposin via 52 kDa and 35 kDa intermediates. The 70 kDa protein was the only form found in cultured medium. Similarly, when using saposin C antibody, a similar co-translational modification was illustrated, and the final product or mature saposin C was also 9-12 kDa [44, 155]. Pulse-chase label experiments of Sertoli cells in culture [11, 152] confirmed the same biosynthetic relationship between the 65 and 70 kDa forms of rat SGP-1 in vivo.

How this maturation process of prosaposin is accomplished within the lysosomes still need to be clarified. Presumbably, dibasic amino acids residues occur at the junctional boundaries of each saposin domain in prosaposin, such as, seven lysine and one arginine, which may be the potential proteolytic cleavage sites [30]. Recently, Hiraiwa et al [139] demonstrated biochemically that cathepsin D may be one of the major proteases involving in the proteolytical processing of prosaposin. The cleavage sites occurred between ^{179}leucin and ^{180}tyrosine and

^{298}leucine and ^{299}valine at the interdomain linker regions between A and B and C, respectively, in the presence of cathepsin D. It was also suggested by time course experiments that the processing of the N-terminal half of prosaposin occured earlier than those of the C-terminal half. Intermediate products (trisaposins and disaposins) are observed during prosaposin processing, however, their functional importance is still not known.

1.7.2 Distribution and Functions of the Precursor of Sphingolipid Activator Protein, Prosaposin

As we mentioned above, in addition to the generation of the four functional saposins within lysosomes, prosaposin also exists as an unprocessed 70 kDa secretory protein present in many tissues and body fluids. The highest concentrations of prosaposin has been reported in testis, seminal plasma, cerebral gray matter, cerebrospinal fluid and human milk, and lower concentration in liver, spleen, and other organs [138, 156]. Recent studies focusing on the roles of prosaposin in human brain was based on the evidence of its high expression level in this organ and on the existence as an integral membrane component of neuronal and other plasma membranes [44, 150]. Northern blot analysis of prosaposin mRNA during embryonic development showed a high expression in mouse brain and dorsal root ganglia, indicating a developmental role of prosaposin [157]. An intriguing function of prosaposin in nerve system has been postulated by O'Brien and colleagues, demonstrating that prosaposin is a neurotrophic factor [3] [158]. The active neurotrophic region is localized to a 12

amino acids residue at the NH_2-terminal end of saposin C (LIDNNKTEKEIL) [159]. Several synthetic peptides derived from this region are equally as bioactive as prosaposin and were called prosaptides [158, 159]. Nanomolar concentrations of prosaptides as well as prosaposin can stimulate neurite outgrowth and choline acetyltransferase activity in neuroblastoma cells [3]. In addition, prosaposin was shown to protect hippocampal neurons from ischemic damage and to prevent apoptosis of cerebellar granule neurons in culture submitted to palitaxol toxicity [14]. Prosaposin appears to bind to a high-affinity receptor that induces protein phosphorylation [3] and which is associated with G protein, $G_{o\alpha}$. [160]. The binding of prosaposin to this receptor triggered a signal transduction cascade, with induction of extracellular signal-regulated protein kinase phosphorylation in neural and glial cells [139, 160-162]. In primary Schwann cells prosaposin has also been found to activate the mitogen-activated protein kinase cascade through a pertussin toxin-sensitive G protein-mediated pathway essential for enhanced sulfatide synthesis by Schwann cells acting as a myelinotrophic factor [14]. And the signaling pathways involved in Schwann cell survival by prosaposin and prosaptide have recently been identified through the PI3K/Akt pathway [163].

Recent observation of colocalization and complex formation between prosaposin and monosialoganglioside G_{M1} and G_{M3} (not G_{M2}) in neural NS20Y cells [164], implicated that the neurotrophic activity of prosaposin in NS20Y neuroblastoma cells might be mediated in part by the increase in content of cell surface gangliosides. The association of prosaposin-G_{M3} complexes on the cell surface appeared to be functionally important in neurite sprouting.

Prosaposin binds gangliosides with the same or greater avidity than saposins and facilitate their transfer form liposomes to biological membranes [165]. Prosaposin has also been suggested to play a role in intracellular transport of glycosphingolipids [129, 134, 156] [166].

SGP-1, the rat homologue of human prosaposin, was initially thought to be secreted to the lumen of seminiferous tubules exclusively [138]. A proline rich segment of 31 amino acids residues present in rat SGP-1 but absent in human prosaposin was implicated in the secretory routing of SGP-1 to the extracellular space, since similar proline-rich regions have been found in many secretory proteins [167]. However, immunocytochemical studies in Sertoli cells of the testis and epithelial cells of the efferent ducts of the rat have demonstrated that SGP-1 can also be localized in the lysosomes [153, 154, 168]. In addition, immunoprecipitation and immunoblotting of lysosomal protein fractions isolated from rat Sertoli cells can light up a 65 kDa as well as a 15 kDa protein [4]. These data confirmed that a lysosomal precursor of SGP-1 also exists in rat Sertoli cells besides its secretory form.

Prosaposin has been found in many body fluids, however, little is known concerning its physiological function. SGP-1 or the rat prosaposin is rich in seminiferous fluids and it has also been demonstrated to be associated with the head and tails of spermatozoa once it is secreted into the lumen [169]. These may suggest that prosaposin may regulate the release and/or maturation of spermatozoa during spermatogenesis. It has also been suggested that prosaposin may be involved in the modification of the sperm membrane by means

glycolipid transport. Since glycolipids were shown to mediate heterologous cell contacts, including the preferential adhesion of different cell types [170], it is possible that glycolipid modification of Sertoli cell and /or germinal cell membranes play a role in certain processes such as the induction of spermiation. Nevertheless, further investigation is required to clarify the functions of secreted prosaposin [152] in the male reproductive system.

1.7.3 Structure and Function of Saposins

1.7.3.1 Discovery of Saposins

Saposins are glycosphingolipid activator proteins, four of which are derived from a single precursor, prosaposin, by proteolytical processing. These small heat stable glycoproteins are required for the hydrolysis of a variety of glycosphingolipids. Saposin B (previously called shingolipid activator protein) was the first activator protein discovered [133]. Saposin B activated the hydrolysis of cerebroside sulfate by arylsulfatase A, the hydrolysis of G_{M1} ganglioside by acid β-galactosidase, and globotriaosylceramide by α-galactosidase [146]. Human hereditary deficiency of saposin B results in tissue accumulation of cerebroside sulfate and other glycolipids and a clinical feature of late infantile or infantile metachramatic leukodystrophy [8] [171].

Saposin C (previously called sphingolipid activator protein-2) was identified by Ho and O'Brien [172]. Saposin C was shown to activate the hydrolysis of glucocerebroside by glucosylceramide β-glucosidase [173]. Later, the activation of the hydrolysis of galactocerebroside β-galactosidase by saposin C was also

reported [174]. Deficiency of saposin C has been linked to a variant form of Gaucher's disease [7].

A cDNA encoding human saposin B was first cloned in 1986 and subsequently longer cDNAs encoding the entire open reading frame of prosaposin had been confirmed by several laboratories [138, 175, 176]. Collard et al [152] first identified four similar polypeptide domains placed in tandem from analysis of a cDNA encoding sulfated glycoprotein-1(SGP-1), the rat homologue of human prosaposin. One of the domains of SGP-1 was identified as homologous with human saposin B. These results suggested that four saposin proteins could be generated by partial proteolytic processing of prosaposin/SGP-1. However, saposin A and D had not been recognized until O'Brien et al [138] analyzed the full sequence of the precursor of human saposin C to be found that it also encoded both saposin B and C and two additional putative saposins, A and D.

1.7.3.2 Structure and Functions of Saposins

All saposins contain about 80 amino acids and each has one N-glycosylation site, except human saposin A, which contains two N-glycosylation sites. Their structures are similar to each other since they contain six identically placed cysteine residues, two-conserved proline residues and one N-glycosylation site. They also have similar circular dichroism (CD) spectra [30]. It has been noted that saposins have a remarkable similarity with other proteins, called SAPLIP (saposin-like proteins), which have a cysteine pattern identical to saposins, a similar size and stability under extreme condition [177].

Based on helical wheels with appropriate positioning of proline residues and glycosylation sites and the localization of three potential disulfide bonds formed by the 6 cysteine residues, a hypothetical secondary structure of saposins were predicted [30] according to the Chou-Fasman rules [178]. This suggested a similar structure between saposin A, C and D, but a different structure for saposin B because of the presence of a large β-sheet region and a lengthy C-terminal helical region not present in saposin A, C, or D. However, they all form three internal disulfide bridges in the hydrophobic interior, which may explain their high stability to heat [138, 179].

Circular dichroism spectroscopic studies of saposins [30] indicated that saposin A, C, and D were enriched in α-helical structure (41%-53% at pH4.5), whereas saposin B had a lower α-helical content (26%) and much higher β-sheet (34%). However, these theoretical models need to be verified by crystal structure.

The similar protein sequences and predicted structures of saposins would indicate a common structure-function rationale. However, the functional properties of saposin B were thought to be different from others because saposin B was shown to interact with lipid substrates forming a lipid and saposin B complex [141] while other saposins interact with enzymes instead of forming complexes of saposin and enzymes [180, 181] [182].

As shown above, saposin B was the first identified saposin. It stimulates the hydrolytic activity of arysulfatase A for sulfatide, α-galactosidase A for globotriaosylceramide hydrolysis, and acid β-galactosidase for G_{M1} ganglioside [183]. The degradation of additional glycolipids and glycerolipids were also shown

to be activated by saposin B [146]. Saposin B seems to act as a detergent-like protein solubilizing multiple lipid substrates for enzyme hydrolysis.

In vitro saposin B-lipids binding assay followed by enzymatic hydrolysis studies [141] demonstrated that saposin B activated more efficiently the hydrolysis of sulfatide by arysulfatase A than globotriaosylceramide by α-galactosidase A, or G_{M1} ganglioside by β-galactosidase A. Furthermore, the molar ratios of lipids, including G_{D1a}, G_{M1}, G_{M2}, G_{M3} gangaliosides and sulfatide were found to be 1:2 [141], which suggested that saposin B may exist as a dimer during its association with lipids. However, this has not been confirmed yet. In summary, saposin B acts on a broad range of glycolipids within an acidic environment, to stimulate their specific hydrolysis within lysosomes. When comparing the interactions between saposin B and G_{M2} activator protein with gangliosides detected in aqueous medium, both showed similar activities. While, the binding on TLC overlay showed that saposin B bound to all glycosphingolipids, G_{M2} activator bound preferentially to the anionic glycosphingolipids [142]. Saposin B was shown to be able to transport glycosphingolipids from donor to acceptor liposomes [145] and facilitate the transfer of many glycolipids [141], suggesting a specific role *in vivo* to transport acidic glycosphingolipids.

Saposin C is considered as a sphingolipid activator because it stimulates the hydrolysis of glucocerebroside by glucosylceramidase and galactocerebroside by galactosylceramidase [30, 173]. Its physiological significance has been confirmed in variant Gaucher's patients due to the lack of Saposin C [7, 132].

In contrast to saposin B, saposin C interacts with the membrane-associated

β-glucocerebrosidase directly to form a more active complex by inducing a conformational change in the enzyme [180]. Saposin C also activates the hydrolysis of galactosylceramide and sphingomyelin. Thus, saposin C does not appear to interact with lipid substrates, such as glucocerebroside. This has been demonstrated when sepharose-linked saposin C used as an affinity column for glucocerebroside, did not form complexes with this lipid [180, 184]. Finally, high molecular aggregates formed by glucocerebrosidase and saposin C has been isolated from human tissue [185].

Saposin A can stimulate the enzymatic hydrolysis of 4-methylumbelliferyl-β-glucoside, glucocerebroside, and galactocerebroside in vitro [179]. Stimulation of acid β-glucosidase by saposin A is similar to that by saposin C but the degree of stimulation is about one-third lower. The binding site of saposin A and C were shown to be the same [173].

Saposin D is the least understood of the saposins. It has been reported to be involved in sphingomyelin and ceramide hydrolysis [186, 187], but no detailed information on its mechanism of action is available so far. However, the addition of saposin D to the culture medium of fibroblasts from patients with prosaposin deficiency leaded to a decrease in the accumulation of ceramide [188], thus the function of saposin D seems to be related to ceramide degradation rather than sphingomyelin degradation. It was also found that saposin D, but not the other three saposins, stimulates the degradation of ceramide by a partially purified preparation of ceramidase and that the saposin poorly interacts with ceramide at acidic pH values [187]. Recently, it has been demonstrated that the association of

saposins with cell membranes was highly dependent on the composition of the bilayer [189]. The presence of acidic phophoslipids such as phosphatidylserine or phosphatidic acid greatly favoured the interaction of saposin D at low pH.

1.7.4 Mechanisms of Action of Saposins

Although the involvement of saposins in the degradation of sphingolipids is well established, their mechanism of action is still under debate. Saposin B, like G_{M2} activator protein, is able to solubilize several sphingolipids in vitro, by binding and bringing them into aqueous solution to make them accessible to specific lysosomal hydrolases [141]. Wynn proposed the triple binding domain theory of a glycosphingolipid to saposin B based on the conformational studies of the glycosphingolipids [190]. He predicted that there are three possible interactions between a glycosphingolipid and the protein: (a) the hydrophobic interaction of the hydrocarbon chains of the ceramide moiety and a complementary hydrophobic domain in the protein molecule; (b) the electrostatic interaction between sialic acid or sulfate group and a positively charged group of the protein; and (c) the hydrophilic interaction between a hydroxyl group in a sugar moiety and a complementary plane of the protein.

In contrast, saposin C, the physiological activator of glucosylceramidase, interacts with the membrane-associated β-glucocerebrosidase directly to form a more active complex, promoting in this way the enzymatic activity [30, 128, 134, 191, 192]. At least two modes of action were proposed for saposin C. 1) The activation effect of saposin C might derive from an induction in the conformational

change of the enzyme for optimal catalysis [180-182]. 2) Saposin C most likely reconstitutes the enzyme activity by favouring the glucosylceramidase localization on lipid surfaces of appropriate composition [193-195]. Saposin C also activates the hydrolysis of galactosylceramide and sphingomyelin.

Saposin A is believed to mediate its activating effect by directly binding to the enzyme [181]. It is not clear if saposin A and C have the same or different mechanism of action on activation of hydrolases.

There is not much information on how saposin D acts as a sphingolipid activator protein, however, it was hypothesized that saposin D activation depends on its interaction with the enzyme rather than with ceramide [187].

1.8 Prosaposin/Saposins Related Diseases

The first demonstration of a role for saposins in human disease came from the discovery of a variant form of metachromatic leukodystrophy (MLD) with normal arylsulfatase A activity and deficiency of saposin B [8]. Patients with this disease present neurological deterioration and demyelination, severe progressive mental retardation, and tissue accumulation of sulfatide in brain and in myelinated nerves. However, unlike the classical form of metachromatic leukodystrophy, in which arysulfatase A is deficient, patients who lack saposin B have normal or nearly normal activities of arysulfatase A [6] [196-198]. Reloading of saposin B in cultured fibroblasts from patients with saposin B deficiency corrects the impaired degradation [8]. However, the fact that saposin B also activates the hydrolysis of other lipids by different enzymes is reflected by the composition of the storage

material, which in addition to sulfatide, it also contains globotriaosylceramide and G_{M3} ganglioside in saposin B deficiencies [146].

Point mutations and amino acid insertions have been reported from three patients with saposin B deficiency, an inherited autosomal recessive disease. One is due to a single C-T transition in the 23rd codon of saposin B domain resulting in a threonine to isoleucine amino acid substitution [6, 196]. A second one is a G to C mutation leading to a substitution of a cysteine residue for a serine residue within the saposin B domain. The last mutation is due to an insertion of 33 nucleotides in the last one third of the saposin B domain. In the first case, a polar amino acid (threonine) is replaced with a nonpolar amino acid (isoleucine) which in turn appears to eliminate the glycosylation signal and to increase its proteolytical degradation owing to exposure of a proteolytical site (arginine) two residues to the amino-terminal side of the glycosylation site. The same proteolytical hydrolase that cleaves prosaposin at dibasic residues at the saposin boundaries could also cleave the mutant protein. The second point mutation destroys the disulfide bonds and the correct three-dimensional structure. The 33 nucleotide insertion occurs in the last one-third of the saposin B domain, changing its hydropathy profile significantly and perhaps leading to its instability [30, 171].

A deficiency in saposin C was first demonstrated in a variant form of Gaucher's disease [7]. Experiments shown that saposin C is an important cofactor for the activity of gluco-and galactoceramidases [173]. A 200-fold elevation of glucocerebroside in spleen but normal glucosylceramide β-glucosidase activity was found in a Gaucher's disease patient [30]. Two point

mutations in the saposin C coding region, G1154 to T [199] and T1153 to G [200], changing the cysteine residues to phenylalanine and glycine respectively, lead to an atypical variant form of Gaucher's disease. This indicates that the importance of the cysteine residues for the stability of mature saposins.

Another mutation resulting in entire prosaposin deficiency was reported in two siblings of fourth cousin parents [131, 132]. Biochemical analysis demonstrated the accumulation of different sphingolipids including glucosylceramide, galactosylceramide, and ceramide in patient's tissues. Sequence analysis demonstrated an A-T transversion in the initiation codon resulting in absence of prosaposin synthesis. Clinically, the patient presented hyperkinesia, respiratory insufficiency, and hepatosplenomegaly and died by 16 weeks. Unfortunately, the defects in other organs such as the male reproductive system had never been examined.

Sphingomyelinase activity was normal in this prosaposin deficient patient and there was no storage of sphingomyelin, which suggest in vivo, that saposins are not essential for sphingomyelinase activity. Thus, the significance of saposin D as an activator protein still needs more investigation.

It is known that saposin C deficiency cause Gaucher's disease in the presence of saposin A, while saposin A has been demonstrated in vitro to activate the same enzymes for glucosylceramide and galactocylceramide. Therefore, it can be concluded that saposin A cannot complement the defective saposin C and may not interact with glucocerebrosidase in vivo.

1.9 Objectives of the Present Research

In summary, saposins A, B, C and D are generated by partial proteolysis of the same precursor, prosaposin in lysosomes. The gene encoding human prosaposin has been partially cloned [175, 176], but not in the mouse and other experimental species. It is well known that saposins share a high degree of structural similarity and that a group of several other proteins (called SAPLIPs) contain saposin-like motif [177]. In addition, prosaposin exists in high concentrations as a secretory protein in human milk, cerebrospinal fluids, and seminal plasma [156] but its physiological role in extracellular fluids remains to be determined. Firstly, to increase our understanding on the biogenesis of prosaposin and the relationship between the structure and function of saposins and saposin-like proteins, we cloned the mouse prosaposin gene and examined the distribution patterns of mRNA variants produced by alternative splicing in various tissues. We also compared the backbone structure of prosaposin cDNAs in mouse, rat, and human, to establish conserved features that are more likely to have functional significance.

The second objective of the present study was to identify the domains that are responsible for the targeting of prosaposin to lysosomes. We used a selective mutagenic strategy by deleting the functional domains of saposin A, B, C and D, as well as the N and C termini of prosaposin. Then, we analyzed the final destination of the truncated constructs as compared to the wild type control using pulse-chase analysis, confocal microscopy and EM immunogold labelling. The

identified targeting domains were verified by attaching them to a secretory protein, albumin. Chimeric constructs of albumin fused with partial sequence of prosaposin were transfected into COS-7 cells and their final destination to lysosomes was examined by confocal microscopy.

Finally, prosaposin was shown to have the highest level of expression in brain as well as in testes. Much attention had been given to the role of prosaposin in the central nerve system, since the diseases (metachromatic leukodystrophy and Gaucher's) caused by mutations that affect saposin B, C or the entire prosaposin, present severe neurodegenerative symptoms. However, SGP-1, the rat homologue of prosaposin is known to be one of the major proteins produced by the testicular Sertoli cells. Therefore, we explored the role of prosaposin in the male reproductive system by using a prosaposin (-/-) mouse model.

CHAPTER TWO

Materials and Methods

2.1 MATERIALS

2.1.1 Chemicals and Supplies

All restriction enzymes and modifying enzymes were purchased from Pharmacia Biotechnology Inc. (Uppsala, Sweden), Promega (Madison, WI), Boehringer Mannheim (Berlin, Germany), Gibco-BRL (Missisaga, ON, Canada), New England Biolabs (Mississauga, Canada) and Stratagene (La Jolla, CA). The pGEM-T, pGEM-3Z(+) and the pGEX vectors were purchased from Promega (Madison, WI), the pcDNA3.1 vector was bought from Invitrogen (Carlsbad, CA), and pMAL vector was from New England Biolabs (Mississauga, Canada). The mouse testicular Unizap XR cDNA library was obtained from PDI BioScience (Aurora, ON, Canada). The rat testicular cDNA library was from Stratagene (La Jolla, CA), the mouse EMBL 3 genomic library was from Clonetech (Palo Alto, CA). The albumin cDNA clone was purchased from ATCC (Manassas, Virginia). Pepstatin A (Isovaleryl-Val-Val-Sta-Ala-Sta) and Phenylmethyl-sulfonylfluoride (PMSF) were purchased from Sigma (Oakville, ON, Canada). Aprotinin, Leupeptin, (+)-Brefeldin A (BFA) were from CalBiochem (La Jolla, CA). Endoglycosidase H (Endo H) was from Roche (Laval, Quebec). Dulbecco's modified eagle medium (DMEM), fetal bovine serum (FBS) and trypsin were bought from Gibco-BRL (Grand Island, NY). Dulbecco's modified eagle medium without methionine and cystine and L-glutamine, L-methionine, L-glutamine and cysteine were purchased from Sigma-Aridrich (Irvine, UK). Nu-Serum V Culture was from Decton Dickinson Labware (Bedford, MA). ECL, Hybond nylon membrane was purchased from Amersham (Oakville, ON, Canada), bovine serum

albumin from Boehringer Mannheim, and Kodak x-omat film from Eastman Kodak Co. (Rochester, NY). Radioisotopes ^{32}P and ^{35}S (Trans^{35}S-Label) were bought from Dupont-NEN (Guelph, ON, Canada) and ICN (Irvine, CA). Glutaraldehyde, osmium tetroxide and Lowicryl K4M were obtained from MecaLab (Montreal, Quebec). LysoTracker Red DND-99 was purchased from Molecular Probe (Eugene, OR).

2.1.2 Antibodies

Anti-procathepsin B polyclonal antibody was a generous gift from Dr. John Mort, Shriner's Hospital, McGill University. Mannosidase II polyclonal antibody was kindly provided by Dr. Marilyn Farquhar, Yale University. Anti-myc monoclonal antibody was purchased from Invitrogen (Carlsbad, CA). Anti-prosaposin polyclonal antibody was generously provided by Dr. Michael D. Griswold, Washington State University. Another prosaposin antibody was generated by immunization of rabbits with recombinant prosaposin expressed in *E.Coli* and affinity purified with a GST purification kit (Amersham Pharmacia, Piscataway, NJ). Goat anti-mouse IgG1 conjugated to agarose, protein A conjugated to agarose, goat anti-mouse IgG conjugated to fluorescein isothiocyanate (FITC), and goat anti-rabbit IgG conjugated to tetramethylrhodamine isothiocyanate (TRITC), peroxidase-conjugated goat anti-rabbit antibody were bought from Sigma-Aldrich (Irvine, UK). Goat anti-mouse IgG conjugated to 10nm colloidal gold particles and goat anti-rabbit IgG conjugated to 15 nm colloidal gold particles were purchased from Cedarlane

(Hornby, ON, Canada).

2.1.3 Oligonucleotides

Table III shows oligonucleotide primers (1-20) used during the sequencing of the mouse prosaposin genomic DNA. Table IV shows oligonucleotide primers utilized in polymerse chain reactions (PCR) during the engineering of wild type and truncated prosaposins aimed at studying its intracellular trafficking. Table V shows the oligonucleotide primers used during the engineering of chimeric proteins consisting of albumin and a functional domain of prosaposin by PCR. All of the oligonucleotide primers were synthesized in the Sheldon Biotechnology Center, McGill University (Montreal, Quebec).

2.1.4 Animals

Prosaposin (+/-) mice were donated by Dr. Kunihiko Suzuki, from The University of North Carolina School of Medicine. Male and female prosaposin heterozygous mice were mated to generate homozygous mice with the disrupted prosaposin gene. Prosaposin (-/-) and littermate control mice (29-40 days old) were anaesthetized and sacrificed for experiments.

For the preparation of an anti-mouse prosaposin antibody, New Zealand white female rabbits weighing 2.5-3 kg were bought from Harlan Sprague-Dawley Inc.(Indianapolis, IN).

Table III: Primers Utilized for Sequencing the Mouse Prosaposin Gene

1:	5' gcagcctgcggagtgaagcgccg 3'	2:	5' atgctcctgccctctggctcacca 3'
3:	5' agaaaaacagcaccaaggag 3'	4:	5' gttcattaccctagaccca 3'
5:	5' tgatctcaaacaagccacc 3'	6:	5' gctcccagaaacctgatg 3'
7:	5' gtctgttctgaacatggctttcc 3'	8:	5' ttgaaatctcccacccgctc 3'
9:	5' actcgaaacacattcagaagg 3'	10:	5' agccatgtgcctcctcagaaga 3'
11:	5' ctcgggtagtatgtatagctt 3'	12:	5' atactgtgcccaaactgggtg 3'
13:	5' gctgcttatcaggcaacccc 3'	14:	5' gaatgccaggccacaccacc 3'
15:	5' ggaggactcattaatttccagg 3'	16:	5' gactgggaacagcgtccag 3'
17:	5' ggcagacgtcctcgttggc 3'	18:	5' atgccctcttctggtgtgtc 3'
19:	5' gaagagctgatgatgggcagc 3'	20:	5' gcctcacaaccatcagtagtaca 3'

Numerals on right side indicate primer's number used in the text.

Table IV: Oligonucleotides Synthesized for Mutagenic Constructs

Names	Sequences
F:	5' CGCCACCATGTACGCCCTCGCCCTC 3',
R:	5' GGAATTCCACACATGGAGTTTGCAAT 3',
ΔA_f:	5' ACAGCGAAATACTTGGCCGAGCAAAAC 3',
ΔA_r:	5' GGCCAAGTAATTTCGCTGTGGGCTTG 3',
ΔB_f:	5' CAACCTAAGAAGAGAGTGCCAATGAAG 3',
ΔB_r:	5' CACTCTCTTCTTAGGTTGGGGCTGGCT 3',
ΔC_f:	5' CAGGCCCACGAGTTGGTGGAGGCACTT 3',
ΔC_r:	5' CACCAACTCGTGGGCCTGGACCAGAT 3',
ΔD_f:	5' CCTCAGAAGCTGCTGCTGGGAACCGA 3',
ΔD_r:	5' CAGCAGCAGCTTCTGAGGAGGCACATG 3',
ΔN_f:	5' AGCCCTGTCTCCCTTCCTTGCGACATA 3',
ΔN_r:	5'AGGAAGGGAGACAGGGCTGGTCAGAG3',
$\Delta COOH_r$:	5' GGAATTCTTATAGGCAGAAGGGCAA 3'.

Table V: Oligonucleotides used in constructing the chimera protein of albumin and partial prosaposin.

Names	Sequences
Alb-F:	5'cgccaccatgaagtgggtaacctttatttc3',
F-alb:	5'gccttagggctgctgctgggaaccga 3'
Dcooh-F:	5' gccttagggaatggtgggttctgtgag 3'
CDcooh-F:	5'gccttagggaatctggtccaggcccac 3',
R-alb:	5'cagcagcagccctaaggcagcttgactt 3',
Dcooh-R:	5' cccaccattccctaaggcagcttgactt 3'
CDcoohR:	5'gaccagattccctaaggcagcttgactt 3'
R:	5' ggaattccacacatggcgtttgcaat 3'

2.2 METHODS

The techniques described in this section were grouped into four categories: molecular biology, protein biochemistry, electron microscopy, and confocal microscopy.

2.2.1 MOLECULAR BIOLOGY

2.2.1.1 Cloning of Mouse cDNA

Primers M_f and M_r were used for the in vitro synthesis of a mouse prosaposin cDNA using a Unizap XR mouse testicular cDNA library as a template in polymerase chain reaction (PCR). The sequences of the primers were M_f: 5' gcagcctgcggagtgaagcgccg 3' and M_r: 5' atgctcctgccctctggctcacca 3'. PCR was performed in a 50 µl volume containing 5 µl of 10 x PCR buffer (with 1.5 mM $MgCl_2$), 0.3 uM of each primer, 0.2 mM of dNTP, 1 µl of the testicular cDNA library (10^6pfu/µl) and 2.5 units of Taq DNA polymerase. Samples were denatured at 94^0C for 5 min, mixed with Taq DNA polymerase and cycled at 94^0C (1min), 55-65^0C (1 min), 72^0C (2 min), with a final extension at 72^0C for 10 min. Approximately 10 µl of amplified sample were resolved on a 1% agarose gel. A 2.2 kb PCR product was obtained and subcloned into a pGEM-T vector following the manufacturer's protocol. The subcloned cDNA fragment was confirmed by double stranded DNA sequencing. The 2.2 kb DNA was then radiolabeled with ^{32}P by random priming according to Sambrook et al (1984). Briefly, 50 ng of the purified PCR product was denatured by boiling for 5 min then kept cool on ice. dNTP (without dCTP), ^{32}P-dCTP (250uci), 1X buffer and T7 DNA polymerase

were added and incubated at 37^{0}C for 30 min. After passing through a Sephadex G-50 column to remove all unlabeled radioactive molecules, radioactive labeled probe was measured.

2.2.1.2 Screening of a Mouse Testicular cDNA Library

To clone the mouse prosaposin cDNA for in vitro mutagenic analysis, a mouse testicular cDNA library subcloned into the Uni-Zap XR vector (Stratagene) was screened by a radioactive ^{32}P labeled PCR-amplified DNA fragment (as described in 2.2.1.1) and used as a probe. An aliquot containing a million recombinants was screened by transfer of plaques onto nitrocellulose membranes. The membranes were prehybridized overnight in 1% BSA, 7% SDS, 0.5 M Na_2HPO_4 (pH 6.8), 1 mM EDTA (pH 8.0) at 65^{0}C, and hybridized in the same incubation solution containing prosaposin cDNA probe (10^6 cpm/ml) labeled with ^{32}P-dCTP at 65^{0}C for 18 h. High stringency washes were performed in 0.5% BSA, 5% SDS, 40 mM Na_2HPO_4 (pH 6.8), 1 mM EDTA (pH 8.0) at 65^{0}C for 30 min. Five positive clones were obtained and verified by PCR with primers 3 and 4 (Table II). Purified positive phages were grown and the cDNA inserts were excised from the phage according to the manufacturer's instructions. A positive clone containing a full-length prosaposin cDNA (2.2 kb) was confirmed by digestion with restriction enzymes (EcoRI/XhoI) and sequencing.

2.2.1.3 Cloning of Rat Testicular cDNA

Two synthetic oligoneucleotide primers were prepared according to the

published cDNA sequences of rat SGP-1 (prosaposin) to generate the cDNA using a rat testicular cDNA library (Lambda dash II) as a template by PCR (as described in 2.2.1.1). The primer sequences of the rat were R_f: 5' attgcatgcggagtgaagcg 3' and R_r: 5' gttcattaccctagaccca 3'. The amplified cDNA fragments were subcloned into the pGEM-T vector and their fidelity was confirmed by sequencing.

2.2.1.4 Screening a Mouse Genomic Library by a PCR-based Method

In order to increase the chances of obtaining positive clones and reducing the strenuous work of sreening a library, a PCR-based method was applied. Forty-two aliquots of the original library (10^6 pfu/μl) containing 2.4 x10^4 plaques forming units (pfus) were amplified by PCR with a pair of oligonucleotide primers 3 and 4 (Table II). The PCR reaction was performed as described above. A positive 1.7 kb DNA fragment was found in 3 out of 42 aliquots. This fragment was subcloned, sequenced, and confirmed to correspond to the prosaposin gene. Then two sets of replica filters were made from the three positive aliquots using Amersham hybond nylon membranes. The filters were rehybridized overnight at 65^0C in 1% BSA, 7% SDS, 0.5 M Na_2HPO_4 (pH 6.8), 1 mM EDTA (pH 8.0), and hybridized at 65^0C for 18 h in the same incubation solution containing the prosaposin cDNA probe (10^6 cpm/ml) labeled with ^{32}P-dCTP. High stringency washes were performed in 0.5% BSA, 5% SDS, 40 mM Na_2HPO_4 (pH 6.8), 1 mM EDTA (pH 8.0), three times for 30 min each. Positive clones were further verified to correspond to the prosaposin gene by repeating the PCR with primers 3 and 4

as described above. After three rounds of plaque purification, the genomic DNA was isolated by the clear lysate method (Sambrook et al., 1989) from the two longest positive clones. Limited restriction mapping with the Sac I restriction enzyme and Southern blot analysis with the prosaposin cDNA probe showed several positive restriction fragments corresponding to the exons of the prosaposin gene that were subcloned into the Sac I site of the plasmid vector pGEM-3Z (+) and sequenced.

2.2.1.5 DNA Sequencing Analysis

The PCR amplified DNA segments and DNA fragments excised from the mouse genomic library were subloned into appropriate vectors for sequencing. Sequencing was done by the dideoxy chain termination method [201] on both strands. The T7 polymerase sequencing kit from Pharmacia was used with appropriate sequencing primers. Sequencing was done at Sheldon Biotechnology Center, McGill University and at the Bio S. & T. Inc. (Montreal, Quebec) using automatic sequencers (ABI).

2.2.1.6 Reverse-Transcripion (RT)-PCR

To determine whether or not exon 8 was spliced out in various tissues, two oligonucleotide primers matching the flanking coding region of this exon were designed. The two primers have the following sequences: sense primer: 5' ggaccacgtgaaggaggat 3' and antisense primer: 5' acagaagccagccagccagcacaca 3'. Total RNA (5 μg) from brain, heart, lung, spleen, pancreas, kidney, muscle

and testis were isolated according to the method of Chomczynski [202]. Total RNAs were denatured at 70^{0}C for 10 min, cooled to room tempreature, and incubated with reverse transcriptase in the presence of 40 pmol of sense primer, 20 μl of Rnasin, 0.5 mM dNTPs, 1 mM DTT, 20 mM Tris buffer pH 8.4, 50 mM KCL, 2.5 mM MgCL2, and 0.1 mg/ml of nuclease-free bovine serum albumin in a total volume of 20 ul. The reaction was started at 23^{0}C for 10 min and the cDNA was synthesized at 42^{0}C for 45 min. The heteroduplex was then denatured at 95^{0}C for 10 min and the PCR amplification was started by adding 1.5 units of Taq DNA polymerase, 40 pmol of antisence primer, and PCR buffer in a total volume of 100 ul. After denaturation at 95^{0}C for 5 min, the reaction was cycled 30 times at 95^{0}C for 40 sec, at 55^{0}C for 30 sec, and 72^{0}C for 45 sec. The cycles were terminated by a polymerization step at 72^{0}C for 15 min. DNA fragments of 106 bp and 115 bp corresponding to the predicted different products of the alternatively spliced exon 8 were separated by non-denatured polyacrylmide gel (12 % w.v) electrophoresis in 90 mM Tris buffer (pH 8.0), 90 mM borate, 2 mM EDTA. The DNA was stained with ethidium bromide.

2.2.1.7 Southern Blot Analysis

To analyze the length of the DNA inserts within the phage plasmid and to determine the presence of exons in the restriction enzyme excised fragments, southern blot analysis were utilized. In every case, 5 μg of phage DNA purified from the positive phages were digested with the restriction enzyme Sac I at 37^{0}C overnight, and the resulting fragments were electrophoresed on a 0.8% agarose

gel. The gel was transferred onto a hybond nylon membrane, prehybridized and hybridized with a ^{32}P labeled prosaposin cDNA as a probe at high stringency incubation condition as described above. The radioautographic film was exposed for 1-2 days at -80^{0}C and developed.

2.2.1.8 Mice Genotyping

Pieces of mice tails (0.5 cm long) were cut and the total genomic DNA extracted using a salt precipitation method. Briefly, tail of mouse was cut into small pieces and incubated in lysis buffer (1% SDS, 0.1M NaCl, 0.1 M EDTA pH 8.0, 0.5 M Tris pH8.0) with proteinase K (10 mg/ml) overnight at 37^{0}C. 1/3 of the volume of saturated NaCl was added to the incubation buffer, samples were centrifuged for 10 min at 13,000xg after vortexing. Supernatants containing DNA were precipitated with 2 volumes of absolute ethanol. DNA precipitates were dissolved in ddH_2O.

Two sets of primers were designed to flank the exon 3 region of the prosaposin gene, where the neomycin-resistant gene was inserted to disrupt the expression of prosaposin. Primers PNF: 5' cgcattgcatcagccatgatgg 3' and PNR: 5' ggagaggctattcggctatgac 3' amplified a 300 bp long DNA fragment in hetero- and homozygous genotypes. While primer PSF: 5' ccagcagatggtctggagcaag 3' and PSR: 5' ttcagcaagttcccagcttcgg 3' amplified a 900 bp fragment in the case of the wild genotype and a 2.2 kb fragment in the case of hetero- and homozygous genotypes.

PCR was performed in a volume of 25 μl, containing 2μl of tail genomic

DNA (200 ng), 0.2 mM of dNTP, 0.2 uM of each primer, 1x PCR buffer (with 1.5 mM of $MgCl_2$), 0.5 unit of DNA taq polymerase (Qiagene) cycled at: denaturing at 94^0C for 1 min, annealing at 60^0C for 1 min and extending for 1 min at 72^0C, with a final extension of 10 min. PCR products were resolved in a 1.5 % agarose gel and stained with ethidium bromide.

2.2.1.9 Recombinant cDNA Constructs

A full-length prosaposin cDNA was obtained by screening a mouse testicular cDNA library as described in 2.2.1.2. The full-length 2.6 kb prosaposin cDNA in the plasmid was used as a template for the different constructs made during this study. The fidelity of individual constructs was confirmed by restriction mapping and DNA sequencing (Sheldon Biotechnology Center, McGill University).

2.2.1.9.1 Wild Type Prosaposin

Pro-WT, is the wild type prosaposin cDNA subcloned into a mammalian expression vector pcDNA3.1B. A pair of primers F: 5' cgccaccatgtacgccctcgccctc 3', R: 5' ggaattccacacatggcgtttgcaat 3', was used to amplify a 1.6 kb fragment consisting of the whole open reading frame of prosaposin by PCR with vent DNA polymerase. A Kozak sequence CGCCACC was added to primer Fc at the 5' end. An EcoRI restriction site (GAATTC) was added to the 5' end of primer R for suitable subcloning. The pcDNA3.1B vector was digested with BamHI and filled in with a Klenow fragment to create a blunt end. The vector was digested with

EcoRI, purified and the DNA concentration was estimated. PCR fragments were digested with EcoRI restriction enzyme, purified and subcloned into the prepared pcDNA3.1B vector. The resulting plasmid was designated Pro-WT.

2.2.1.9.2 Truncation of the N- and C-termini of Prosaposin

ΔN-term and ΔC-term, are prosaposin constructs lacking part of the N-terminus (residues17-59) and C-terminus (residues 520-556). For the ΔN-term truncated construct, part of its N-terminal region in front of saposin A was eliminated. An upstream primer N_f: 5' agccctgtctcccttccttgcgacata 3' and downstream primer N_r: 5' aggaagggagacagggctggtcagag 3' were designed according to the sequence of prosaposin cDNA. Two pairs of primers, F/N_r and N_f/R, were used in the first run of PCR. F/R primers were utilized in the second run of PCR using amplified F/N_r fragment and N_f/R fragment as templates. PCR fragment (1.6 kb) was digested by EcoRI restriction enzyme and purified before subcloning into the prepared pcDNA3.1B vector. The resulting plasmid construct was called ΔN-term.

For the ΔC-term truncated construct, the same upstream F primer and a new downstream primer $COOH_r$: 5' ggaattcttataggcagaaggggcaa 3' were used to eliminate a sequence of 36 amino acid residues ($_{520}$-LLLGTEKCVWGPSYWCQNMETAARCNAVDHCKRHVWN-$_{556}$) in the C-terminus and subcloned into the pcDNA3.1B vector.

2.2.1.9.3 Truncation of the Saposin A, B, C and D Domains

ΔA (residues 57-147), ΔB (residues 189-278), ΔC (residues 309-396), and ΔD (residues 434-522) mutant plasmids, were prosaposin constructs lacking individual saposin functional domains. Three pairs of primers were used for each construct. The external primers F/R were the same as for the Pro-WT construct. The two internal primers were A_f: 5' acagcgaaatacttggccgagcaaaac 3' and A_r: 5'ggccaagtatttcgctgtgggcttg 3' for ΔA; primers B_f: 5' caacctaagccgagagtgccaatgaag 3'and B_r: 5'cactctcttcttaggttggggctggct 3' for ΔB; primers C_f: 5' caggcccacgagttggtggaggcactt 3' and C_r: 5'caccaactcgtgggcctggaccagat 3' for ΔC and primers D_f: 5' cctcagaagctgctgctgggaaccga 3' and D_r: 5' cagcagcagcttctgaggaggcacatg 3' for ΔD. All these primers were backwards to each other. The primers F/A_r and A_f/R, F/B_r and B_f/R, F/C_r and C_f/R, and F/D_r and D_f/R were used in the first run of PCR for ΔA, ΔB, ΔC, and ΔD constructs, respectively. Primers F/R were used in the second run of PCR using the amplified F/A_r and A_f/R fragments, F/B_r and B_f/R fragments, F/C_r and C_f/R fragments, and F/D_r and D_f/R fragments as templates for each construct. The final PCR products were purified and digested with EcoRI and then subcloned into the prepared pcDNA3.1 B vector.

2.2.1.9.4 Chimeric Constructs of Albumin with Partial Prosaposin Domains

Alb/Pro-c-term, Alb/(Pro-D+Pro-c-term), Alb/(Pro-C,D+Pro-c-term), were fusion protein constructs containing the full length albumin and partial prosaposin sequences, i.e. the C-terminus of prosaposin (Alb/Pro-c-term), domain D plus the

C-terminus of prosaposin (Alb/Pro-D+Pro-c-term), and domains C and D plus the C-terminus of prosaposin (Alb/Pro-C,D+Pro-c-term). Alb-WT was wild type albumin. Three pairs of primers were used in each of the chimeric constructs except in the wild type albumin which had one pair of primers (Alb-F/Alb-R) prepared according to the nucleotide sequence of albumin. Primers Alb-F: 5'cgccaccatgaagtgggtaacctttatttc3', R-alb: 5' cagcagcagccctaaggcagcttgactt 3', F-alb: 5' gccttagggctgctgctgggaaccga 3' and R were used for Alb/Pro-c-term; Primers Alb-F, Dcooh-R: 5' cccaccattccctaaggcagcttgactt 3', Dcooh-F: 5' gccttagggaatggtgggttctgtgag 3' and R were used for chimera Alb/(Pro-D+Pro-c-term). Primers Alb-F, CDcooh-F: 5'gccttagggaatctggtccaggcccac 3', CDcooh-R: 5' gaccagattccctaaggcagcttgactt 3' and Rc were used for the chimeric construct Alb/(Pro-C,D+Pro-c-term). Primers Alb-F/R-alb and F-alb/R were used for chimeric construct Alb/(Pro-c-term); primers Alb-F/Dcooh-R and Dcooh-F/Rc were for chimeric construct Alb/(Pro-D+Pro-c-term), and primers Alb-F/CDcooh-R and CDcoohF/R were for chimeric construct Alb/(Pro-C,D+Pro-c-term) in the first PCR run, the amplified two fragments of each construct were mixed and used as templates in the second run of PCR with the same pair of primer Alb-F/Rc. Alb-F and Alb-R: 5' ggaattccctaaggcagcttgactt 3' were the primers used for amplification of the wild type albumin (1.8 kb). Final PCR products were purified and digested with EcoRI restriction enzyme and subcloned into the same pcDNA3.1B vector.

2.2.1.10 Cell Culture and Transfections

Cos-7 cells were maintained in Dulbecco's modified eagle's medium (D-

MEM) supplemented with 10% fetal bovine serum, 100 units/ml penicillin and 100 ug/ml streptomycin in an atmosphere of 5% CO_2 at 37^{0}C. Cells (60% confluence) grown on cover slips (12 mm in diameter) within 6 well dishes were transfected with LipofectAMINE according to the manufacture's instruction. Cells grown in 100 mm petri dish were transfected according to DEAE-dextran method [203]. Briefly, COS-7 cells ($5x10^{5)}$ were seeded into DMEM containing 10% Nu-serum overnight. 5 μg of plasmid DNAs were mixed with 40 μl of 5% DEAE-dextran, 5 μl of 0.1M chloroquine phosphate in 5 ml of DMEM with 10% Nu-Serum for 4 hours. Cells were then shocked with 10% DMSO in PBS for 1 min, rinsed with PBS and fresh DMEM containing 10% FBS was added for at least 48 hours.

2.2.2 PROTEIN BIOCHEMISTRY

2.2.2.1 Western Blotting

After 48 h of transfection with different plasmid constructs, cells were rinsed twice with cold PBS, lysed with 1x sample buffer (125 mM Tris pH6.8, 2% SDS, 5% glycerol, 1% β-mecaptoethanol), boiled for 5 min. Approximately 50 μg of total protein was loaded and resolved in 10% SDS-PAGE gel and transferred to 0.45 μm nitrocellulose membranes. Membranes were blocked in 5% non-fat dry milk in TTBS (10 mM Tris pH 7.5, 150mM NaCl, 0.05% Tween 20) and probed with anti-myc antibody (1:1000). The blots were washed three times in TTBS buffer before incubation with a goat anti-mouse IgG (1:2000) conjugated with horseradish peroxidase antibody. After washing three times in TTBS, the membranes were developed by enhanced chemiluminescence reagent (ECL) and

exposed to X-ray films for 1-60 min.

2.2.2.2 Metabolic Labelling and Immunoprecipitation

Cells were washed twice with cold PBS after 48 hours of transfection with different plasmid constructs, starved for one hour in starvation medium (DMEM lacking of methionine and cysteine but containing 5% of dialysed fetal bovine serum and 200 mM glutamine). Cells were then pulsed in starvation medium supplemented with Trans^{35}S-label (300 uCi/ml) for the times indicated. For experiments including chase periods, the radiolabelled medium was removed and the cells were washed twice with PBS and incubated with cell growth medium supplemented with unlabelled methionine (1.5 mg/ml) and cysteine (2.4 mg/ml) for the chase time indicated. When specified, cells were incubated with brefeldin A (20 ug/ml) for 1 hour prior to the addition of medium containing the radiolabelled and fresh brefeldin A.

Monolayers of cells and media were collected. Cells were lysed with 1x lysis buffer (1% Triton X-100, 150 mM NaCl, 10 mM. Tris pH 7.4, 1 mM EDTA, 1 mM EGTA pH 8.0, 0.2 mM sodium ortho-vanadate, 2 mM PMSF, 0.5% NP-40, 10 ug/ml pepstatin A, 10 ug/ml Aprotinin, 10 mg/ml leupeptin). After incubating with primary anti-myc antibody or antibody against prosaposin bound to anti-mouse IgG-agarose or protein A agarose, the immunoprecipitates were washed three times with 1x lysis buffer. Samples were then resolved by SDS-PAGE and radioactive signals were visualized by fluorography. A 15% tricine-SDS-PAGE [204] was performed to resolve smaller molecular weight proteins.

2.2.2.3 EndoH Treatment

To digest the immunoprecipitates with endoglycosidase H, they were released from the agarose and antibodies first, by boiling in 50 μl of 1 % SDS and 200 mM dithiothreitol for 5 min. An equal volume of 100 mM citric acid buffer (pH 5.5) and 1U of endoglycosidase H was added to the immunoprecipitates and incubated at 37^0C for 16 h. The processed samples were resolved by 10% SDS-PAGE and detected by fluorography.

2.2.2.4 Antibody Production

A pair of primer was prepared (Forward primer: 5' acagcgaaatcccttccttg 3'; Reverse primer: 5' gacctcattacagaagcc 3') to synthesize part of the domain of prosaposin (containing the domains encoding saposin A and B, residue 57-275) by PCR. A 1.2 kb fragment was amplified and subconed into *E.coli* expression vectors pMAL (producing maltose binding fusion protein) and pGEX (making glutathione S-transferase (GST) fusion protein) for the purpose of antigen preparation and antibody purification respectively. Inserts within the plasmids were confirmed to be the prosaposin sequence by using the dideoxy chain termination method with T7 Polymerase (Pharmacia). Expressed prosaposin fused with the maltose binding protein was purified by maltose affinity chromatography with amylose resin column according to the manufacturer's instruction. Purified prosaposin fusion protein was then concentrated by Microcon-30 (Amicon, Beverly, MA) to produce the final antigen with a concentration of 1mg/ml. Antibody was prepared by immunizing rabbits with 0.5

ml of Freund's adjuvant (Sigma) mixed with the expressed fusion prosaposin (1mg/ml) according to conventional methods. Briefly, after 3-4 times immunization, 100-120 ml of blood was collected through the hearts of the rabbits. Crude anti-serum was immunoaffinity chromatography purified by passing over Affi-Gel 15 column (Pharmacia) coupled with GST fusion of the same amino acid residues of prosaposin following the manufacturer's instruction. The affinity-purified antibody was immunoblotted to test for its immunoreactivity and purity.

2.2.2.5 Secondary Structure Predictions

The secondary structure predictions of rodent and human prosaposins and predicted mature saposins were generated on the PredictProtein server at EMBL-Heidelberg according to the Profile network prediction HeiDelberg (PHD) methods of Rost and Sander [205], which employ a subroutine (MaxHom) to align homologue identified in the Swissprot database [206]. Maxhom identified guinea pig (SwissProt entry P20097) and bovine (P26779) saposin C as homologues of mouse saposins A, C, D and SGP-1; mouse (P50405) and rat (P22355) surfactant-associated proteins (SP-B) were identified for mouse saposin A; a canine (P17129) pulmonary surfactant protein was identified for mouse saposin C.

2.2.2.6 Hydropathy Profile

The deduced structures of mouse prosaposin and human prosaposin with and without (rat) a QDQ insertion in domain B or with (rat and mouse) and without (human) a proline-rich segment located between domain C and D were

analysed by the method of Kyte and Doolittle [207]. A unique histidine in the human sequence was included and analyzed in the human prosaposin.

2.2.2.7 Measurement of Serum Testosterone

Blood samples were collected from anaesthetized prosaposin homozygous (-/-) mice and prosaposin heterozygous (+/-) mice (as controls). Serum testosterone was measured in triplicates by radioimmunoassay at the Endocrinology Unit, Royal Victoria Hospital (Montreal, Quebec).

2.2.3 LIGHT AND ELECTRON MICROSCOPY

2.2.3.1 Light Microscopy

2.2.3.1.1 Perfusion, Tissue Preparation and Morphological Examination

Prosaposin homozygous (-/-) and prosaposin heterozygous (+/-) control mice from the same litters were anesthetized with sodium pentobarbital administered intraperitoneally. Tissues including testes, prostate glands, seminal vesicles, and epididymis were fixed with Bouin's fixative by perfusion through the left ventricle of the heart for 15 min. Subsequently, the organs were removed and sectioned in smaller blocks. The tissue was immersed in Bouin's fixative 2-3 days at 4^{0}C, after which it was dehydrated sequentially in 30%, 50% and 70% enthanol for several hours, and then embedded in paraffin. The paraffin sections of the tissues (5 um thick) were stained with hematoxylin and eosin and examined under light microscope.

2.2.3.1.2 Immunoperoxidase Staining

Paraffin sections were deparaffinized in xylene and hydrated in a series of graded ethanol solutions. During hydration, residual picric acid was neutralized in 70% ethanol containing 1% lithium carbonate, and endogenous peroxidase activity was abolished in 70% ethanol containing 1% (vol/vol) hydrogen peroxide. Once dehydrated, the tissue sections were washed in distilled H_2O containing 300 mM glycine to block free aldehyde groups.

Prior to immunostaining, sections were blocked for 15 min with 10 % goat serum in TBS (20 mM Tris-HCl-buffered saline pH 7.4). This and subsequent treatments were accomplished by placing 50 µl of a solution on a coverslip and overturning the tissue face of the slide onto the drop, thus ensuring that the entire tissue was treated with minimal fluid. Coverslips were removed by dipping the slides in TBS containing 0.1% tween-20 (TWBS). Sections were then incubated in a 37^0C humidified incubation chamber for 1.5 hr with primary antibody. Following four consecutive 5 min washes in TWBS, sections were once again blocked with 10% goat serum in TBS. They were incubated for 30 min with goat anti-rabbit IgG conjugated to peroxidase diluted 1:250 in TBS. This was followed by four 5 min washes in TWBS.

The final reaction product was achieved by incubating the sections for 10-12 min in 500 ml of TBS containing 0.03% H_2O_2, 0.1M imidazole and 0.05% diaminobensidine tetrahydrochloride (pH7.4). Slides were then washed in distilled H_2O and counterstained with 0.1% methylene blue for 10 min. The tissue was dehydrated by passing slides through a graded ethanol series, after which the

sections were cleared and mounted with permount medium. Normal rabbit serum at a dilution of 1:20 served as a control.

2.2.3.2 Electron Microscopy

Prosaposin homozygous (-/-) and prosaposin heterozygous (+/-) control mice from the same litters were anesthetized with sodium phenobarbital and fixed by intracardiac perfusion with 2.5% glutaraldehyde in 0.1 M phosphate buffer at pH 7.4 at the age of the late onset of the symptomatic phenotype [10]. Fixed tissues including testes, prostate glands, seminal vesicles, and epididymis were excised and cut into 1 mm^3 pieces. After washing in 0.1 M cacodylate washing buffer, samples were postfixed in ferrocyanide reduced osmium, washed in 0.1M cacodylate buffer, dehydrated sequentially in 30%, 50% and 70% enthanol and propylene oxide and then embedded in epon. The epon blocks were trimmed and ultrathin sections of tissues were mounted on copper grids and examined with a Philips 400 electron microscope.

2.2.3.2.1 Immunocytochemical Gold Labelling

After 48 h of transfection with different plasmid constructs, culture cells were detached from the culture dishes with 0.1% trypsin in HBSS (Hank's Balanced Salt Solution). The cells were pelleted and fixed with 4% paraformaldehyde and 0.5% glutaraldehyde in 0.05M phosphate buffer (pH 6.8). The cell pellets were washed several times in phosphate buffered saline (PBS) and dehydrated in cold methanol and embedded in Lowicryl K11M as described

previously by Sylvester et al. [153] and Hermo et al. [208].

Ultrathin Lowicryl sections were mounted on 300-mesh Formvar-coated nickel grids (Polyscience Inc., Warrington, PA). Each grid containing 5-6 section was floated for 15 min on a drop of 20 mM Tris-HCl-buffered saline (TBS) containing 15% (v/v) goat serum and then incubated for 30 min on a drop of anti-myc monoclonal primary antibody diluted in 1:100 in TBS. The grids were then washed in TBS containing 0.05% Tween-20. After blocking again with 15% goat serum, grids were incubated with goat anti-mouse IgG conjugated to colloidal gold (10 nm). For double staining with a lysosomal marker, grids were blocked and incubated with procathepsin B (1:50) following the same procedure as mentioned above. A goat anti-rabbit secondary antibody conjugated with colloidal gold (15 nm) was used. Grids were counterstained with uranyl acetate in 30% ethanol (2 min) followed by lead citrate (0.5 min). Normal rabbit serum served as control. Electron micrographs were taken on a Philips 400 electron microscope (Philips Electronics, Toronto, ON).

2.2.4 CONFOCAL MICROSCOPY

2.2.4.1 Immunofluorescent Labelling and Image Processing

For immunofluorescent staining, culture cells transfected with the wild type and mutated constructs on coverslips were fixed with 3.8% paraformaldehyde in 0.1 M phosphate buffer (pH 7.2) at room temperature and washed with PBS. Cells were permeabilized with 0.5% Triton X-100 in PBS for 30 min at room temperature, then blocked with 10% goat serum in PBS for 1 hour. After washing

with PBS, the cells were incubated with monoclonal antibody against myc (1:100) and polyclonal antibody against mannosidase II (1:500) at 4^0C overnight. Following three washes in 0.05% Tween-20 in PBS, the cells were incubated with a 1:100 dilution of FITC conjugated goat anti-mouse and TRITC conjugated goat anti-rabbit secondary antibodies. After three washes in 0.05% Tween-20 in PBS, the cells were rinsed with ddH2O. Subsequently, the coverslips were mounted on slides using Mowiol (CalBiochem). For colocalization of lysosomes with myc antibody, an acidic sensitive dye (fluorescence emission at 577 nm), called LysoTracker, was used to stain all acidic compartments including endosomes and lysosomes on live COS-7 cells. To perform this, 50 nM of Lysotracker was added to culture medium for 30 min at 37^0C, followed by incubation of the cells grown on coverslips in normal medium without LysoTracker for 15 min. Cells were then immunostained with myc antibody as mentioned above. Cells were observed using a Zeiss Axiovert microscope with a 63x objective and the appropriate filter set. Fluorescent images of stained cells were then resized using Adobe Photoshop.

CHAPTER THREE

Results

Figure 3-1: Electrophoresis of the murine prosaposin cDNA fragments by PCR. (A): Lane 1 shows a 1 kb DNA ladder, lane 2 shows a 2.2 kb long DNA fragment amplified by PCR using a mouse testicular cDNA library as a template. (B) Lane 1 shows a 1 kb DNA ladder, lane 2 shows a 1.7 kb long DNA fragment amplified by PCR using a rat testicular cDNA library as a template. 10 ul of the PCR reaction was electrophoresed on 1% agarose gel, and stained with ethidium bromide.

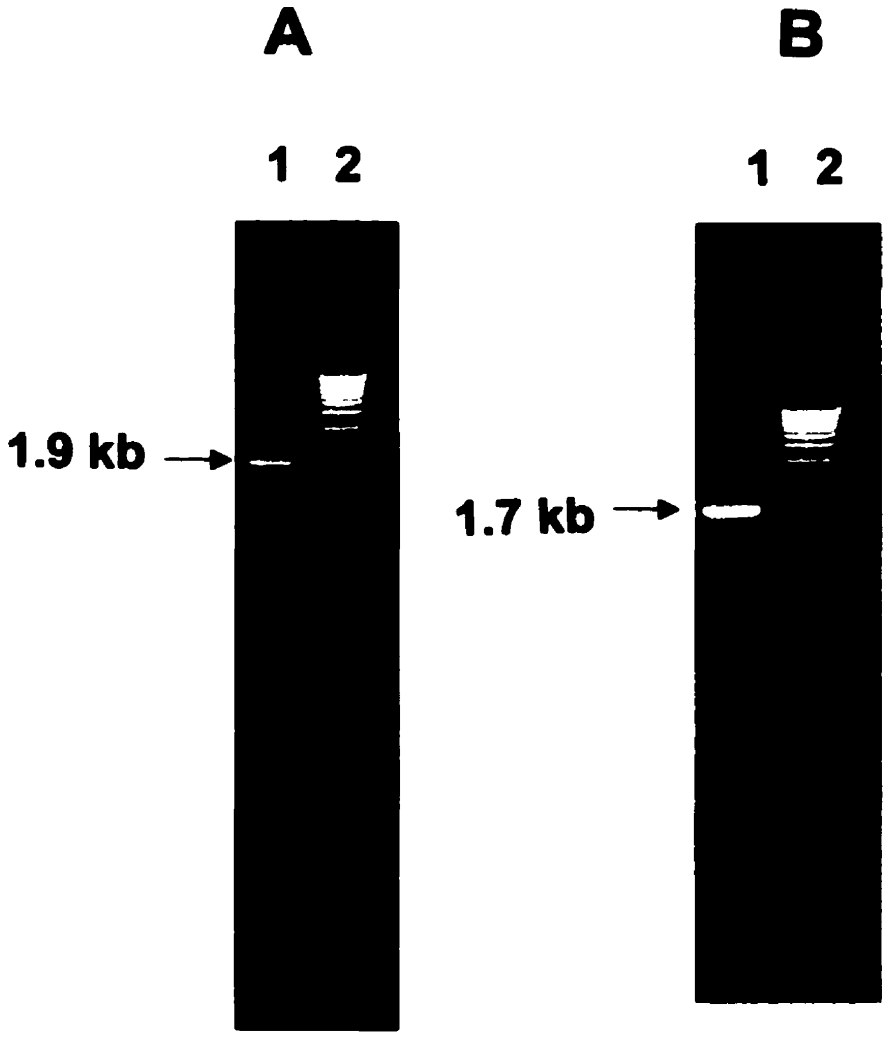
A
B
1 2
1 2
1.9 kb
1.7 kb

According to the proposed objectives, the results are grouped in three sections. The first part focuses on the structural and functional analysis of the prosaposin gene and its translation products. It also deals with the cloning of the mouse and rat prosaposin cDNAs, the analysis of their deduced amino acid backbone structure and their sequence comparison with other species. Special emphasis is given to differential expression of transcribed prosaposin mRNA in different tissues due to alternative splicing. The second part of this chapter focuses on the study of the mechanism of transport of prosaposin to the lysosomes. The last section deals with effect of the inactivation of the prosaposin gene on the development of male reproductive organs by using a prosaposin homozygous mice model.

3.1 Structural Analysis of the Mouse Prosaposin (SGP-1) Gene and Its Translation Product

3.1.1 Cloning of Murine Prosaposin cDNAs

Two sets of synthetic oligonucleotide primers were prepared to generate mouse and rat cDNAs from testicular sources by applying PCR. An amplified 2.2 kb and a 1.7 kb cDNA fragment representing the cDNAs of mouse and rat prosaposin were subcloned into the pGEM-T vector and confirmed by sequencing. The 2.2 kb (Figure 3-1A) mouse cDNA fragment contained the 5' and 3' untranslated region, while the 1.7 kb (Figure 3-1B) rat cDNA fragment only contained the open reading frame encoding the rat prosaposin. The nucleotide sequences, the restriction maps generated by Dnasis program, and the predicted

amino acid sequences are presented in Figures 3-2, 3-3, 3-4A and 3-4B. The obtained mouse amino acid sequence demonstrates that it contains 557 amino acids, while the rat sequence contains 554 amino acid residues, with 3 amino acids (QDQ, glutamine-aspartate-glutamine) less in the region encoding saposin B, underlying the presence of different isoforms of prosaposin in testis and possibly in other tissues as well by alternative splicing.

3.1.2 PCR-based Method to Clone the Mouse Prosaposin Gene

A mouse genomic DNA library was sreened using a PCR-based method in conjunction with a ^{32}P-labeled mouse cDNA probe. Two positive clones (Figure 3-5) of approximately 19 kb were identified and isolated (Figure 3-6). Both clones were digested with restriction enzyme Sac I (Figure 3-7). To determine if the Sac I digested fragment contained prosaposin sequences, they were examined by Southern blot analysis with the same cDNA probe (Figure 3-8). The precise location of individual exons and introns and their boundaries were determined by sequencing the DNA fragments digested with Sac I restriction enzyme, which were previously subcloned into the pGEM-3Z(+) vector. Figure 3-9 shows the deduced genomic organization of the mouse prosaposin gene (NCBI Genbank accession number; U57999).

Sequence analysis revealed that the mouse prosaposin gene consists of 15 exons ranging from nine base pairs to 298 base pairs and 14 introns, which ranged from 89 base pairs to over 8 kb in length (Table VI). The largest intron (> 8 kb) was located upstream of exon 2 and was therefore regarded as intron 1.

Figure 3-2: Nucleotide and amino acid sequence of the mouse prosaposin cDNA. The open reading frame is indicated by "*" above the amino acid residues of initiation (ATG) and termination code (TAG) of translation. Nucleotide numbering is placed on the left margins.

Mouse prosaposin

```
  1  CAG CCT GCG GAG TGA AGC GCC GCC ATG TAC GCC CTC GCC CTC
       Q   P   A   E   -   S   A   A   M   Y   A   L   A   L

 43  TTC GCC AGC CTT CTG GCC ACC GCT CTG ACC AGC CCT GTC CAA
       F   A   S   L   L   A   T   A   L   T   S   P   V   Q

 85  GAC CCG AAG ACA TGC TCT GGG GGC TCA GCA GTG CTG TGC AGA
       D   P   K   T   C   S   G   G   S   A   V   L   C   R

127  GAT GTG AAG ACG GCG GTG GAC TGT GGG GCC GTG AAG CAC TGC
       D   V   K   T   A   V   D   C   G   A   V   K   H   C

169  CAG CAG ATG GTC TGG AGC AAG CCC ACA GCG AAA TCC CTT CCT
       Q   Q   M   V   W   S   K   P   T   A   K   S   L   P

211  TGC GAC ATA TGC AAA ACT GTT GTC ACC GAA GCT GGG AAC TTG
       C   D   I   C   K   T   V   V   T   E   A   G   N   L

253  CTG AAA GAT AAT GCT ACG CAG GAG GAG ATC CTT CAT TAC CTG
       L   K   D   N   A   T   Q   E   E   I   L   H   Y   L

295  GAG AAG ACC TGT GAG TGG ATT CAT GAC TCC AGC CTG TCG GCC
       E   K   T   C   E   W   I   H   D   S   S   L   S   A

337  TCG TGC AAG GAG GTG GTT GAC TCT TAC CTG CCT GTC ATC CTG
       S   C   K   E   V   V   D   S   Y   L   P   V   I   L

379  GAC ATG ATT AAG GGC GAG ATG AGC AAC CCT GGG GAA GTG TGC
       D   M   I   K   G   E   M   S   N   P   G   E   V   C

421  TCT GCG CTC AAC CTC TGC CAG TCC CTT CAG GAG TAC TTG GCC
       S   A   L   N   L   C   Q   S   L   Q   E   Y   L   A

463  GAG CAA AAC CAG AAA CAG CTT GAG TCC AAC AAG ATC CCG GAG
       E   Q   N   Q   K   Q   L   E   S   N   K   I   P   E

505  GTG GAC ATG GCC CGT GTG GTT GCC CCC TTC ATG TCC AAC ATC
       V   D   M   A   R   V   V   A   P   F   M   S   N   I

547  CCT CTC CTG CTG TAC CCT CAG GAT CAC CCC CGC AGC CAG CCC
       P   L   L   L   Y   P   Q   D   H   P   R   S   Q   P

589  CAA CCT AAG GCT AAC GAG GAC GTC TGC CAG GAC TGT ATG AAG
       Q   P   K   A   N   E   D   V   C   Q   D   C   M   K

631  CTG GTG TCT GAT GTC CAG ACT GCT GTG AAG ACC AAC TCC AGC
       L   V   S   D   V   Q   T   A   V   K   T   N   S   S

673  TTT ATC CAG GGC TTC GTG GAC CAC GTG AAG GAG GAT TGT GAC
       F   I   Q   G   F   V   D   H   V   K   E   D   C   D

715  CGC TTG GGG CCA GGC GTG TCT GAC ATA TGC AAG AAC TAC GTG
       R   L   G   P   G   V   S   D   I   C   K   N   Y   V
```

```
757  GAC CAG TAT TCC GAG GTC TGT GTC CAG ATG TTG ATG CAC ATG
       D   Q   Y   S   E   V   C   V   Q   M   L   M   H   M

799  CAG GAT CAG CAA CCC AAG GAA ATC TGT GTG CTG GCT GGC TTC
       Q   D   Q   Q   P   K   E   I   C   V   L   A   G   F

841  TGT AAT GAG GTC AAG AGA GTG CCA ATG AAG ACT CTG GTC CCT
       C   N   E   V   K   R   V   P   M   K   T   L   V   P

883  GCC ACC GAG ACC ATT AAG AAC ATC CTC CCT GCC CTG GAG ATG
       A   T   E   T   I   K   N   I   L   P   A   L   E   M

925  ATG GAC CCC TAT GAG CAG AAT CTG GTC CAG GCC CAC AAT GTG
       M   D   P   Y   E   Q   N   L   V   Q   A   H   N   V

967  ATT TTA TGC CAG ACC TGT CAG TTT GTG ATG AAT AAG TTT TCT
       I   L   C   Q   T   C   Q   F   V   M   N   K   F   S

1009 GAG CTG ATT GTC AAT AAT GCC ACT GAG GAG CTC CTA GTT AAA
       E   L   I   V   N   N   A   T   E   E   L   L   V   K

1051 GGT TTG AGC AAC GCA TGC GCA CTG CTC CCC GAT CCT GCC AGA
       G   L   S   N   A   C   A   L   L   P   D   P   A   R

1093 ACC AAG TGC CAG GAG GTG GTG GGA ACA TTT GGC CCC TCC CTG
       T   K   C   Q   E   V   V   G   T   F   G   P   S   L

1135 TTG GAC ATC TTT ATC CAT GAG GTA AAC CCC AGC TCT CTG TGC
       L   D   I   F   I   H   E   V   N   P   S   S   L   C

1177 GGT GTG ATC GGC CTC TGT GCT GCC CGC CCG GAG TTG GTG GAG
       G   V   I   G   L   C   A   A   R   P   E   L   V   E

1219 GCA CTT GAG CAG CCT GCG CCA GCC ATT GTA TCT GCA CTG CTC
       A   L   E   Q   P   A   P   A   I   V   S   A   L   L

1261 AAA GAG CCC ACA CCG CCA AAG CAG CCC GCA CAG CCC AAG CAG
       K   E   P   T   P   P   K   Q   P   A   Q   P   K   Q

1303 TCG GCA TTG CCC GCC CAT GTG CCT CCT CAG AAG AAT GGT GGG
       S   A   L   P   A   H   V   P   P   Q   K   N   G   G

1345 TTC TGT GAG GTG TGC AAG AAA CCT GTC CTC TAT TTG GAA CAT
       F   C   E   V   C   K   K   P   V   L   Y   L   E   H

1387 AAC CTG GAG AAA AAC AGC ACC AAG GAG GAA ATC CTG GCC GCA
       N   L   E   K   N   S   T   K   E   E   I   L   A   A

1429 CTT GAG AAG GGC TGC AGC TTC CTG CCA GAC CCT TAC CAG AAG
       L   E   K   G   C   S   F   L   P   D   P   Y   Q   K

1471 CAG TGC GAT GAC TTT GTG GCT GAG TAT GAG CCC TTG CTA TTG
       Q   C   D   D   F   V   A   E   Y   E   P   L   L   L

1513 GAG ATC CTC GTG GAA GTG ATG GAT CCT GGA TTT GTG TGC TCG
       E   I   L   V   E   V   M   D   P   G   F   V   C   S
```

```
1555  AAA ATT GGA GTT TGC CCT TCT GCC TAT AAG CTG CTG CTG GGA
        K   I   G   V   C   P   S   A   Y   K   L   L   L   G

1597  ACC GAG AAG TGT GTC TGG GGC CCT AGC TAC TGG TGT CAG AAC
        T   E   K   C   V   W   G   P   S   Y   W   C   Q   N

1639  ATG GAG ACT GCC GCC CGA TGC AAT GCT GTC GAT CAT TGC AAA
        M   E   T   A   A   R   C   N   A   V   D   H   C   K

                            *
1681  CGC CAT GTG TGG AAC TAG TTT CCC AGC TGC AGA AGT CAC CTA
        R   H   V   W   N   -   F   P   S   C   R   S   H   L

1723  CTT GTG GGT CTA GGG TAA TGA ACA CAT AGA TCT ATT TGA CTT
        L   V   G   L   G   -   -   T   H   R   S   I   -   L

1765  AAT AAG TAG GAA CCC CCT TTG CCC TTC CCC CAT CTC CTC TCC
        N   K   -   E   P   P   L   P   F   P   H   L   L   S

1807  CTT ACT GTA GCA TTT CTG TCA TGT AAG AGG TTC TGA CAG CAC
        L   T   V   A   F   L   S   C   K   R   F   -   Q   H

1849  CTT CCG TGT CCC CTT TCT GCT CGA AGG ATG AGG ATA CCT TGG
        L   P   C   P   L   S   A   R   R   M   R   I   P   W

1891  GCA TCA GCT CCC CGG CTG CCC TTT TCA CCC ACC TGC TGG AGG
        A   S   A   P   R   L   P   F   S   P   T   C   W   R

1933  GGG GTG GTG AGC CAG AGG GCA GGA GCA T
        G   V   V   S   Q   R   A   G   A
```

Figure 3-3: Nucleotide and amino acid sequence of the rat prosaposin cDNA. The open reading frame is indicated by "•" above the amino acid residues of initiation (ATG) and termination code (TAG) of translation. Nucleotide numbering is placed on the left margins.

Rat prosaposin

```
                                                    •
  1  GCA GCC TGC GGA GTG AAG CGC GCC ATG TAT GCT CTC GCT CTC
       A   A   C   G   V   K   R   A   M   Y   A   L   A   L

 43  CTC GCC AGC CTT CTG GTC ACC GCT CTG ACC AGC CCT GTC CAG
       L   A   S   L   L   V   T   A   L   T   S   P   V   Q

 85  GAC CCG AAG ATC TGC TCT GGG GGC TCA GCA GTA GTG TGC AGA
       D   P   K   I   C   S   G   G   S   A   V   V   C   R

127  GAT GTG AAG ACG GCG GTG GAC TGT AGG GCT GTG AAG CAC TGC
       D   V   K   T   A   V   D   C   R   A   V   K   H   C

169  CAG CAG ATG GTC TGG AGC AAG CCC ACA GCA AAA TCC CTT CCT
       Q   Q   M   V   W   S   K   P   T   A   K   S   L   P

211  TGT GAC ATA TGC AAA ACG GTT GTC ACC GAA GCT GGG AAC TTG
       C   D   I   C   K   T   V   V   T   E   A   G   N   L

253  CTG AAA GAT AAT GCT ACT GAG GAG GAG ATC CTC CAT TAC CTG
       L   K   D   N   A   T   E   E   E   I   L   H   Y   L

295  GAG AAG ACC TGT GCG TGG ATT CAT GAC TCC AGC CTG TCA GCC
       E   K   T   C   A   W   I   H   D   S   S   L   S   A

337  TCT TGC AAG GAG GTG GTT GAC TCT TAC CTG CTT GTC ATC CTG
       S   C   K   E   V   V   D   S   Y   L   L   V   I   L

379  GAC ATG ATT AAG GGG GAG ATG AGC AAC CCC GGG GAA GTG TGC
       D   M   I   K   G   E   M   S   N   P   G   E   V   C

421  TCT GCG CTC AAC CTC TGC CAG TCC CTT CAG GAG TAC TTG GCC
       S   A   L   N   L   C   Q   S   L   Q   E   Y   L   A

463  GAG CAA AAC CAG AGA CAG CTG GAG TCC AAC AAG ATC CCG GAG
       E   Q   N   Q   R   Q   L   E   S   N   K   I   P   E

505  GTG GAC CTG GCC CGC GTG GTT GCC CCC TTC ATG TCC AAC ATC
       V   D   L   A   R   V   V   A   P   F   M   S   N   I

547  CCT CTC CTG CTG TAC CCT CAG GAT CGG CCT CGC AGC CAG CCG
       P   L   L   L   Y   P   Q   D   R   P   R   S   Q   P

589  CAG CCC AAG GCT AAC GAG GAC GTC TGC CAG GAC TGT ATG AAG
       Q   P   K   A   N   E   D   V   C   Q   D   C   M   K

631  TTG GTG ACT GAC ATC CAG ACT GCT GTG AGG ACC AAC TCC AGC
       L   V   T   D   I   Q   T   A   V   R   T   N   S   S

673  TTT GTC CAG GGC TTG GTG GAC CAC GTC AAG GAG GAT TGT GAC
       F   V   Q   G   L   V   D   H   V   K   E   D   C   D

715  CGC CTC GGG CCA GGC GTG TCT GAC ATA TGC AAG AAC TAT GTT
       R   L   G   P   G   V   S   D   I   C   K   N   Y   V
```

```
757  GAC CAG TAT TCT GAG GTC GCC GTC CAG ATG ATG ATG CAC ATG
       D   Q   Y   S   E   V   A   V   Q   M   M   M   H   M

799  CAA CCC AAG GAA ATC TGT GTG ATG GTT GGC TTC TGT GAT GAG
       Q   P   K   E   I   C   V   M   V   G   F   C   D   E

841  GTC AAG AGA GTG CCA ATG AGG ACT CTG GTC CCC GCC ACT GAG
       V   K   R   V   P   M   R   T   L   V   P   A   T   E

883  GCC ATC AAG AAT ATC CTC CCT GCC CTG GAG CTG ACG GAC CCC
       A   I   K   N   I   L   P   A   L   E   L   T   D   P

925  TAT GAG CAG GAT GTG ATC CAG GCC CAA AAT GTG ATT TTC TGC
       Y   E   Q   D   V   I   Q   A   Q   N   V   I   F   C

967  CAA GTT TGT CAG CTT GTG ATG CGC AAG TTG TCT GAA CTG ATT
       Q   V   C   Q   L   V   M   R   K   L   S   E   L   I

1009 ATC AAC AAT GCC ACT GAG GAA CTT CTA ATT AAA GGT TTG AGT
       I   N   N   A   T   E   E   L   L   I   K   G   L   S

1051 AAA GCC TGC TCC CTG CTC CCT GCT CCT GCT TCA ACC AAG TGC
       K   A   C   S   L   L   P   A   P   A   S   T   K   C

1093 CAG GAA GTG CTG GTA ACA TTT GGC CCC TCC CTG TTG GAC GTC
       Q   E   V   L   V   T   F   G   P   S   L   L   D   V

1135 CTC ATG CAT GAG GTG AAC CCG AAC TTT CTG TGC GGT GTG ATC
       L   M   H   E   V   N   P   N   F   L   C   G   V   I

1177 AGC CTC TGT TCT GCC AAC CCG AAT TTG GTG GGG ACC CTT GAA
       S   L   C   S   A   N   P   N   L   V   G   T   L   E

1219 CAA CCT GCA GCA GCC ATT GTA TCT GCA CTG CCC AAA GAG CCT
       Q   P   A   A   A   I   V   S   A   L   P   K   E   P

1261 GCA CCG CCA AAA CAG CCT GAA GAG CCC AAG CAG TCT GCA TTG
       A   P   P   K   Q   P   E   E   P   K   Q   S   A   L

1303 CGC GCC CAT GTG CCT CCT CAG AAG AAC GGG GGG TTC TGT GAG
       R   A   H   V   P   P   Q   K   N   G   G   F   C   E

1345 GTG TGC AAG AAG CTG GTC ATC TAT TTG GAA CAT AAC CTG GAG
       V   C   K   K   L   V   I   Y   L   E   H   N   L   E

1387 AAA AAC AGC ACC AAG GAG GAG GTC CTG GCT GCA CTT GAG AAG
       K   N   S   T   K   E   E   V   L   A   A   L   E   K

1429 GGC TGC AGC TTC CTG CCC GAC CCT TAC CAG AAG CAG TGT GAT
       G   C   S   F   L   P   D   P   Y   Q   K   Q   C   D

1471 GAA TTT GTG GCT GAG TAT GAG CCC TTA CTG CTG GAA ATC CTT
       E   F   V   A   E   Y   E   P   L   L   L   E   I   L

1513 GTG GAG GTG ATG GAT CCT TCC TTT GTG TGC TCG AAA ATT GGA
       V   E   V   M   D   P   S   F   V   C   S   K   I   G
```

```
1555  GTC TGC CCT TCT GCC TAT AAG CTG CTG CTG GGA ACC GAG AAG
        V   C   P   S   A   Y   K   L   L   L   G   T   E   K

1597  TGT GTC CGG GGC CCA GGC TAC TGG TGT CAG AAC ATG GAG ACT
        C   V   R   G   P   G   Y   W   C   Q   N   M   E   T

1639  GCT GCC CGA TGC AAT GCT GTC GAT CAT TGC AAA CGC CAT GTG
        A   A   R   C   N   A   V   D   H   C   K   R   H   V

1681  TGG AAC TAG CTT TCC AGC TTG CAG AAG TCG CCT ACT TGT GGG
        W   N   -   L   S   S   L   Q   K   S   P   T   C   G

1723  TCT AGG GTA ATG AAG
        S   R   V   M   K
```

Figure 3-4: Restriction enzymes maps of mouse and rat prosaposin cDNAs. **A)** Sites of restriction enzymes distributed in the open reading frame (marked by "•" indicating the initiation and termination sites) of mouse prosaposin cDNA are indicated by vertical dotted bars. **B)** Sites of restriction enzymes distributed in the open reading frame of the rat prosaposin cDNA sequence (marked by '•' indicating the initiation and termination sites) are indicated by vertical dotted lines. Analysis was done by computer with Clone program.

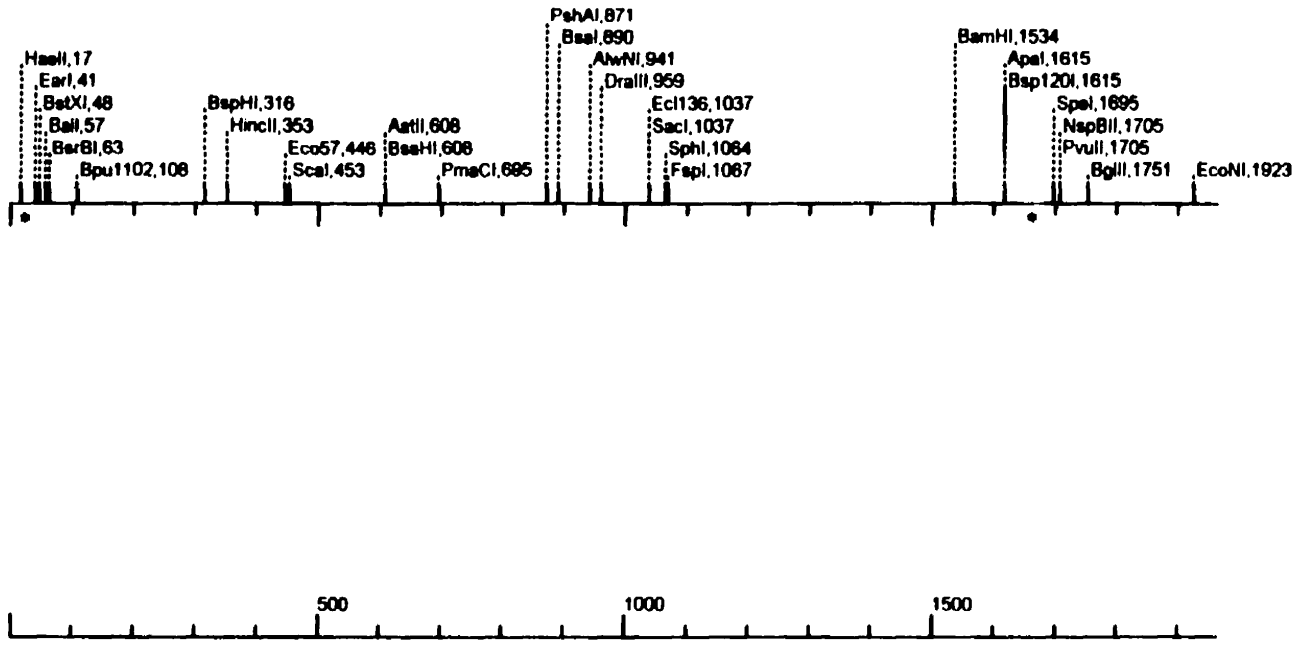

Mouse prosaposin (1961 bps)

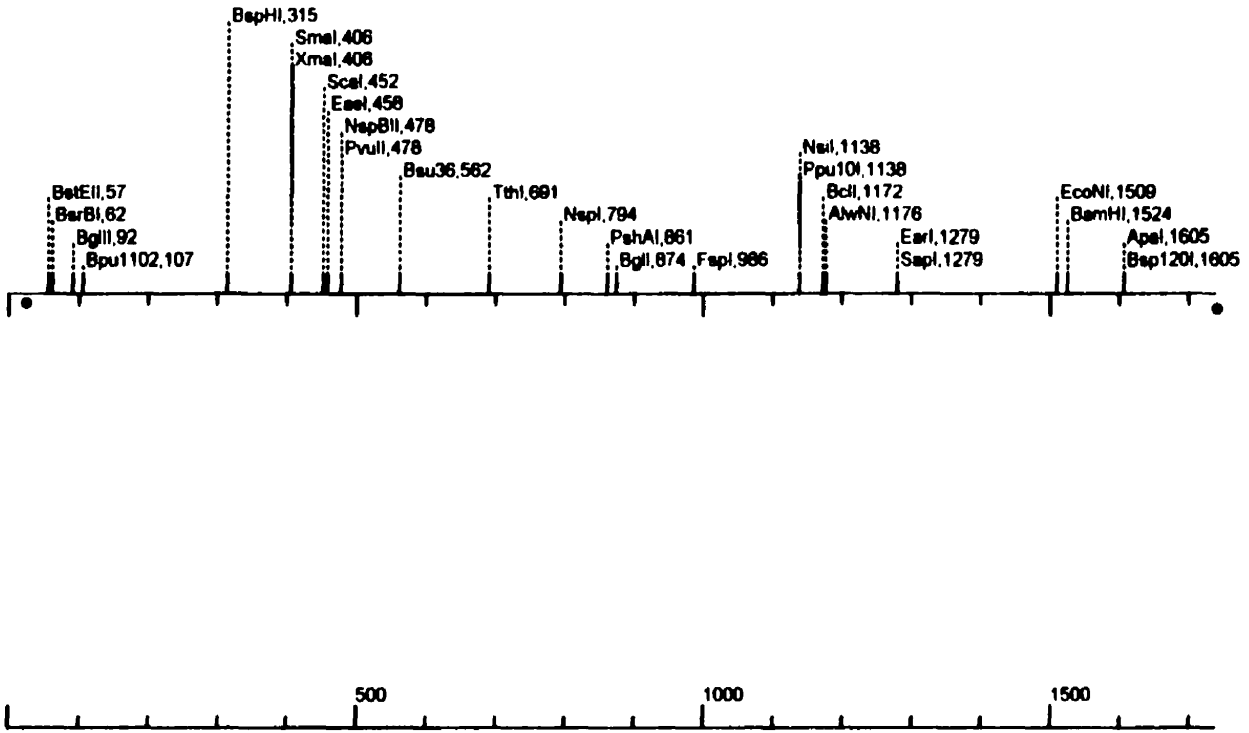

Rat prosaposin (1737 bps)

Figure 3-5: Representative of a positive clone obtained after three-round-screening (first, secondary and tertiary) from a mouse genomic library (10^6 pfu/ul). Two sets of replica were made and hybridized with a prosaposin cDNA probe labeled with ^{32}P-dCTP (10^6cpm/ml). Phage DNA was isolated by the clear lysate method (Sambrook et al., 1989).

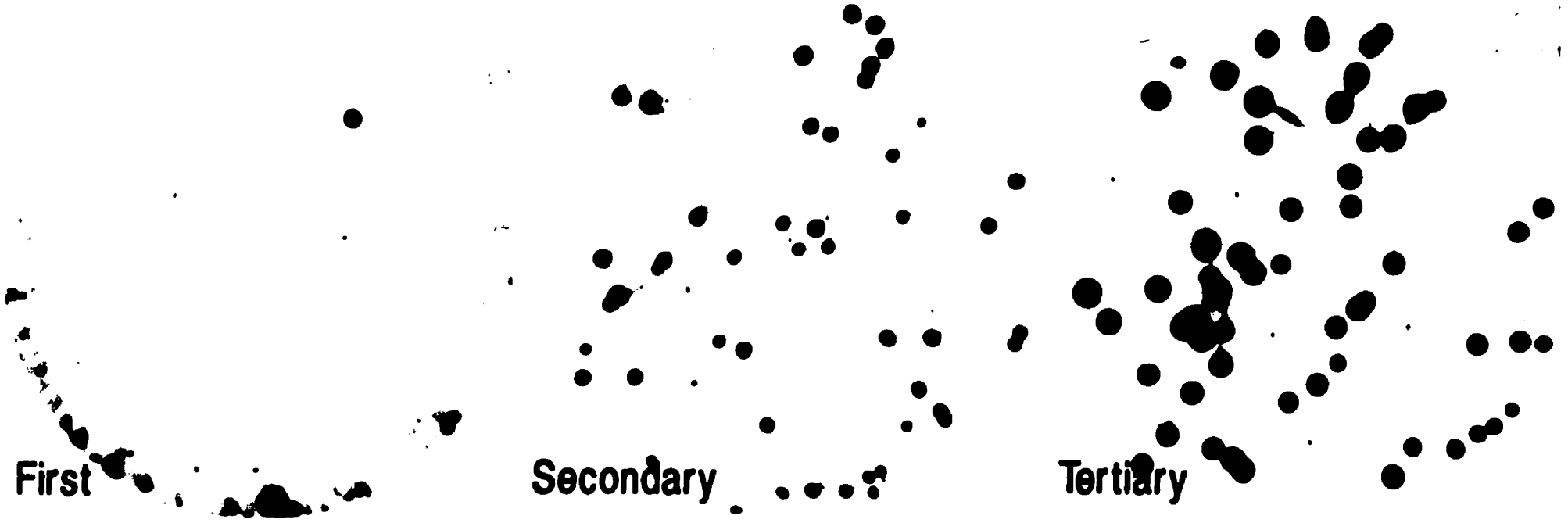
First
Secondary
Tertiary

Figure 3-6: Agarose gel electrophoresis of two positive clones digested with Xho I restriction enzyme and stained with ethidium bromide (lane 1 and lane 2). Note that the excised genomic fragments are approximately 19 kb. Arrowheads indicate the arms of the phagemid. Lane 3 is a DNA ladder.

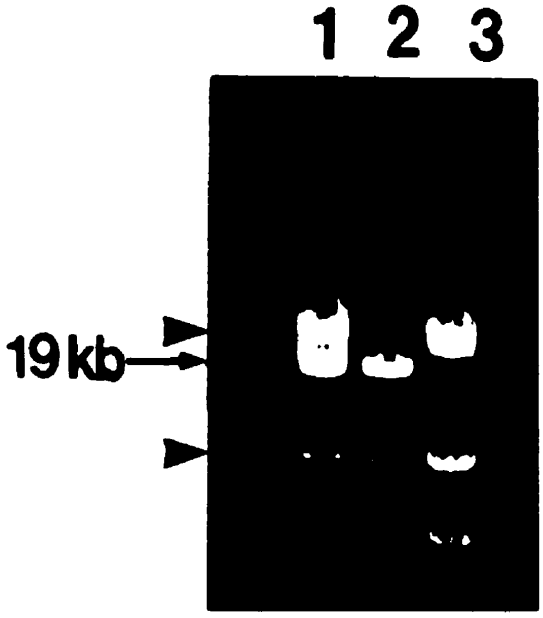
1 2 3
19kb

Figure 3-7: Agarose gel electrophoresis of two positive clones (lane 2 and 3) digested with SacI restriction enzyme and stained with ethidium bromide. Six restriction fragments of 8.3 kb, 4.0 kb, 2.5 kb, 2.2 kb, 1.1 kb and 0.4 kb long were generated from one clone in lane 3 and 8.3 kb, 3.7 kb, 2.5 kb, 2.2 kb, 1.1 kb and 0.4 kb long fragments were generated from another clone in lane 2. Lane 1 is a Hind III digested DNA ladder, lengths are pointed by arrowheads.

Figure 3-8: Southern blot analysis of two positive clones digested with SacI restriction enzyme and hybridized with a ^{32}P-dCTP labeled mouse prosaposin cDNA probe. Note that four restriction fragments of 8.3 kb, 2.2 kb, 1.1 kb and 0.4 kb, hybridized to the radiolabeled probe.

Fig.3-7

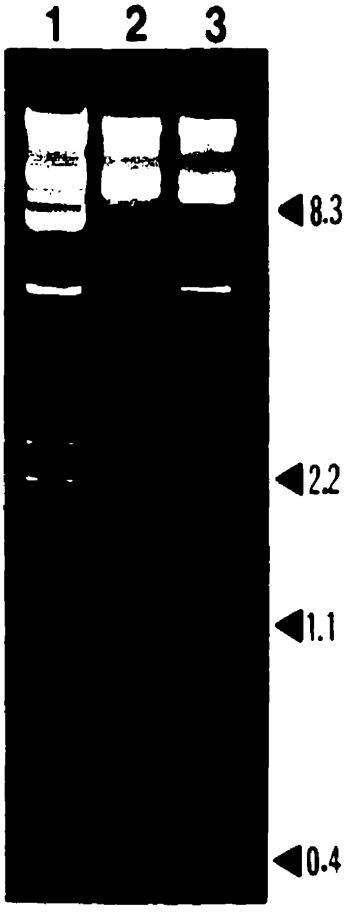

Fig.3-8

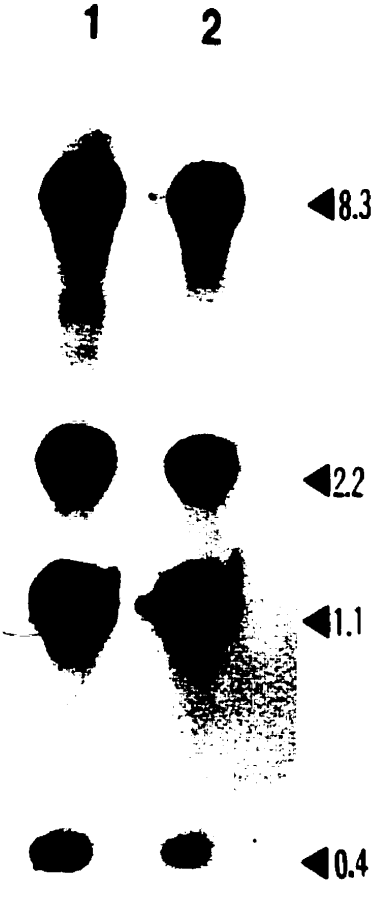

Table VI: Consensus Sequence of Splicing Donor and Acceptor Sites in Mouse Prosaposin Gene

Intron Exon size[a]	3' splice site	5' splice site	Exon size[a]	
1	ATGTAC		64[c]	
8000[c]				
2	ttcctttagGCTCTG ————	ACAGCGgtgagt	135	734
3	tcctgttagAAATCC ————	ACGCAGgtaagg	75	771
4	cgcttgcagGAGGAG ————	GAGATGgtaggt	126	1061
5	cctttccagAGCAAC ————	CCTAAGgttagc	198	
236				
6	ctcttgtagGCTAAC————	GACATAgtaagc	144	
837				
7	tctctgcagTGCAAG————	CACATGgtaggt	57	1533
8[b]	gttcaacag CAGGATCAG	gtatgt	9	
1555				
9	tttcttcagCAACCC ————	TATGAGgtacct	132	234
10	ccttcacagCAGAAT————	AATGAGgtatgc	96	217
11	ctgtttcagGAGCTC ————	TTGCCCgtaagt	279	89
12	ttttgtagGCCCAT————	AAGCAGgtatgg	159	232
13	tcttggcagTGCGAT————	TGCTCGgtaagc	81	155
14	gtcatacagAAAATT————	TGCAATgtgagt	108	815
15	tcctcatagGCTGTC		298[c]	

- Dashed lines show unknown sequences. Continous lines indicate known exon sequences.
- [a] sizes are expressed as base pairs
- [b] Note that exon 8 is formed by only nine base pairs
- [c] Indicates incomplete number of base pairs

However, the full-length sequence of this intron is still incomplete due to the fact that it is too long to characterize.

Our sequence analysis also allowed us to identify the coding regions of each saposin. Saposin A is encoded by the exons 3, 4, and 5; saposin B is encoded by exons 6, 7, 8 and 9; saposin C is encoded by exons 10, and 11 and saposin D is encoded by exons 12, 13, and 14 (Figure 3-9). Sequence analysis showed that each saposin molecule does not start or end exactly at the beginning or end of the exons due to the partial proteolytic processing of these proteins. The translation start codon is located within the first exon and the translation stop codon is located within exon 15. Finally, the exon/intron boundaries were in accordance with the AG/GT consensus sequences. Table VI shows the consensus sequences of splicing donor and acceptor sites in the mouse prosaposin gene. Moreover, the conservation and size of each exon, the size of each intron between the mouse and human was compared (Table VII). The results demonstrated that the sizes of the mouse and human exons are quite similar except the exon 11 of the human which lacks 93 nucleotides. The average conservation of the exons between the mouse and human is 79% by nucleotide and 69 % by amino acids. The sequence and size of introns between the mouse and human are quite different, though the introns in the mouse are smaller than in the human.

3.1.3 Expression of Mouse Prosaposin Gene by Alternative Splicing

Exon 8 is the smallest exon of the prosaposin gene and consists of nine

Figure 3-9: Schematic diagram of the organization of mouse prosaposin gene (upper panel) and of the translated prosaposin protein (lower panel). The red boxes are exons and the blue bars in between are introns. Exonic sequences are numbered (1-15). The color boxes marked by A, B, C and D represent the translated product, composing of saposins A, B, C and D domains. SP represents the signal peptide. Big arrow head indicates the alternative splice site (AS) of saposin B. Other two arrows indicate the proline-rich sequence (31 amino acids) located between saposin C and D (PP). Dashed lines identify the coding regions for each saposin. Note that saposin A is encoded by the exons 3, 4, and 5; saposin B by exons 6, 7, 8 and 9; saposin C by exons 10, and 11 and saposin D by exons 12, 13, and 14.

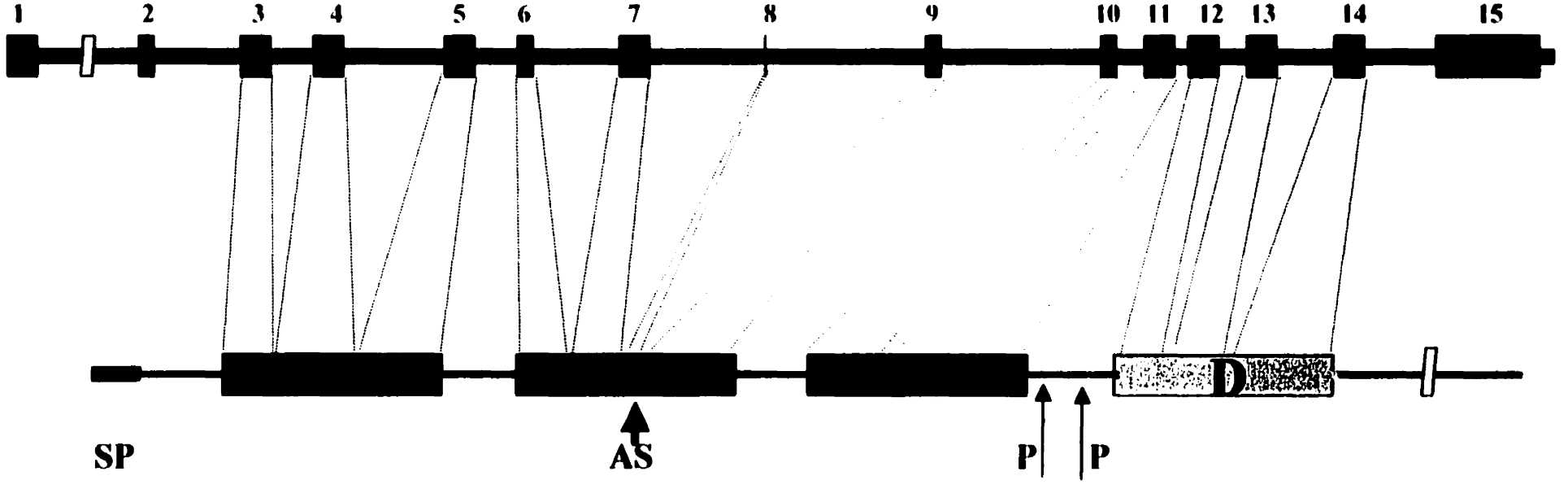
1
2
3
4
5
6
7
8
9
10
11
12
13
14
15
D
SP
AS
P
P

Table VII: Number and Size of Exons and Introns in Mouse (M) and Human (H) Prosaposin Genes

	Exon size (bp)		% homology			Intron size (bp)	
	M	H	Exon	Amino acid		M	H
1	64	40	82.8	69	1	8000	1787
2	135	134	74.1	64	2	734	2441
3	75	75	84	80	3	771	594
4	126	126	77.8	78.6	4	1061	2046
5	198	201	82.8	80.3	5	236	717
6	144	144	81.9	66	6	837	2126
7	57	57	80.7	68.4	7	1533	---
8[a]	9	---	---	---	8	1555	3812
9	132	132	80.3	59.1	9	234	1539
10	96	96	61.5	31	10	217	338
11	279	187	54.3	32	11	89	91
12	159	158	85.9	84.9	12	232	354
13	81	81	87.7	85.2	13	155	305
14	108	108	83.3	81.8	14	815	1136
15	198	1200	88.7	91.7	15		

[a] Exon and intron 8 have not been reported in the human prosaposin gene (Rorman et al., 1992; NCBI GeneBank accession number 86181)

base pairs. To evaluate the abundance of prosaposin gene transcripts with or without the nine base pairs by alternative splicing, a RT-PCR was applied to amplify specific regions of the prosaposin gene encoding saposin B domain flanking the area of the 9 amino acids. Total RNAs were isolated from brain, heart, muscle, lung, spleen, kidney, pancreas and testis. The sense and antisense primers were designed to match the flanking regions of exon 8. The amplified PCR products were resolved in a 12 % polyacrylamide gel after stained with ethidium bromide (Figure 3-10). Comparison of the mobility's of the bands to a DNA ladder revealed that a larger fragment was 115 bp and a smaller fragment was 106 bp by 9-nucleotide difference. The results also showed that three of the eight tissues (muscle, heart and brain) contained mostly the larger 115 bp fragment due to the presence of exon 8 and that the five remaining tissues (testis, lung, pancreas, spleen and kidney) contained mostly the 106 bp fragment devoid of exon 8. It was also observed that the corresponding fragments of the muscle not only consisted of the larger 115 bp band, but also seemed to have a faint lower band representing the smaller fragment of 106 bp. On the other hand, in testis, the 106 bp band appeared to be more dominant than the 115 bp band.

In order to confirm unequivocally the presence of exon 8 in brain, heart and skeletal muscle, and the absence of exon 8 in kidney, spleen, pancreas and lung, the PCR fragments were electrophoreses on a 1% agarose gel. The bands were then cut from the gel, purified and subcloned into the pGEM-T vector and sequenced. Two representative tissues (brain and kidney) were selected as examples showing their different sequences (Figure 3-11). The sequence

Figure 3-10: RT-PCR products with specific primers flanking the exon 8 were electrophoresed in a 12 % polyacrylamide gel. Note that brain (B), heart (H) and skeletal muscle (M) generated a 115 bp band and that kidney (K), spleen (S), pancreas (P), lung (L) and testis (T) generated a 106 bp band.

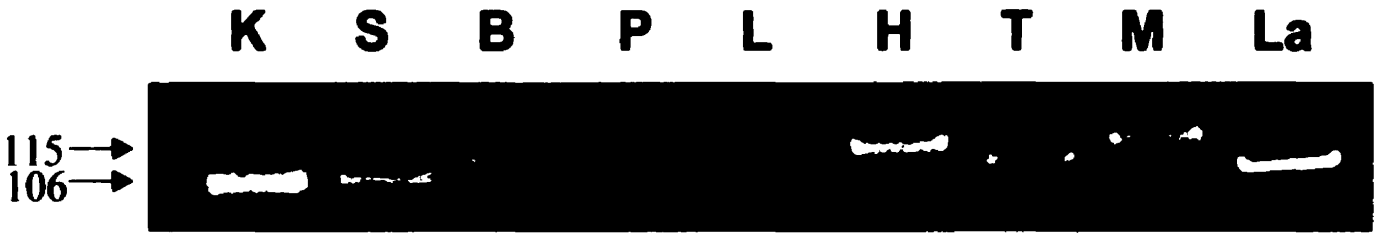
K
S
B
P
L
H
T
M
La
115
106

Figure 3-11: Sequence analysis of RT-PCR products form brain and kidney as representatives. The results showed that the brain fragment (B) contains a nine base pair insertion of (CAG GAT CAG) corresponding to exon 8 (on the right), whereas the kidney fragment (K) did not (arrow, on the left).

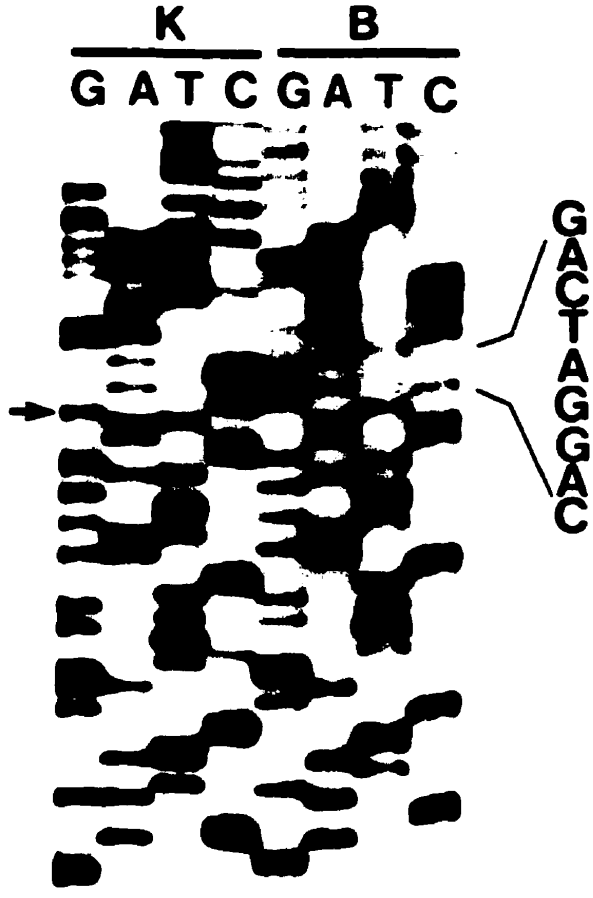
K
B
G A T C G A T C
GACTAGGAC

analysis showed that both fragments matched with the corresponding sequences of the mouse prosaposin gene, and the sequences of the brain fragment contained a nine base pairs insertion (CAG GAT CAG) corresponding to the exon 8, whereas the kidney fragment did not (Figure 3-11).

The abundance of prosaposin transcripts with or without the 9 bp by alternative splicing in the testis was confirmed in a separate experiment by using the same sense and antisence primers in RT-PCR (Figure 3-12). The smaller band (106 bp) without the exon 8 was more prominent than the larger band (115 bp). The identities of these PCR fragments have been determined by sequencing.

3.2 Sequence Analysis of the Common Backbone Structure of Prosaposin among Different Species.

3.2.1 Amino Acid Sequence Alignment of the Mouse, Rat and Humam Prosaposin cDNAs

The deduced amino acid sequences of mouse and rat prosaposin were used for a database search employing the Blast network [209] against the nonredundant NCBI database. Several mouse, rat (SGP-1) and human prosaposin homologues were found. For comparison purpose, the mouse and rat prosaposin cDNAs from this study and the human prosaposin sequence from Dewji et al [210] were selected and aligned (Figure 3-13). The predicted mouse prosaposin amino acid sequence of 557 residues has a 94% similarity (88% identity) to the rat homologue (also known as SGP-1) which is 554 amino acids in length and has a 75 % similarity (64%) to human prosaposin (524 amino acids)

Figure 3-12: Polyacrylamide (12%) gel electrophoresis of RT-PCR products performed on total RNA extracted from mouse testis and stained who ethidium bromide. Note the presence of a 115-bp and a 106-bp band representing transcripts bearing or not the exon 8. The 106-bp band is obviously more abundant.

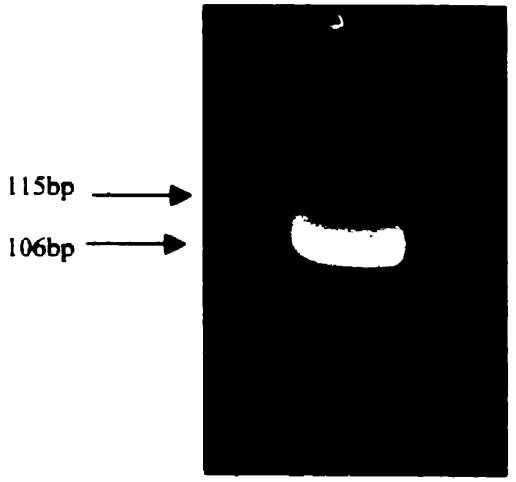
115bp
106bp

Figure 3-13: Amino acid sequence alignment of rat, mouse and human Prosaposins. Identical residues are highlighted in black, whereas conservative replacements are shaded. White boxes depict amino acid heterogeneities. Single dots between the conserved N (Asn) 149 and Q (Gln) 150 identify a histidine (H) residue insertion in the segment connecting human saposin A and B that is absent from rodent prosaposins. Asterisks between the conserved M (Met) 258 and Q (Gln) 262 indicate the absence of a QDQ insertion (Gln,Asp, Gln) in the rat. Dots indicate the deletion of a proline-rich segment in human prosaposin that is present in rodent prosaposins.

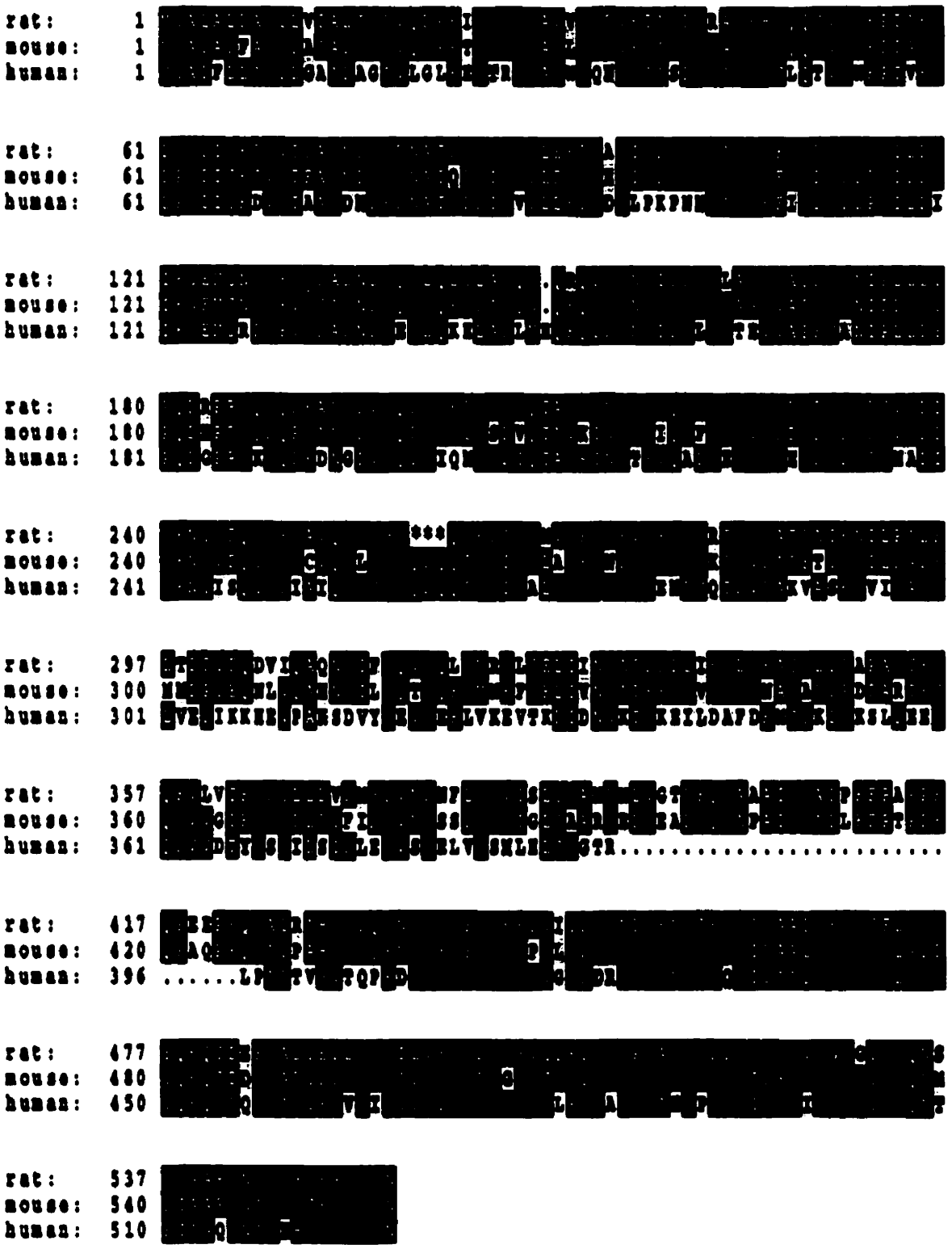
rat: 1
mouse: 1
human: 1
rat: 61
mouse: 61
human: 61
rat: 121
mouse: 121
human: 121
rat: 180
mouse: 180
human: 181
rat: 240
mouse: 240
human: 241
rat: 297
mouse: 300
human: 301
rat: 357
mouse: 360
human: 361
rat: 417
mouse: 420
human: 396
rat: 477
mouse: 480
human: 450
rat: 537
mouse: 540
human: 510

sequences when conservative amino acid replacements are taken into account (Figure 3-13). The alignments of the mouse and rat sequences yielded a perfect match. However, the rat sequence corresponded to the mouse splicing variant lacking the three amino acids QDQ (Gln, Asp, Gln), that are encoded by exon 8 (NCBI 138152). Alignment of the human prosaposin sequence was also direct (Figure 3-13) and identified a histidine residue insertion between the conserved Asn 149-Gln 150 (mouse numbering) in the segment connecting saposins A and B, and a deletion of a proline-rich segment of 31 amino acids in the segment connecting saposin C and D, of the human sequence. The most conserved region (Figure 3-13) was noticed at the 3' end of the three sequences (residues 428-557 of the mouse numbering) which contained the domain encoding saposin D and the C-terminus of prosaposin.

3.2.2 Pairwise Comparison of Sequence Identities/Similarities among Mouse, Rat and Human Prosaposin

We have chosen to analyze the similarity among the three sequences of the mouse, rat (SGP-1) and human prosaposin on a segmental basis, based on the predicted saposin domains. A subdomain structure of four saposin sequences that are separated by segments of about 40 amino acids was present among the full-length rat SGP-1 and the mouse and human prosaposin sequences. Furthermore, the comparison in pairwise fashion (mouse vs. rat; mouse vs. human; rat vs. human) was conducted to accentuate similarities and differences between rodent (mouse or rat) versus the human sequence rather than an overall

comparison. The computed percent identity and percent similarity scores for these segments are presented in Figure 3-14. Generally, sequence identity has not been retained uniformly throughout the SGP-1/prosaposin molecule. Identifying regions that share a conserved function reveals that there has been a tendency to retain the structure-function relationship in other segments by conservative amino acid replacements. The overall similarity between the three sequences is 74% (62 % identity). This indicates that the similarities observed for the mouse, rat and human are not arranged at random and that they follow the same modes.

The segment-pairwise comparison of the SGP-1/prosaposin sequences revealed that saposin D and the adjacent C-terminal (residue 518-557) segment were the most conserved (83-95% identity) among the three species (Figure 3-14). Four other regions were highly identical only between the mouse and rat sequences (e.g. the N-terminal segment, saposin A, saposin B, and the intervening segment between saposin A and saposin B, residues 144-193), although saposin A and saposin B from the three species were much more closely related when conservative replacements were taken into consideration (88-95% conserved). The relatively low degree of conservation in the N-terminal segment (residues 1-59) between rodent and human prosaposins reflects species-related targeting/processing differences in the secretory pathway rather than differences in the function of SGP-1/prosaposin. A 31-amino acid loss of a proline-rich segment connecting saposin C and saposin D in human, but presence in rodents, has not been related to the differences in their roles. However, it may reflect

Figure 3-14: Pair-wise comparison of prosaposin sequence identities/similarities between rat (r) and mouse (m), rat (r) and human (h), mouse (m) and human (h) on the predicted saposin/nonsaposin domains. Sequence identities and similarities, when taken into account of the conservative replacements, are expressed as percentages and are shown as the first and second column, respectively, above the pair being compared. Numbers identify the nonsaposin domains.

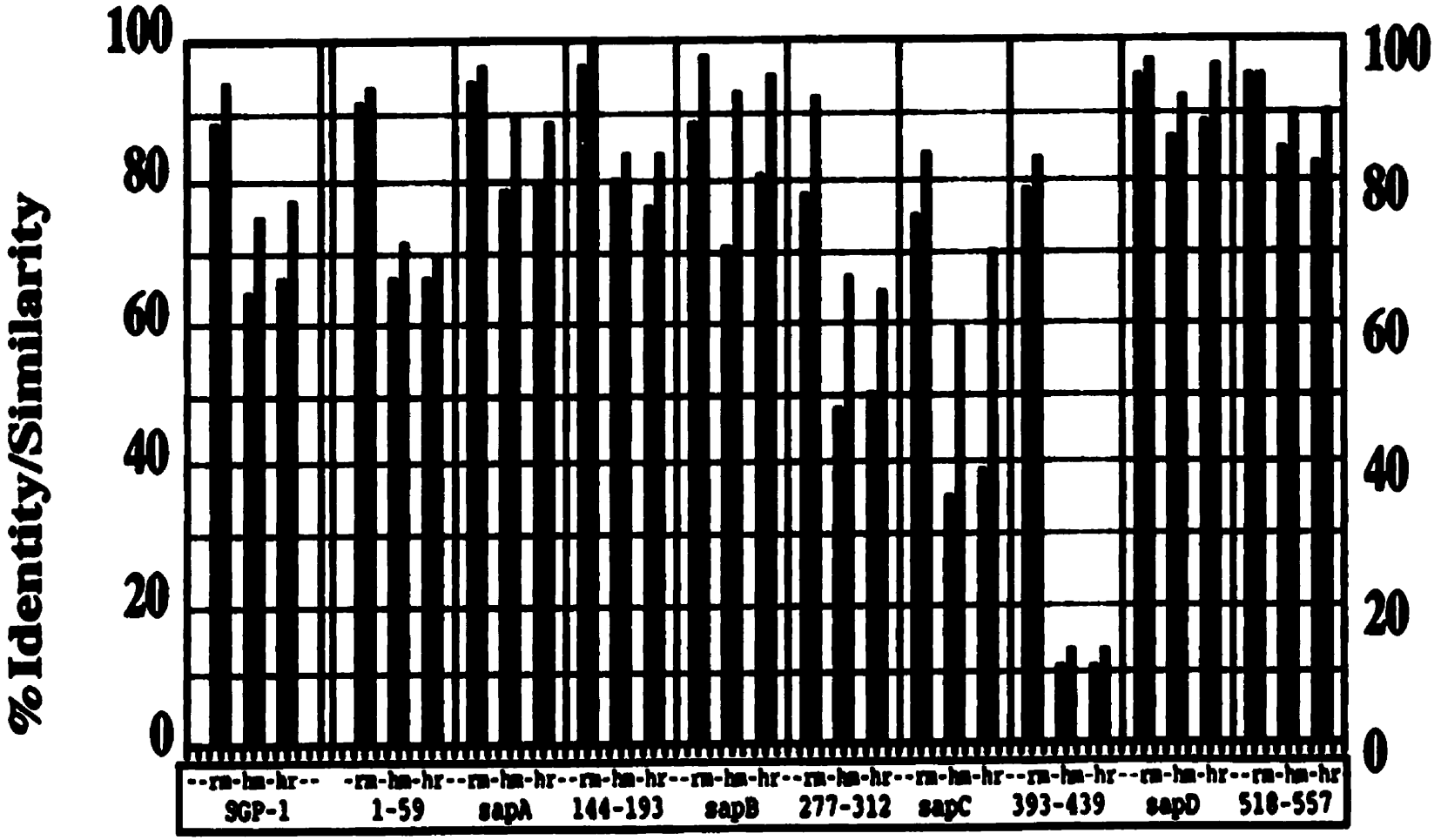
% Identity/Similarity
100
80
60
40
20
0
--rm-hm-hr--
SGP-1
-rm-hm-hr--
1-59
rm-hm-hr--
sapA
rm-hm-hr--
144-193
rm-hm-hr--
sapB
rm-hm-hr--
277-312
rm-hm-hr--
sapC
rm-hm-hr--
393-439
rm-hm-hr--
sapD
rm-hm-hr--
518-557
Prosaposin

either a loss of function of SGP-1/prosaposin and /or the strict requirement to regain functional saposin processing with a much shortened hinge segment. Of all the saposins, the saposin C appears to be the least conserved between rodents and humans (Figure 3-14). Interestingly, when comparing mouse or rat saposin sequences to human's, rat saposin B shows significantly greater identity with human saposin B (81% vs. 71%) than that with the mouse. In general, with the exception of saposin A, all rat saposins are more similar to the human saposins (Figure 3-14).

3.3 Alignment and Secondary Structure Predictions of Saposins in Mouse, Rat and Human

Sequence comparison of the four-saposin domains of rat SGP-1 and mouse and human prosaposin revealed that these molecules share common structural features. Saposins A, B, C and D have essentially identical placement of six cysteines, a conserved N-linked glycosylation site, and a conserved proline residue (Figure 3-15, in shaded area). Secondary structure predictions for the saposin domains within the SGP-1/prosaposin structure predict that there are three α helices in saposin A, B and D with an extended small helices at each end and four α helices in saposin C with an extended α helix in the end too. The α helices, together with the disulfide bonding patterns, most likely produce a stable helical bundle. The alignment also revealed that 15 amino acid positions are conserved (Figure 3-15) and occupied by bulky hydrophobic amino acids (Val, Ile, Leu, Met, Phe, or Tyr). This alignment of bulky hydrophobic amino acids

Figure 3-15: Secondary structure predictions for aligned saposins in mouse, rat and human. Alignments and secondary structure predictions have been grouped as saposins (sap) A, B, C and D. Amino acid alignment of mouse, rat, and human saposins (uppercase) and adjoining N-terminal prosaposin amino acid sequences (lower case). Spaces within the saposin sequences represent gaps that have been introduced for the alignment of the six conserved cysteines, the conserved N-linked glycosylation site, and the conserved proline residue found in all saposins (arrows). Conserved hydrophobic positions occupied by the bulky amino acids V (Val), I (Ile), L (Leu), M (Met), F (Phe) and Y (Tyr) are identified by arrowheads. Secondary structure predictions (PHD sec) are shown for aligned saposins groups and for that saposin within the context of aligned prosaposin: H, helix; E, extended. The analysis predicts a motif of three α helices in a bundle stabilized by disulfide bonds. Splice sites are identified above the aligned sequences by an asterisk (*) over the first amino acid of the exon. Note that only two pairs of splice sites, 3*4-10*11 and 9*10-11*12, are conserved exactly with respect to the alignment. Amino acid positions within mouse saposins and within mouse prosaposin are indicated below the alignment and below the secondary structure predictions. Decade positions are numbered. Dots (.) represents consecutive positions, and commas (,) identify every fifth residue.

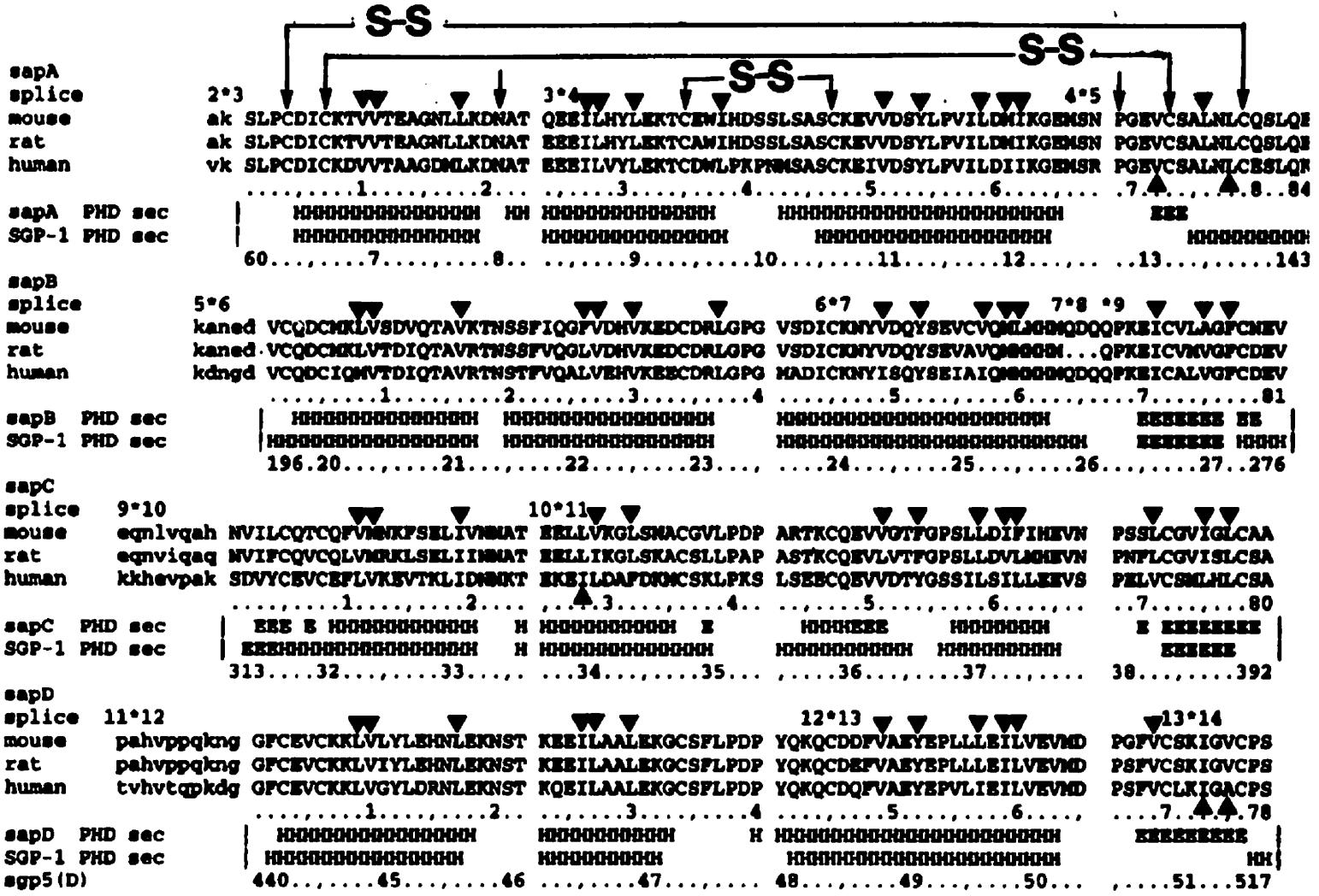
S-S
S-S
S-S
sapA
splice
mouse
rat
human
sapA PHD sec
SGP-1 PHD sec
sapB
splice
mouse
rat
human
sapB PHD sec
SGP-1 PHD sec
sapC
splice
mouse
rat
human
sapC PHD sec
SGP-1 PHD sec
sapD
splice
mouse
rat
human
sapD PHD sec
SGP-1 PHD sec
sgp5(D)

occupying equivalent positions suggests that their side chains are buried in the folded structure and that their interactions contributed to the stability of saposins.

3.4 Hydropathy Profiles of Mouse, Rat and Human Prosaposin

The hydropathy profiles of rat SGP-1 and mouse and human prosaposin were determined to compare the saposin and nonsaposin domains (Figure 3-16). The profiles were generated by computer, based on the algorithm described by Kyte and Doolittle [207]. The shaded areas span the regions corresponding to the four saposins (Figure 3-16). In general, the hydropathy profiles are characteristically conserved among the same saposins, with the least similarity within the human saposin C. On average, the N-terminal region of the individual saposin is more hydrophilic than the C-terminal region. However, they were both highly hydrophobic. This analysis also reveals the dramatic effect of inclusion (arrow heads) or exclusion of the three amino acids (QDQ) contributed by exon 8 to the local hydropathy profile of the saposin B domain (Figure 3-16). The QDQ insertion accentuates the local hydrophilicity of mouse and human saposin B. A similar dramatic different, characterized by an increase in relative hydrophobicity were also apparent in the N-terminal region of human saposin A and in the C-terminal region of human saposin C relative to the corresponding regions in mouse and rat saposin A and C. Lack of the 31 amino acid residues of proline rich segment in human prosaposin accounts for the removal of a local structure, of predicted alternating hydrophobic and hydrophilic nature (Figure 3-16, lower panel), without any significant change in the adjoining hydropathy profile

Figure 3-16: Hydropathy profiles of rat prosaposin (upper panel), mouse prosaposin (middle panel) and human prosaposin (lower panel), obtained according to Kyte and Doolittle (1982) employing a moving window of seven amino acids. Shaded areas depict the predicted nonsaposin regions. The QDQ insertion is identified by arrowheads. Arrow indicates a similar increase in hydrophilicity in the human saposin C sequence relative to the rodent saposin C. A, B, C and D identify saposin domains.

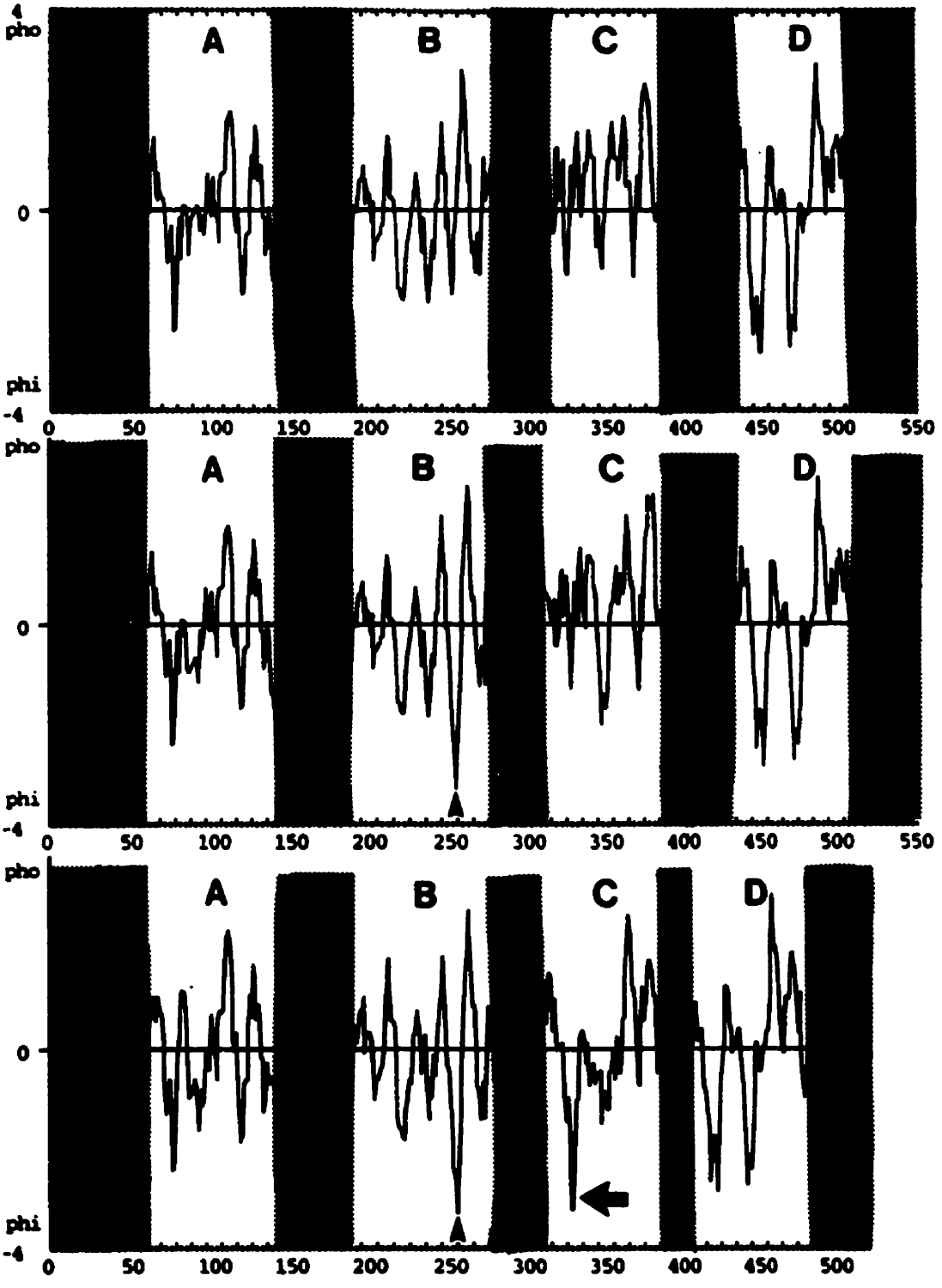
4
pho
A
B
C
D
0
phi
-4
0
50
100
150
200
250
300
350
400
450
500
550

comparing to the rodent's. The hydropathy profile for saposin D is almost identical in the three species and consistent with the high degree sequence identity.

3.5 Identification of a Novel Sequence Involved in Lysosomal Sorting of the Sphingolipid Activator Protein, Prosaposin

Most of the lysosomal soluble hydrolases are delivered to lysosomes via the mannose 6-phosphate (M6P) receptor pathway [43]. Lysosomal membrane proteins, however, do not have a mannose 6-phosphate tag and are transported to the lysosomes based on their cytosolic tyrosine or or dileucine residues [102, 104, 211] [112, 212].

Prosaposin reaches lysosomes by a mannose 6-phosphate independent mechanism [11, 12, 44, 56]. Cultured human fibroblasts from human patients with I-cell disease, which fail to phosphorylate mannose residues on newly synthesized lysosomal proteins have near normal levels of prosaposin and saposins in the lysosomes [12]. The 70 kDa secretory prosaposin is a post-translationally modified form of the 65 kDa lysosomal prosaposin [4, 213]. This observation suggests that the Golgi apparatus must decode a sorting signal from the 65 kDa prosaposin to target it to the lysosomes before it is fully glycosylated in the distal compartment of this organelle.

To identify the sequence responsible for the lysosomal routing of prosaposin, deletion of different domains within this protein were done.

3.5.1 Analysis of Prosaposin Domains

Alignment of amino acid residues for saposins as well as the N- and C-termini of prosaposin showed a similarity of 70-90 % among different species [30, 134, 214, 215]. Each saposin contains 80 amino acids, 6 conserved cysteine residues which form three internal disulfide bonds, a N-glycosylation site, a conserved proline residue and 14-15 hydrophobic amino acid residues at the same position [215]. Alignment between the N- (residues 1-60) and C-termini (residues 521-557) of prosaposin showed a 40% identity and 66% similarity. A Genebank database search revealed a 70% similarity between a 29 amino acid stretch of the N-terminus of the human surfactant protein B (SP-B) and the C-terminus of prosaposin. This N-terminus of surfactant protein B is involved in the transport of this protein to the lamellar bodies of pneumocyte type II [216]. A unique characteristic of the lysosomal nature of lamellar bodies is the content of hydrolases and a lysosomal membrane glycoprotein [217, 218].

3.5.2 Deletion of Prosaposin Functional Domains

Based on the analysis of prosaposin, saposin functional domains A, B, C, D, the N- and C-termini of prosaposin were deleted. The truncated constructs were designated ΔA, ΔB, ΔC, ΔD, ΔN-term and ΔC-term, to indicate the deleted region of the protein. Wild type prosaposin was designated Pro-WT (Figure 3-17). The constructs were subcloned into a mammalian expression vector pcDNA3.1B which harbors a myc epitope tag before the stop codon. Pro-WT and all truncated mutants were transiently transfected into COS-7 cells. The intracellular

Figure 3-17: Schematic representation of wild type and truncated prosaposin constructs subcloned into the pcDNA3.1B expression vector. Pro-WT is the wild type prosaposin containing the full- length cDNA of prosaposin encoding the N-terminus (N-term), the saposin A, B, C and D domains, and the C-terminus (C-term). The truncated constructs were designated ΔN-term (deletion of residues 17-59), ΔA (deletion of residues 57-147), ΔB (deletion of residues 189-278), ΔC (deletion of residues 309-396), ΔD (deletion of residues 404-522), and ΔC-term (deletion of residues 520-556) to indicate the specific regions deleted from prosaposin (shown by dotted lines).

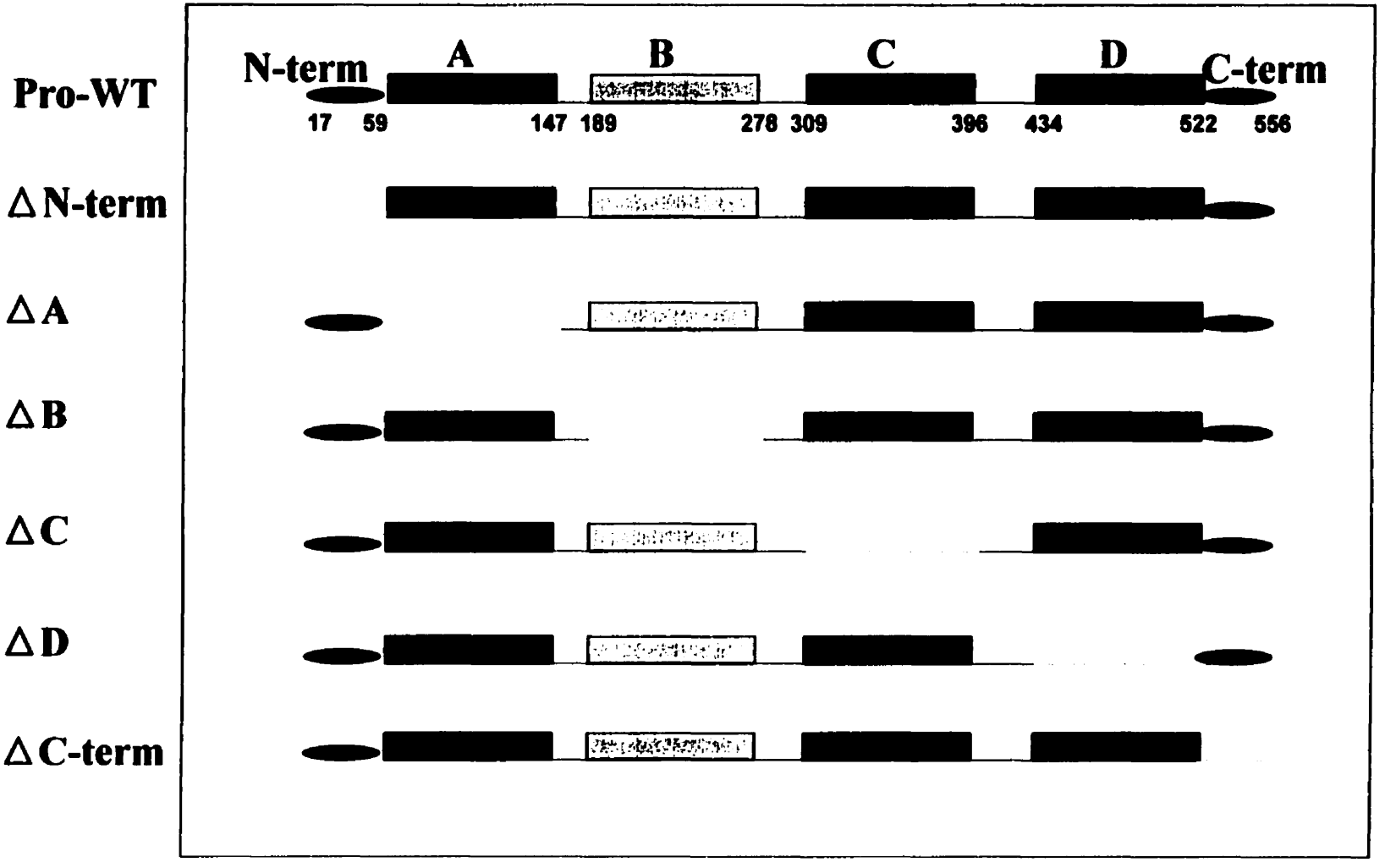
Pro-WT
N-term
A
B
C
D
C-term
17
59
147
189
278
309
396
434
522
556
ΔN-term
ΔA
ΔB
ΔC
ΔD
ΔC-term

distribution of the constructs was assessed by immunofluorescent staining with primary anti-myc monoclonal antibody, and secondary FITC conjugated goat anti-mouse antibody.

The two forms of wild type prosaposin, i.e, the 65 kDa lysosomal form and the 70 kDa secretory form were found by western blot analysis with antibody against myc in Pro-WT (Figure 3-18). All mutants also produced the two forms of prosaposin with lower molecular weights due to the truncation of their corresponding domains. Confocal immunofluorescence of COS-7 cells transfected with wild type prosaposin Pro-WT and ΔA, ΔB, ΔC, ΔD and ΔN-term mutants with myc antibody yielded both a perinuclear and a granular reaction. Cells transfected with the ΔC-term mutant did not yield any granular staining but the reaction persisted in the perinuclear region (Figure 3-19).

To confirm whether the granular structures observed in Pro-WT and ΔA, ΔB, ΔC, ΔD and ΔN-term were lysosomes, the lysosomal marker LysoTracker was used as a probe. This marker is sensitive to low pH and stains all acidic vesicles including the trans-Golgi region. The LysoTracker (red fluoresence) showed overlap with the punctate structures stained with myc antibody (green fluorescence) in Pro-WT, ΔA, ΔB, ΔC, ΔD and ΔN-term (Figure 3-20). In ΔC-term mutant although the LysoTracker detected numerous lysosomes, myc antibody staining was negative in these granules (Figure 3-20).

Since the myc antibody yielded a perinuclear reaction reminiscent of the Golgi apparatus in all the constructs including the ΔC-term mutant, an anti-mannosidase II antibody was used as a Golgi marker. Confocal immunostaining

Figure 3-18: Expression of wild type and truncated prosaposins after transfection into COS-7 cells. Approximately 50 ug of whole cell lysates were subjected to a 10% SDS-PAGE, transferred onto a nylon membrane and immunoblotted with anti-myc monoclonal antibody. Two bands representing the 65 kDa and 70 kDa wild type prosaposins (WT) are shown by arrows. Mutants (ΔN-term, ΔA, ΔB, ΔC, ΔD and ΔC-term) also produced two slightly lower bands depending on the size of the truncated sequences. Non transfected COS-7 cells (COS-7) and COS-7 cells transfected with the vector alone (V) were used as negative controls.

Cos-7
Vector
WT
ΔC-term
ΔA
ΔB
ΔC
ΔD
ΔN-term
70 kDa
65 kDa

Figure 3-19: Immunofluorescent staining of COS-7 cells after transfection with expression vectors containing wild type (Pro-WT) and truncated prosaposin (ΔN-term, ΔA, ΔB, ΔC, ΔD, and ΔC-term). Primary anti-myc monoclonal antibody was visualized with a FITC conjugated goat anti-mouse antibody. Pro-WT (WT) and the mutant constructs ΔN-term, ΔA, ΔB, ΔC and ΔD yielded a Golgi-like perinuclear and granular reactions. Cells transfected with ΔC-term show a Golgi-like perinuclear staining, but the granular reaction is seemingly absent.

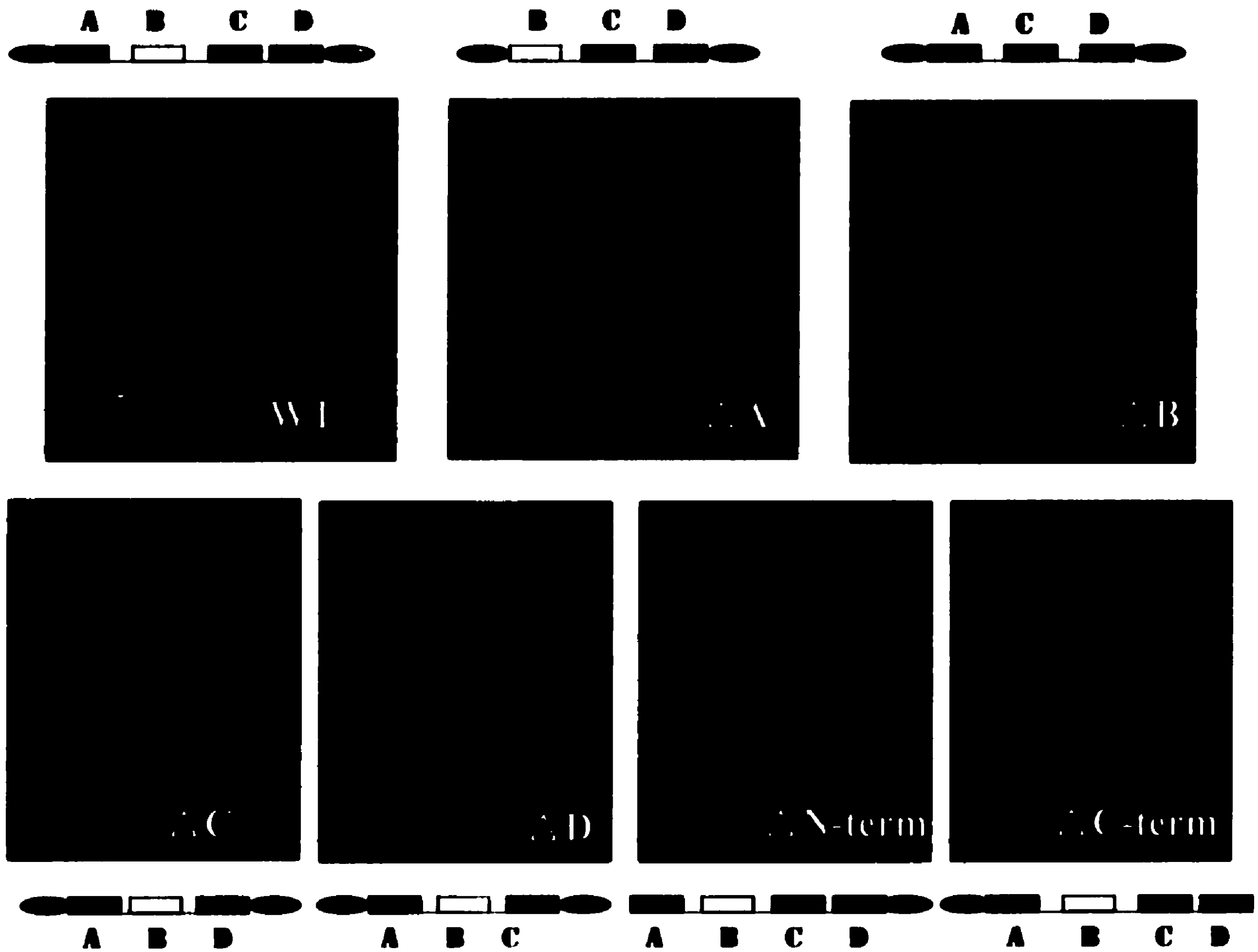

A B C D
WT
B C D
ΔA
A C D
ΔB
ΔC
A B D
ΔD
A B C
ΔN-term
A B C D
ΔC-term
A B C D

Figure 3-20: Colocalization of wild type and truncated prosaposin in COS-7 cells. Colocalization of wild type and truncated prosaposins after immunostaining with anti-myc antibody and LysoTracker LysoTracker (red fluorescence) overlapped with punctate structures stained with anti-myc monoclonal antibody (green fluorescence). A partial overlap was detected on a Golgi-like perinuclear region in wild type, Pro-WT (WT), and ΔN-term (panel A), ΔA, ΔB, ΔC and ΔD mutants (panel B). No overlap of punctate structures stained by LysoTracker was found in ΔC-term mutant (panel A) due to the absence of granular staining with anti-myc antibody.

A

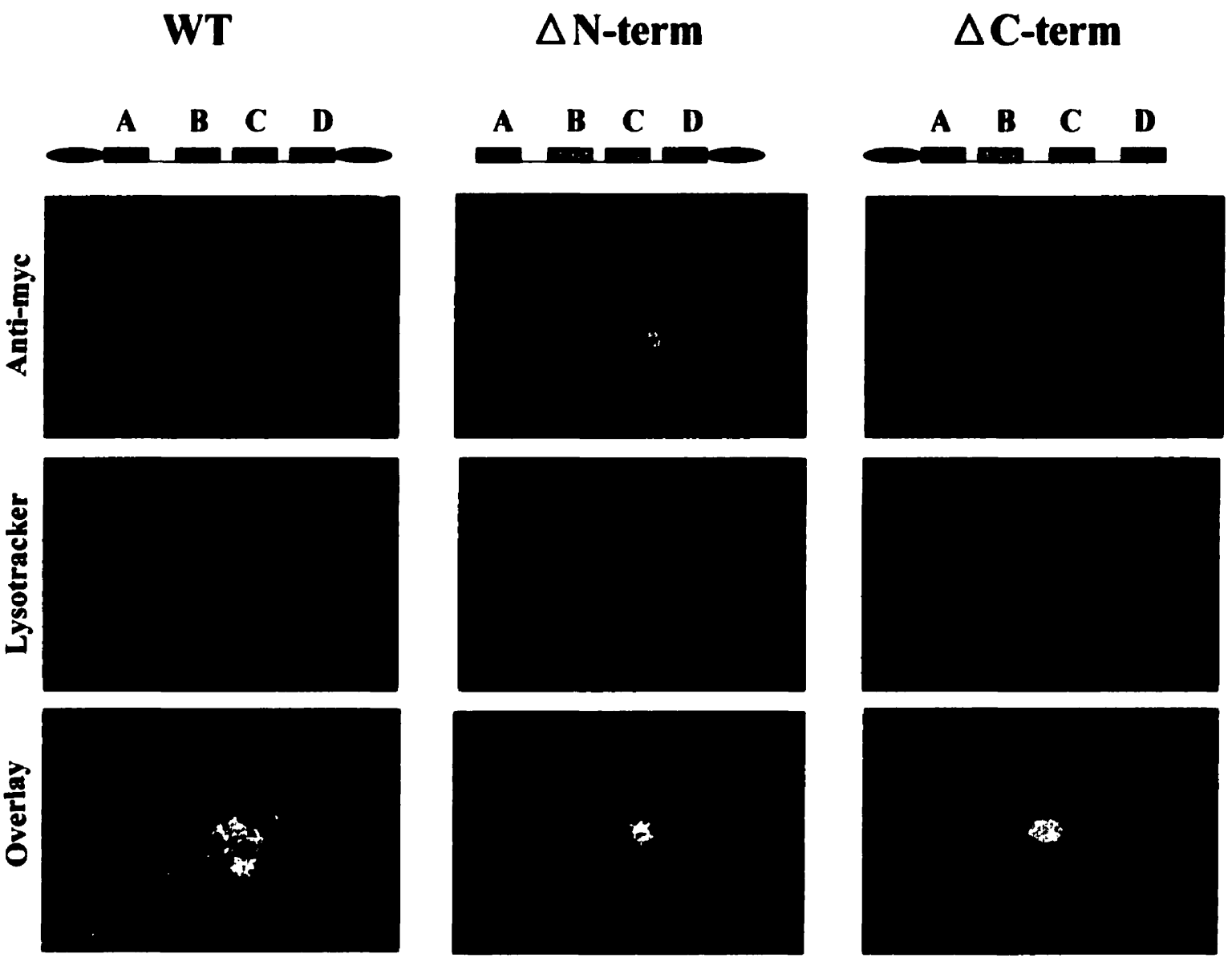
WT
ΔN-term
ΔC-term
A B C D
A B C D
A B C D
Anti-myc
Lysotracker
Overlay

B

revealed an overlap between the two antibodies in all constructs including in the ΔC-term mutant (Figure 3-21).

To further confirm the immunofluorescence results, a double immunogold labeling was conducted on COS-7 cells transfected with the Pro-WT, ΔA, ΔB, ΔC, ΔD, ΔC-term and ΔN-term constructs and analyzed by electron microscopy. To accomplish this objective, goat anti-mouse IgG conjugated to 10 nm gold was used to detect the monoclonal myc antibody, and goat anti-rabbit IgG conjugated to 15 nm gold was used to detect the rabbit pro-cathepsin B antibody. The results showed a strong labeling with 10 nm gold particles and a weak labeling with the 15 nm gold particles of electron dense membrane bound structures in COS-7 cells transfected with the Pro-WT, ΔA, ΔB, ΔC, ΔD and ΔN-term (Figure 3-22). These structures were considered to be lysosomes. However, in cells transfected with the ΔC-term construct, no labeling was found with anti-myc antibody in the lysosomes.

3.5.3 Metabolic Labelling Study

To study the biosynthetic processing of the wild type and truncated prosaposin in vivo, to examine whether they were properly folded within the endoplasmic reticulum (ER) and therefore transported to their destinations, pulse chase experiments were conducted using Trans^{35}S-label. COS-7 cells transfected with pcDNA3.1B vector alone or containing the Pro-WT and the truncated constructs were incubated with Trans^{35}S-label for 30 min and chased for 30 min and 2h. Cell lysates and samples from the medium were

Figure 3-21: Colocalization of ΔC-term mutant and mannosidase II. Anti-mannosidase II polyclonal antibody was used as a Golgi marker and visualized with a TRITC conjugated goat anti-rabbit antibody. ΔC-term mutant was stained with anti-myc monoclonal antibody and visualized with a FITC conjugated goat anti-mouse antibody. An overlap between the myc (green fluorescence) and mannosidase II (red fluorescence) antibodies was observed in a Golgi-like perinuclear region of COS-7 cells transfected with the ΔC-term construct. This result demonstrated that prosaposin mutations did not affect the transit of the truncated protein from the ER to the Golgi apparatus.

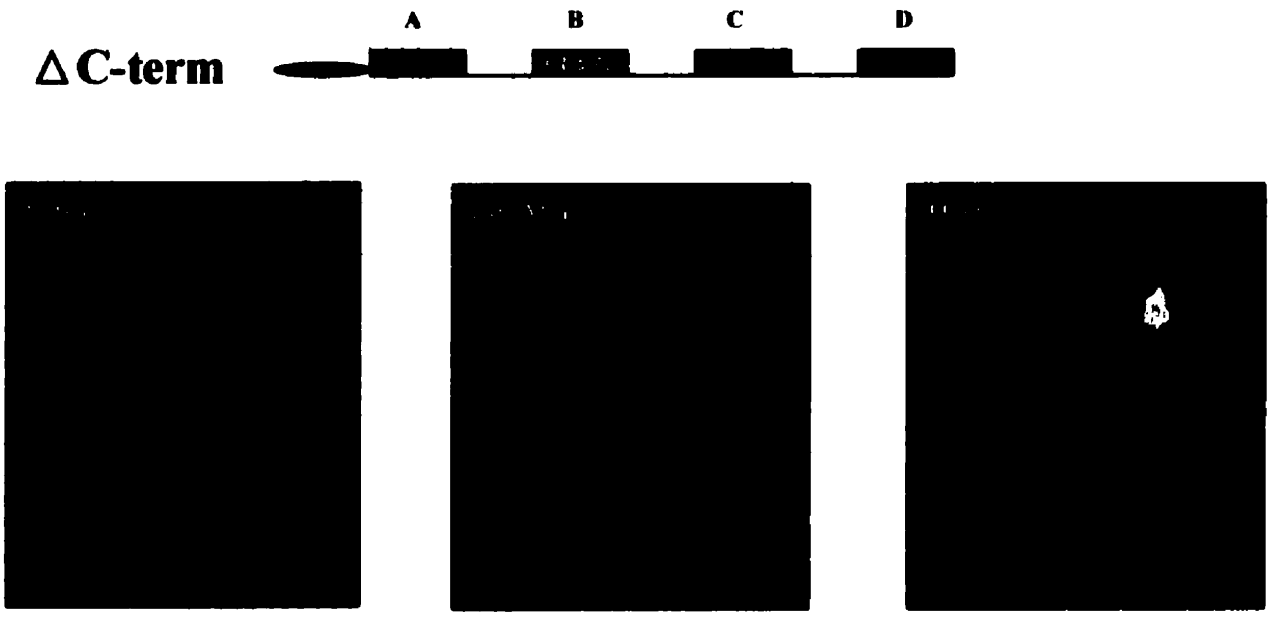
A
B
C
D
ΔC-term

Figure 3-22. Immunogold labeling of COS-7 cells transfected with Pro-WT (WT), ΔN-term, ΔA, ΔB, ΔC, ΔD and ΔC-term constructs. Goat anti-mouse IgG conjugated to 10 nm gold particles was used to detect monoclonal myc antibody. Goat anti-rabbit IgG conjugated to 15 nm gold particles (encircled) was employed to detect polyclonal pro-cathepsin B antibody used as a lysosomal marker. A strong immunogold labeling with 10nm gold particles and weak immunogold labeling with 15 nm gold particles were observed within the lysosomes of COS-7 cells transfected with the Pro-WT, ΔN-term, ΔA, ΔB, ΔC and ΔD constructs. No labeling with anti-myc antibody was found in the lysosomes of COS-7 cells transfected with ΔC-term mutant. Negative control (con) was immunogold labeled in absence of the primary antibodies.

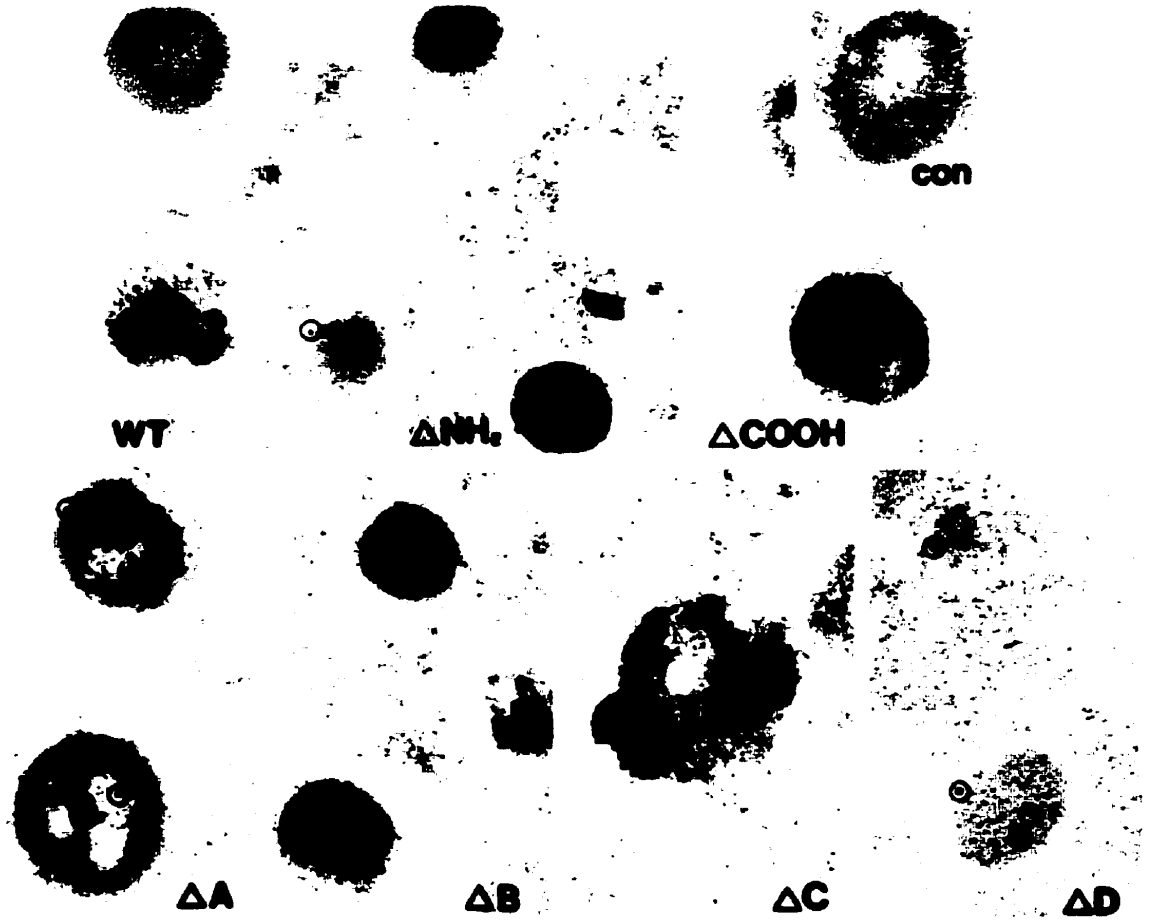
con
WT
ΔNH2
ΔCOOH
ΔA
ΔB
ΔC
ΔD

immunoprecipitated with anti-myc antibody and then subjected to SDS-polyacrylamide gel electrophoresis and fluorography. As shown in Figure 3-23A, the 65 kDa form was visualized after 30 min in Pro-WT and in each of the truncated mutants including the ΔC-term. After chasing for 2 hours, the amount of 65 kDa protein decreased in cell lysates while the 70 kDa secretory protein increased in the spent media. In the mutants, the equivalent of the 65 kDa and 70 kDa proteins were slightly smaller due to their truncation. In the case of the ΔC-term mutant, the increase of the secretory form in the medium was more prominent as confirmed by densitometry (Figure 3-23B). These data suggest that cells transfected with the Pro-WT and the truncated mutants including ΔC-term, produced properly folded proteins within the ER, and that the transport to the Golgi apparatus and secretion in the media was not altered.

Although the ΔC-term mutation abolished the transport of prosaposin to the lysosomes, it did not interfere with its secretion. Since the ΔC-term mutant protein did not reach the lysosomes, it was predicted that COS-7 cells transfected with this construct would not yield mature saposins as oppose to cells transfected with the Pro-WT construct. To confirm if this was the case, cells transfected with ΔC-term and Pro-WT were subjected to a longer pulse labeling experiment with Trans^{35}S-label (Figure 3-24) to detect the proteolytically cleaved saposins. After 5 hours of labeling, cell lysates were immunoprecipitated with anti-prosaposin antibody, which recognizes both prosaposin and mature lysosomal saposins. The immunoprecipitates were resolved in a 15% tricine-SDS-PAGE and fluorographed. Wild type 65-70 kDa and ΔC-term slightly smaller prosaposins were detected in

Figure 3-23. Effect of truncation on the synthesis, targeting and processing of prosaposin. Pulse chase analysis of COS-7 cells transfected with pcDNA3.1B alone (V), or with the same vector containing Pro-WT (WT) and truncated constructs ΔN-term, ΔA, ΔB, ΔC, ΔD and ΔC-term. Cells were pulsed with Trans^{35}S-label (300uci/ml) for half-hour and chased for 30 min and 2 h. Cell lysates and culture medium were immunoprecipitated with anti-myc antibody and subjected to 10% SDS-PAGE and fluorographed. (A) Both the 70 kDa and 65 kDa prosaposins were present intracellularly. (B) In the medium, only the 70 kDa secretory form was present.

A.

Pulse: 0.5 hour	Cell							
	Vector	WT	ΔC-term	ΔA	ΔB	ΔC	ΔD	ΔN-term
Chase : (hour)	0 0.5 2	0 0.5 2	0 0.5 2	0 0.5 2	0 0.5 2	0 0.5 2	0 0.5 2	0 0.5 2

70 kDa
65 kDa

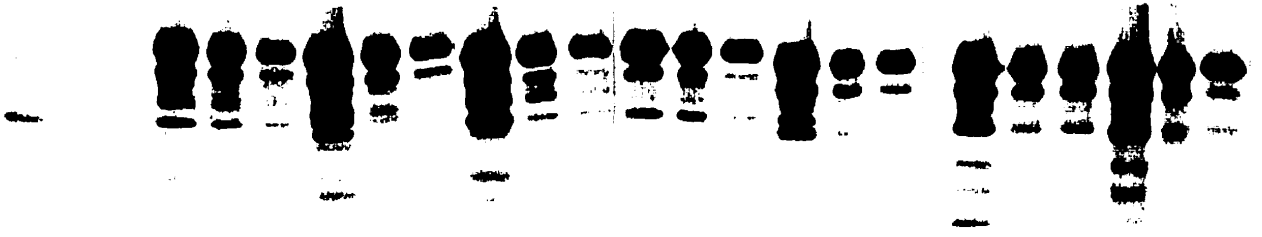

B.

Pulse: 0.5 hour	Medium							
	Vector	WT	ΔC-term	ΔA	ΔB	ΔC	ΔD	ΔN-term
Chase : (hour)	0 0.5 2	0 0.5 2	0 0.5 2	0 0.5 2	0 0.5 2	0 0.5 2	0 0.5 2	0 0.5 2

70 kDa →

Figure 3-24: Detection of mature saposins in COS-7 cells transfected with Pro-WT and ΔC-term after labeling with Trans^{35}S-label. COS-7 cells transfected with Pro-WT (WT) and ΔC-term were labeled with Trans^{35}S-label (300uci/ml) for 5 hours prior to immunoprecipitation with anti-prosaposin antibody. Immunoprecipitates were subjected to a 15% Tricine-SDS-PAGE followed by fluorography. A 15 kDa band corresponding to saposins was observed in cells transfected with the Pro-WT but absent in cells transfected with the ΔC-term. The major band (65 kDa) in WT and a slightly smaller band in the ΔC-term mutant represent the lysosomal precursor of saposins. COS-7 cells transfected with pcDNA3.1B vector alone were used as negative control.

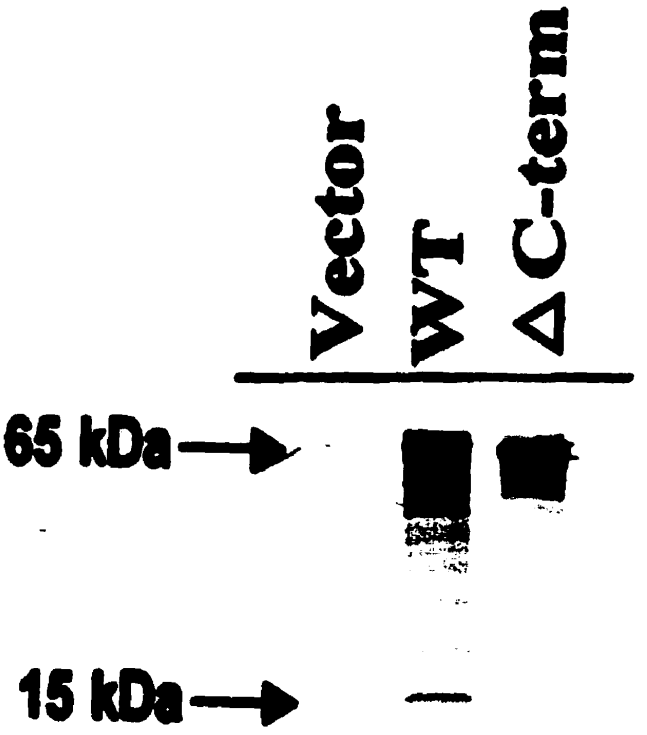
Vector
WT
Δ C-term
65 kDa
15 kDa

cell lysates (Figure 3-24). As expected, mature saposins were not observed in cells transfected with the ΔC-term construct but were present in the cells transfected with the Pro-WT construct.

3.5.4 Addition of Prosaposin Functional Domains to a Secretory Protein

To determine whether the C-terminus alone was sufficient for intracellular targeting, a chimeric protein encoding the full length cDNA of albumin plus the C-terminus of prosaposin (Alb/Pro-c-term) was constructed and subcloned into the pcDNA3.1B vector and transfected into COS-7 cells. Wild type albumin cDNA was also prepared as a control (Alb) (Figure 3-25). Albumin is a secretory protein, which reaches the extracellular space by constitutive secretion. After transfection, cells were immunostained with anti-myc antibody, followed by a secondary FITC conjugated goat anti-mouse antibody. Some cells were simultaneously stained with LysoTracker. Myc antibody (green fluorescence) produced a perinuclear Golgi-like reaction (Figure 3-26). However, the punctate structures stained by LysoTracker (red fluorescence) did not react with anti-myc antibody. This suggested that the C-terminus alone was insufficient to drive albumin to lysosomes. Based on this result and on the mutational analysis of prosaposin, it was hypothesized that one or more saposin domains should also be present along with the C-terminus to direct albumin to the lysosomes.

To test this hypothesis, a chimeric protein was engineered by fusing an albumin cDNA with nucleotide sequences encoding domain D and the C-terminus of prosaposin (Alb/Pro-D, c-term). In addition, an albumin fusion protein

Figure 3-25: Chimeric constructs of albumin with partial prosaposin functional domains. Alb-WT (1-551) is the wild type albumin subcloned into pcDNA 3.1 B vector. Alb/Pro-c-term represents the chimera of albumin attached by the C-terminus (522-556) of prosaposin at its 3' end; Alb/(Pro-D+Pro-c-term) represents the chimera of albumin fused with domain D (434-552) plus the C-terminus of prosaposin; and Alb/(Pro C, D +Pro-c-term) represents the chimera of albumin fused with domain C (309-396), D and the C-terminus of prosaposin. Numbers indicate the amino acids of albumin in black or prosaposin in the same colors as the attached parts.

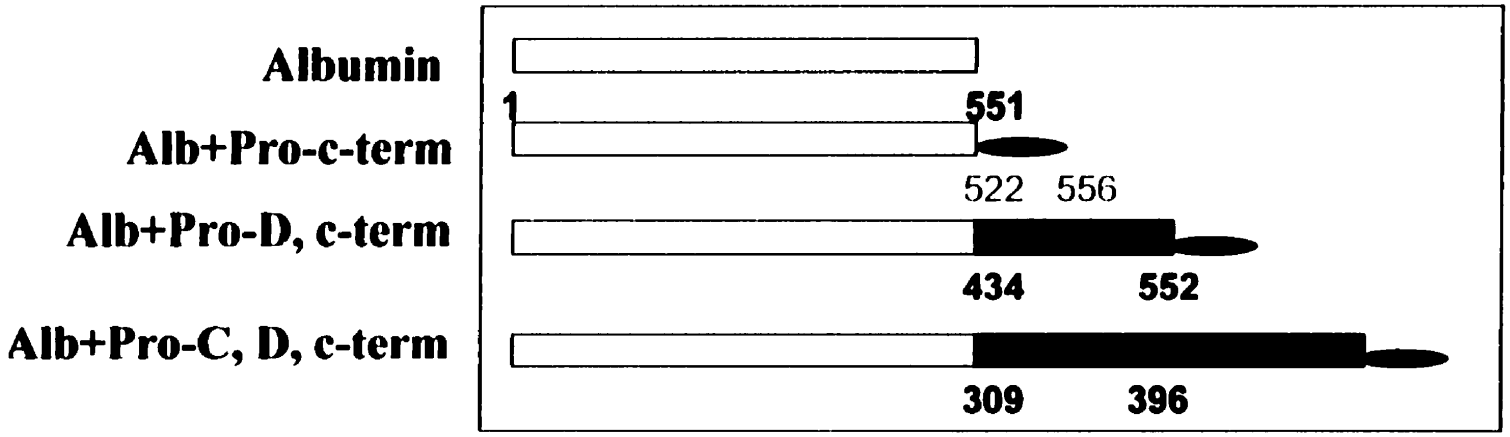
Albumin
1
551
Alb+Pro-c-term
522
556
Alb+Pro-D, c-term
434
552
Alb+Pro-C, D, c-term
309
396

Figure 3-26: Expression and targeting of chimeric constructs

(A) Targeting of chimeric proteins to the lysosomes. A typical Golgi-like reaction (green fluorescence) was observed in COS-7 cells transfected with Alb/Pro-c-term as well as with the wild type albumin (Alb-WT). A Golgi-like reaction plus a prominent lysosome-like staining was achieved with the Alb/(Pro-D+Pro-c-term) and Alb/(Pro-C,D+Pro-c-term) constructs (green fluorescence). LysoTracker staining (red fluorescence) was seen in COS-7 cells transfected with the different constructs. The punctate reaction obtained with anti-myc (green fluorescence) in Alb/(Pro-D+Pro-c-term) and Alb/(Pro-C,D+Pro-c-term) overlapped with LysoTracker staining (red fluorescence). This experiment demonstrated that prosaposin domain plus the C-terminus are required for the transport of albumin to the lysosomes.

(B). Western blot analysis of wild type and albumin chimeric proteins. COS-7 cells transfected with wild type albumin (Alb-WT) and chimeric constructs Alb/Pro-c-term, Alb/(Pro-D+Pro-c-term), and Alb/(Pro-C,D+Pro-c-term) were lysed and subjected to a 10% SDS-PAGE, transferred onto a nylon membrane, and immunostained with anti-myc monoclonal antibody. Molecular weight of wild type albumin (Alb-WT) is indicated by an arrow (66 kDa). Other bands with higher molecular weights correspond to the chimeric proteins.

containing domains C and D plus the C-terminus of prosaposin (Alb/Pro-C, D, c-term) was also constructed (Figure 3-25). Anti-myc antibody yielded a punctate reaction in both chimeras (Figure 3-26) which overlapped with LysoTracker staining. Western blotting with myc antibody confirmed the expression of wild type and chimeric albumin proteins (Figure 3-26).

3.6 Endo H Treatment of Prosaposin

The difference between the 65 kDa and 70 kDa prosaposins is due to their glycosylation state [168]. To determine the structures of their N-linked carbohydrates, and to identify the potential sorting compartment for the lysosomal precursor within the Golgi apparatus, endoglycosidase H digestion was performed on immunoprecipitated proteins. Anti-myc antibody was used to immunoprecipitate recombinant prosaposins from lysates of COS-7 cells transfected with wild type Pro-WT and mutated constructs. Results (Figure 3-27) revealed that in all cases, the 65 kDa band shifted to a 53 kDa band which corresponds to the molecular weight of the native form of prosaposin [168]. The less prominent protein band corresponding to the 70 kDa protein was resistant to Endo H treatment. Similarly, the 70 kDa secretory protein immunoprecipitated from the medium was Endo H resistant (Figure 3-27). This result suggested that the 65 kDa lysosomal form of prosaposin exits from the cis/medial compartment of the Golgi while the 70 kDa protein traversed the Golgi apparatus completing its terminal glycosylation.

Figure 3-27. Treatment with endoglycosidase H (Endo H) of COS-7 cells transfected with wild type Pro-WT (WT) and ΔN-term, ΔA, ΔB, ΔC, ΔD and ΔC-term prosaposin constructs.

After transfection with Pro-WT and truncated constructs, COS-7 cells were labeled with Trans^{35}S-label (300uci/ml) for 30 min and chased for 2 h. Cell lysates and culture medium were immunoprecipitated with anti-myc antibody and incubated with Endo H (1U) at 37^{0}C for 16 h. Immunoprecipitated proteins were resolved in a 10% SDS-PAGE followed by fluorography.

(A) In cell lysates the 65 kDa protein band shifted to a 53 kDa band and the less prominent 70 kDa band remained unchanged (Endo H +). Similar band patterns were also observed with the truncated prosaposins (ΔN-term, ΔA, ΔB, ΔC, ΔD and ΔC-term) with slightly smaller molecular weights due to the truncations.

(B) In culture medium the 70 kDa (WT) band, representing the secretory form of prosaposin, was not modified after incubation with Endo H. Similar results were obtained with truncated prosaposins (ΔN-term, ΔA, ΔB, ΔC, ΔD and ΔC-term). COS-7 cells transfected with the vector alone (Vector) was used as a negative control.

A

	Cell							
	Vector	WT	ΔC-term	ΔN-term	Δ A	Δ B	Δ C	Δ D
Endo H	- + - +	- + - +	- + - +	- + - +	- + - +	- + - +	- + - +	- + - +
Chase: (hour)	0 0 2 2	0 0 2 2	0 0 2 2	0 0 2 2	0 0 2 2	0 0 2 2	0 0 2 2	0 0 2 2

B

	Medium							
	Vector	WT	ΔC-term	ΔN-term	Δ A	Δ B	Δ C	Δ D
Endo H	- + - +	- + - +	- + - +	- + - +	- + - +	- + - +	- + - +	- + - +
Chase: (hour)	0 0 2 2	0 0 2 2	0 0 2 2	0 0 2 2	0 0 2 2	0 0 2 2	0 0 2 2	0 0 2 2

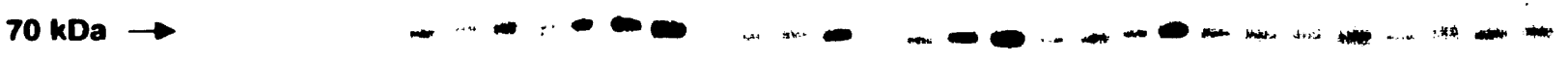

3.7 Treatment with Brefeldin A (BFA)

To verify whether the Golgi apparatus was the site where the 65 kDa lysosomal precursor was sorted, brefeldin A (BFA) was used prior to Trans^{35}S-labeled pulse chase experiments. BFA is a fungal metabolite that causes rapid redistribution of the components of the Golgi apparatus to the endoplasmic reticulum (ER) [219, 220]. COS-7 cells transfected with the wild type prosaposin (Pro-WT) were incubated with BFA 1 hour prior to Trans^{35}S-labeling. In the presence of BFA, the amount of intracellular protein in cell lysates remained unchanged after chasing for 4h, while in cells not treated with BFA, the amount of protein decreased after chasing for 2h (Figure 3-28). In the medium of cells incubated with BFA, there was a very low amount of the 70 kDa protein after chasing for 30 min, 2h and 4h. This indicated that the 70 kDa secretory protein present before the supplementation of BFA was beyond the proximal compartment of the Golgi apparatus. In contrast, in cells incubated without BFA, the amount of protein in the medium increased after 30 min and 2h (Figure 3-28). Taken together, these data suggest that the 65 kDa lysosomal precursor contains mainly high mannose sugar residues and that it is present in the proximal aspect of the Golgi apparatus. On the other hand, the 70 kDa secretory form is glycosylated with complex/hybrid sugar residues and appear to exit from the distal region of the Golgi apparatus.

Figure 3-28: Pulse chase of COS-7 cells transfected with the wild type prosaposin (Pro-WT) treated with Brefeldin A (BFA). Cells were incubated with BFA (20ug/ml) (+BFA) 1 hour prior to the addition of Trans^{35}S-label (300uci/ml). Replicas of COS-7 cells were grown in absence of BFA and used as controls. After labeling for 30 min, cells were chased for an additional 30 min, 2 h and 4h. Immunoprecipitates of cell lysates and culture medium were resolved in a 10% SDS-PAGE and fluorographed. BFA caused intracellular retention of the 65 kDa protein. In control cells, the 65 kDa protein decreased intracellularly, while the 70 kDa protein increased in control medium.

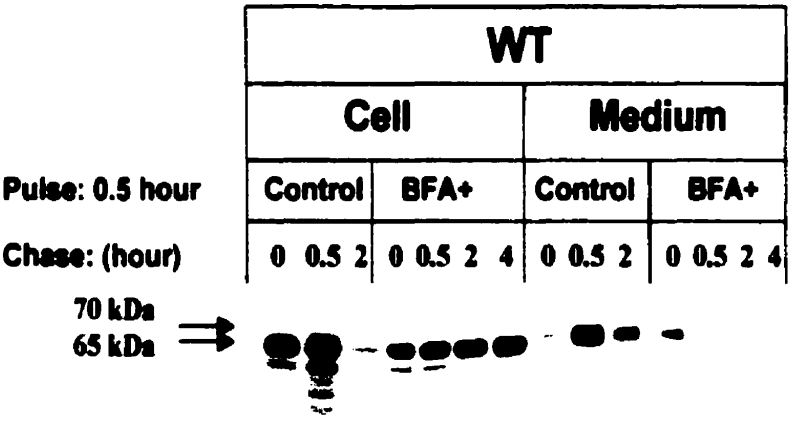
WT
Cell
Medium
Pulse: 0.5 hour
Control
BFA+
Control
BFA+
Chase: (hour)
0 0.5 2
0 0.5 2 4
0 0.5 2
0 0.5 2 4
70 kDa
65 kDa

3.8 Effect of the Disruption of the Prosaposin Gene on the Male Reproductive System

Saposin A-D are well established sphingolipid activator proteins which function as essential cofactors for physiological degradation of sphingolipids with relatively short hydrophilic oligosaccharide chain [31]. Besides, another identified sphingolipid activator protein, G_{M2} activator protein, is known to stimulate the degradation of G_{M2} ganglioside and asialo G_{M2} gangliosides (GA2) by β-hexosaminidase A.

The product of the prosaposin gene appears to have other important physiological functions in vivo in addition to its role as sphingolipid activators. The following postulated functions have been assigned to the product of prosaposin gene based on the experimental evidence: 1) As a neurotrophic factor, prosaposin appears to be involved in stimulating neurite outgrowth in murine cells and choline acetyltransferase activity in human neuroblastoma cells [3]; 2) As a ganglioside binding/transport protein [165], the secretory form of prosaposin may be involved in glycolipid modification of certain cell membranes, such as in Sertoli and germinal cells, which may play a role in processes such as the induction of spermiation [1, 152]; 3) As one of the major glycoproteins secreted by Sertoli cell in the male reproductive system, prosaposin may play a role in the regulation of spermatogenesis [152] and in gonadal development [221].

The recent development of a prosaposin -/- mouse model has provided an opportunity to explore the functions of prosaposin in various tissues [10]. Inactivation of the prosaposin gene causes accumulation of multiple

glycosphingolipids within the lysosomes of affected cells, such as, lactosylceramide, glucosylceramide, digalactosyl ceramide, sulfatide, ceramide, and globotriaosylceramide [10]. Ultrastructural analysis of these cells shows an accumulation of undigested membranes in multivesicular bodies. However, there is lack of information on the effect of disruption of prosaposin gene in male reproductive system. Morphological investigations were performed in the present study to analyze the abnormalities in relationship with the development of the male reproductive organs including the testis, the prostate gland, the seminal vesicles and epididymis by anatomical examination, and under the light and electron microscopes. The heterozygous mice from the same littermates were used as comparison.

3.8.1 Anatomical Examination of the Affected Organs

A morphometric analysis of the organs of the male reproductive system of 37 day old mice reveals that disruption of the prosaposin gene produces a reduction in size and weight of 30% of the testes, 37% of the epididymis, 75% of the seminal vesicles and 60% of the prostate glands (Figure 3-29). Seminal vesicles and dorsal lobules of prostate gland are significantly smaller in the prosaposin homozygous mutant.

3.8.2 Examinations under Light Microscope on the Affected Testes, Prostate Gland, Seminal vesicles and Epididymis

Light microscopy showed that small sized testes from homozygous mutant

Figure 3-29: Male reproductive organs affected by the inactivation of prosaposin gene (-/-) as compared to heterozygous organs (+/-) from mice of the same age (37 days old). a, b, Seminal vesicles (stars) and ventral lobules of prostate gland (arrows). c, Testes; d, Epididymis. Note that inactivation of the prosaposin gene caused a significant reduction in size of the male reproductive organs.

mice, is associated with reduced spermiogenesis, with the late spermtids being particularly affected (Figure 3-30). Involution of the prostate glands in homozygous mutant affects equally the dorsal and ventral lobules. Light microscope showed that the diameter of the tubuloalveolar glands is considerably reduced and that the prostatic epithelial cells were shorter in homozygous mutant than in heterozygous and normal control animal mice of the same age (Figure 3-30). In addition, in the homozygous mice, secretion in the lumen of prostate gland disappears, and there is a tremendous increase in interstitial connective tissues among alveolar glands in a disorganized appearance. Smaller tubular diameter and shorter undifferentiated epithelial cells were also observed in seminal vesicles and epididymis (data not shown). Interestingly, in efferent ducts of homozygous mutants, the lining epithelia is formed almost exclusively by ciliated cells in contrast to the heterozygous which show a majority of non ciliated cells in this epithelium (Figure 3-31).

3.8.3 Testosterone Measurements

To determine the relationship between the involution of the the testis in prosaposin homozygous mice with the level of blood testosterone, radioimmunoassay of blood samples from prosaposin homozygous (-/-) and prosaposin heterozygous (+/-) mice (as control) (n=6) was analyzed, results (Figure 3-32) demonstrated that blood testosterone levels are normal or higher in mice with the inactivated prosaposin gene.

Figure 3-30: Light microscopy of male reproductive organs affected by the inactivation of prosaposin gene (-/-) as compared to the same organs of heterozygous (+/-) littermates of the same age (37 days). a, b, testes from homozygous (a) and heterozygous (b) mice. A reduced number of late spermatids, is observed in the lumen of seminiferous tubules (stars), prior to spermiation, in homozygous testis as compared to heterozygous testis (stage VIII of the seminiferous epithelium cycle) x400. Section of ventral prostate showing a smaller diameter of the tubuloalveolar glands in homozygous mutant (c) as compared to the heterozygous (d) x400. Only one layer of cells lines the tubuloalveolar glands in homozygous mutant indicating that the epithelium is composed of basal cells. In heterozygous both basal and secretory cells are present and the tubuloalveolar glands contain secretory product. Scale bar, 12.5 um.

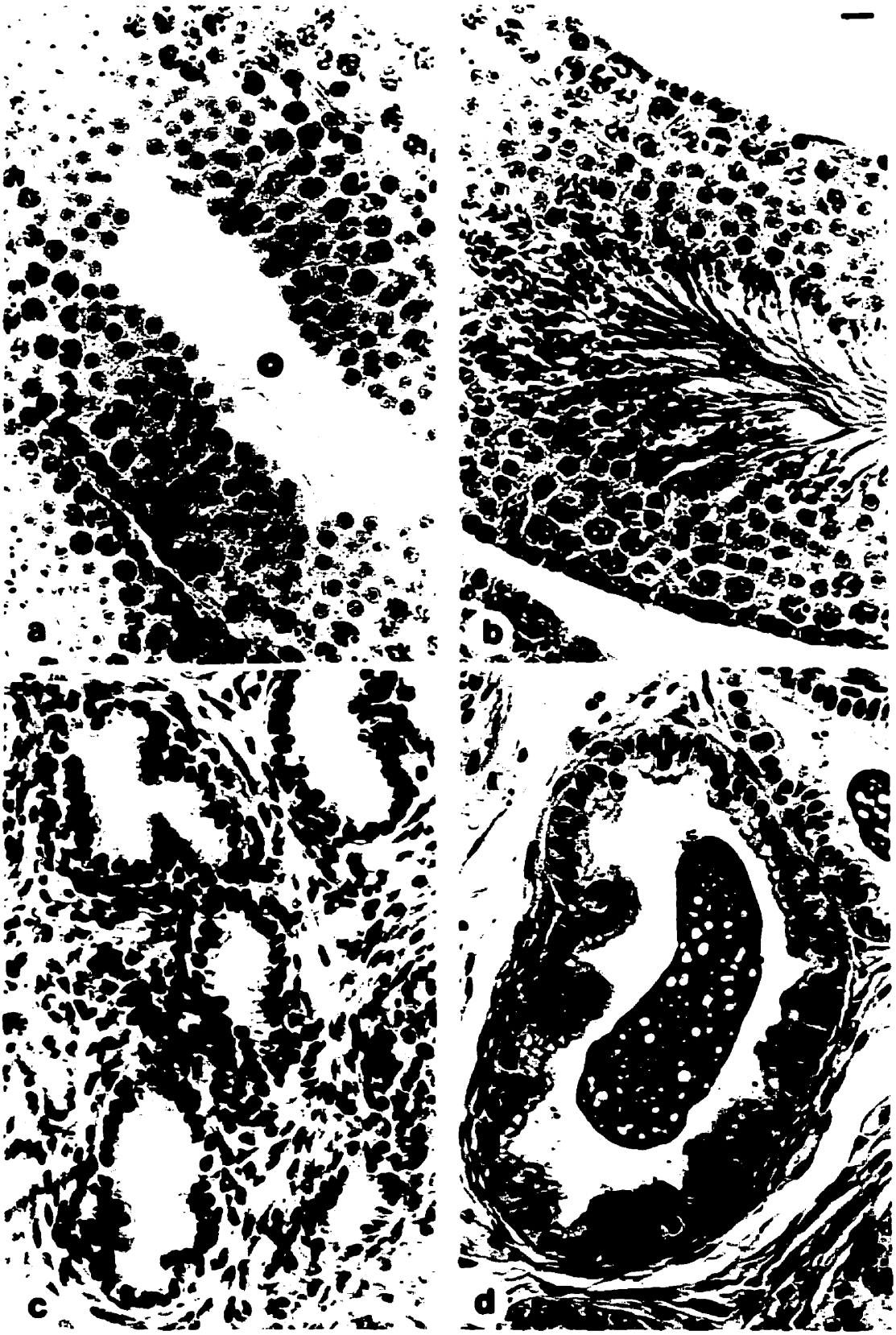
a
b
c
d

Figure 3-31: Electron micrographs of efferent ducts. A, homozygous mutant (-/-) x18,000. Scale bar, 270nm. B, heterozygous (+/-) x9,000. Scale bar, 540 nm. Notice in homozygous, that ciliated cells (arrow) predominate over nonciliated cells (aterisks). Ciliated cells from homozygous often contain large irregular multivesicular bodies (arrowheads). L, lumen.

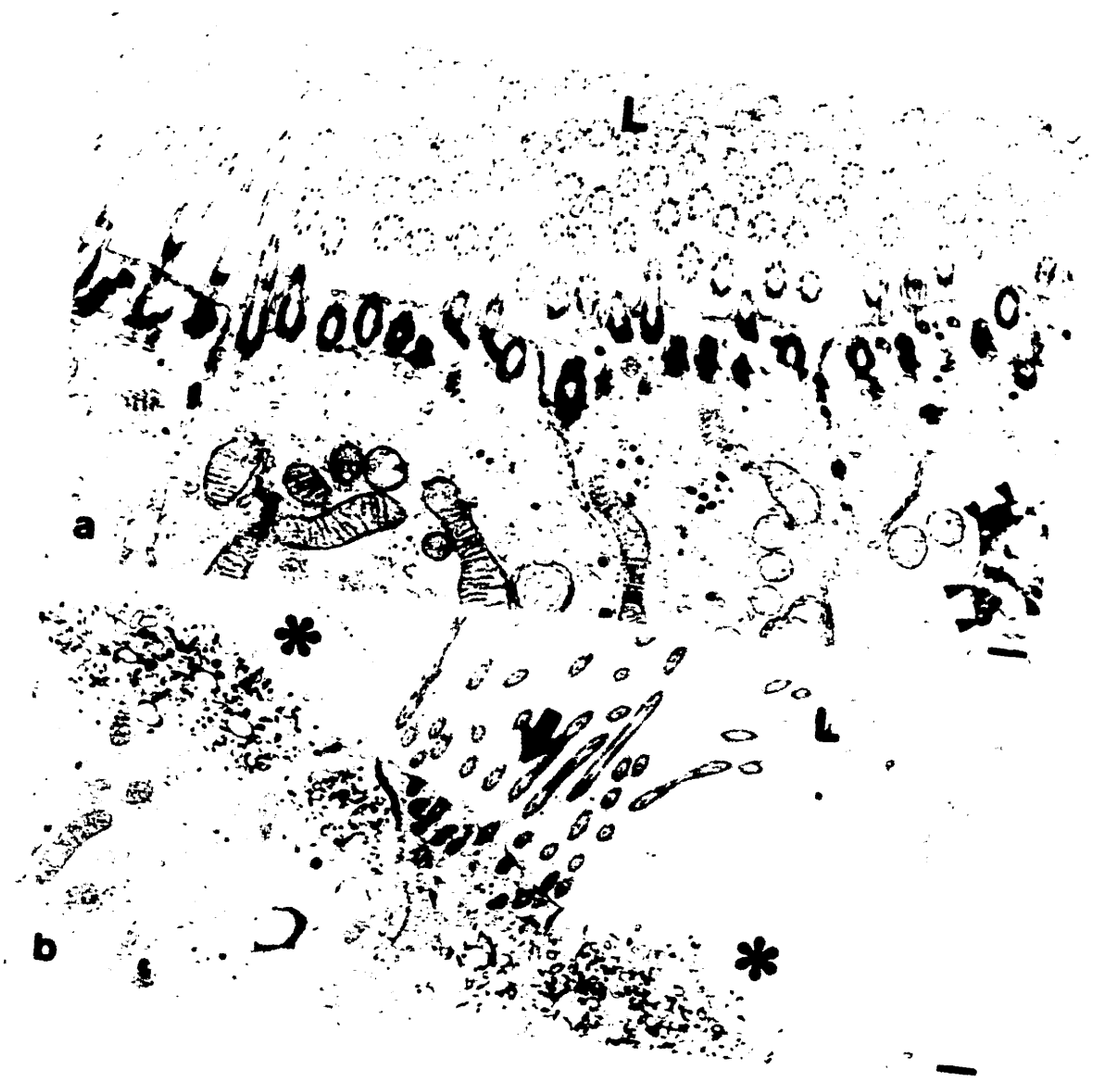
L
a
*
L
b
*

Figure 3-32: Histogram illustrated that testosterone level is more elevated in homozygous mutant (-/-) as compared to heterozygous mice (+/-). The difference is statistically significant ($p \leq 0.005$; n=6).

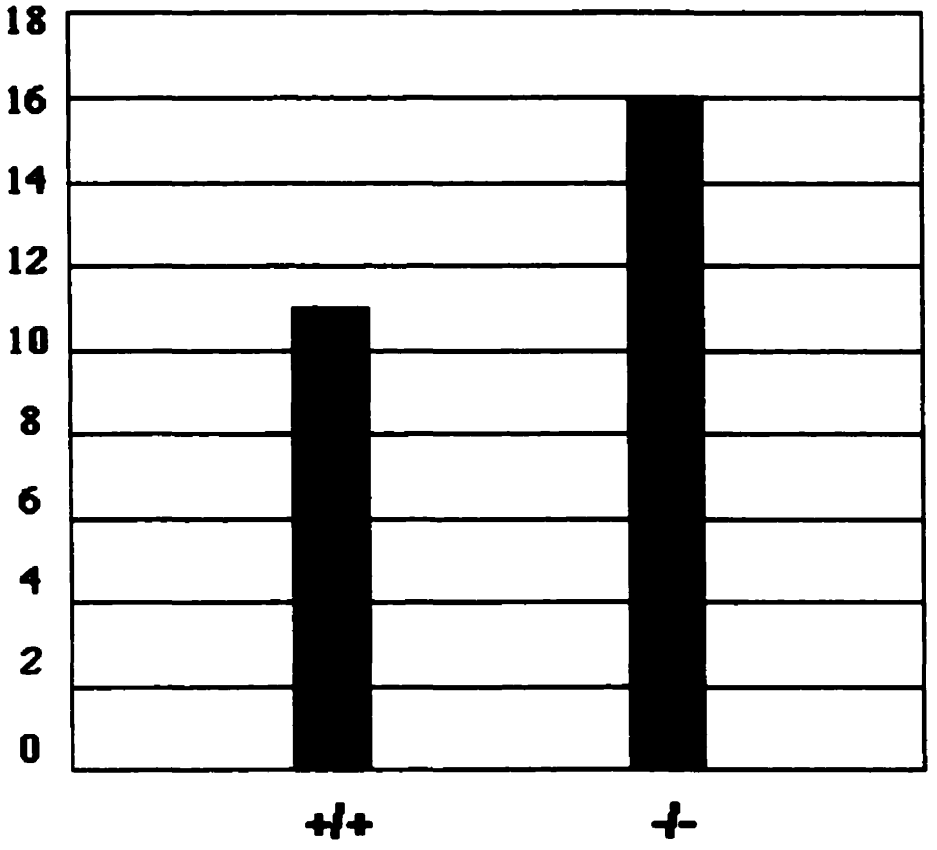
18
16
14
12
10
8
6
4
2
0
+/+
-/-

3.8.4 Expression of Androgen Receptor

To further determine whether the underdevelopment of the prostate gland and other male reproductive organs is due to downregulation of the expression level of androgen receptor, the immunostaining of prostate sections with an anti-androgen receptor antibody was performed. Results indicated that the epithelial cells lining the alveoli express androgen receptor in both the heterozygous and homozygous tissues (Figure 3-33).

3.8.5 Status of Mitogen Activated Phosphorylated Kinase (MAPK) in Prosaposin Homozygous Mice (-/-)

To examine if inactivation of the prosaposin gene could result in the inactivation of the MAPK pathway, prostate sections from homozygous and hetreozygous mice were immunostained with two monoclonal antibodies, which recognize the phosphorylated and non phosphorylated forms of ERK1/2. Sections immunostained with the antibody to the non phosphorylated form of ERK1/2 reacted with all epithelial cells in heterozygous and homozygous prostates (Figure 3-33). Sections immunostained with the antibody to the phosphorylated ERK1/2 strongly reacted with tall prostatic secretory cells in prostate from heterozygous mouse (Figure 3-33). On the other hand, the epithelial cells in the homozygous prostate remained unstained (Figure 3-33).

Figure 3-33: Immunoperoxidase staining of prostate sections with anti-androgen receptor antibody (a,b) and with nonphosphorylated MAPK (c, d) and phosphorylated MAKP antibodies (e,f). a,b, prostate sections immunostained with androgen receptor antibody. A strong nuclear staining of the alveolar cells is observed in the prostate of the heterozygous (a) and homozygous mice (b). c, d, Prostate sections immunostained with a monoclonal antibody to nonphosphorylated MAKP. A moderate reaction is observed in the epithelial cells lining the alveoli of heterozygous (c) and homozygous prostates (d). f, g, prostate sections immunostained with a monoclonal antibody to phosphorylated MAKPs. Some epithelial cells are strongly stained in the prostate of the heterozygous mouse (f). The epithelial cells in the homozygous are unstained (g). This result suggests that the MAKP pathway is inactive in the homozygous.

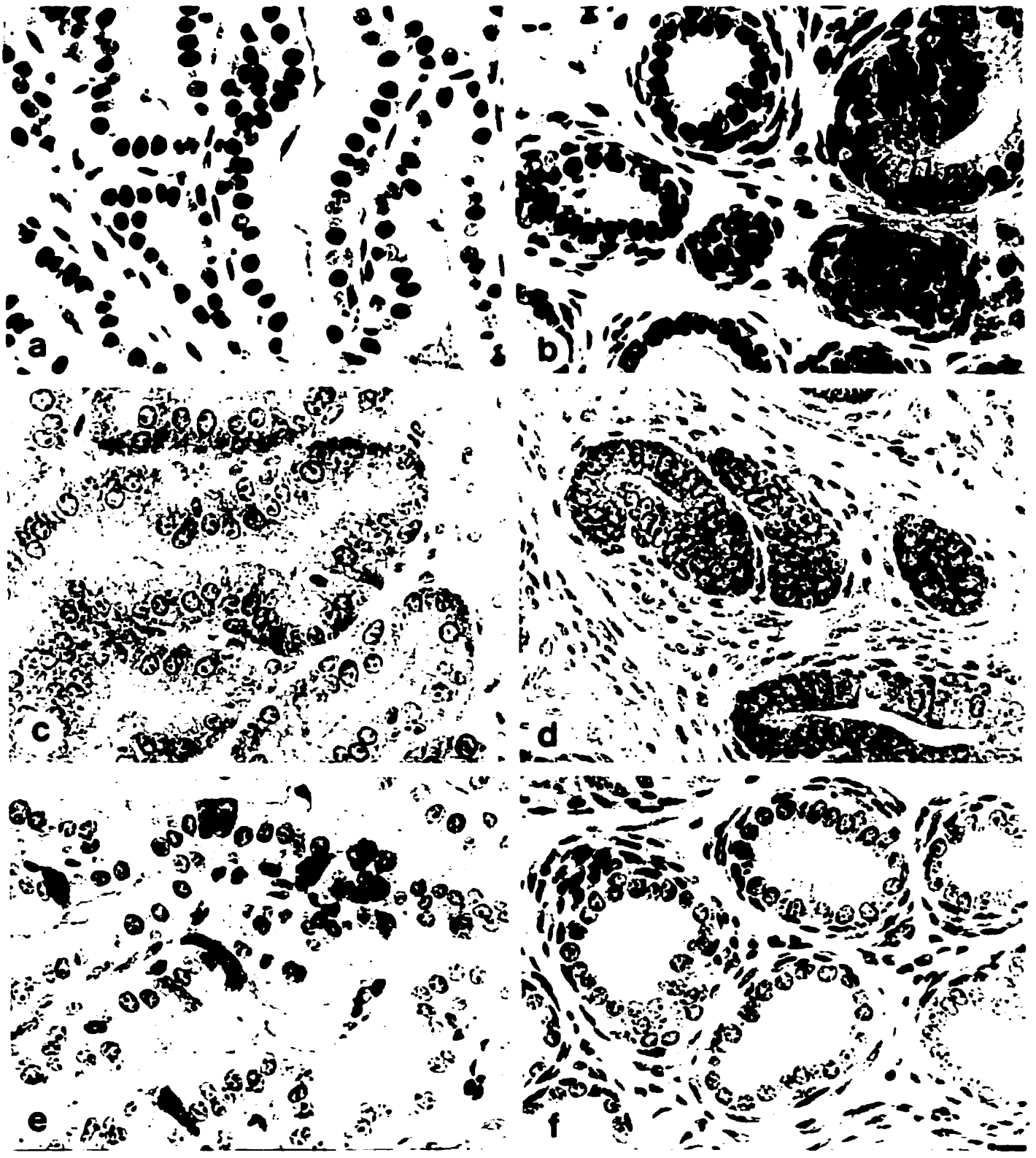
a
b
c
d
e
f

CHAPTER FOUR

Discussion

Prosaposin is a multifunctional protein with specific intracellular and extracellular functions. Intracellular prosaposin modulates the flux of glycosphingolipids in the lysosomes by promoting the activity of several lysosomal hydrolases [31]. Extracellularly, prosaposin participates in glycosphingolipids transfer between heterogeneous membranes [165]. Prosaposin may also acts as a potent neurotrophic factor that induces neurite outgrowth [3, 158] and promotes peripheral nerve regeneration [222]. Extracellular prosaposin has been found in the reproductive system of prenatal and postnatal mice [223]. Prosaposin expression is limited to the genital ridge, the primordium for both male and female gonads. In the seminiferous epithelium, the localization of prosaposin mRNA is restricted to the Sertoli cells [223] but not in germ cells of adult mice and rat. Sertoli cells are responsible for creating a unique milieu in which germ cells proliferate and differentiate. In the reproductive system the expression of prosaposin appears to be regulated by a pituitary factor [213]. Nevertheless, the function of prosaposin in the reproductive system is still unknown. Many other relavant aspects of the biology of prosaposin are still obscure, such as, the mechanism that determines when prosaposin should be targeted to the extracellular space or to the lysosomes.

Thus, the main objectives of this research are: 1) To study the structure and organization of the mouse prosaposin gene, and to compare the protein backbone structure among different species; 2) To study the mechanism of sorting and targeting of prosaposin using a mutational analysis; 3) To analyze the role of prosaposin in male reproductive system, using a prosaposin knock out mice

model (prosaposin -/-).

4.1 Structure and Function of the Mouse Prosaposin Gene and Its Translation Product

4.1.1 Structural Analysis of the Mouse Prosaposin Gene

Recently, the human prosaposin gene was cloned [175] and localized in chromosome 10q21-22 [176]. Interestingly, several genes structurally related to prosaposin, such as surfactant protein A (SP-A) and D (SP-D), also map to this region of chromosome 10 [224], suggesting that prosaposin and surfactant proteins may derive from a common ancestral gene. The close similarities of the four saposins and the analysis of the intronic positions in the human prosaposin gene also suggests that it evolved from an ancestral protosaposin gene by two duplication events and at least one gene rearrangement involving a double crossover after the insertion of introns [175, 176]. In the mouse, the prosaposin gene is also located in chromosome 10 [225], but its gene organization has not been examined yet.

In this study, we have isolated and characterized the gene encoding mouse prosaposin and disclosed its structural organization. We also examined its differential expression patterns due to alternative splicing in different tissues by applying RT-PCR. The mouse prosaposin gene consists of 15 exons, which is similar to the human prosaposin gene. The size of exons varies from nine base pairs to 298 base pairs. The size of introns varies from 89 base pairs to over 8 kilobase pairs. The sequence similarity of the coding regions of the mouse and

human prosaposin gene is striking, indicating that prosaposin is a highly conserved protein between this two species. The exons of the mouse and human genes (Table VII) have almost identical sizes except for exon 11, which lacks 93 base pairs in the human, present in the rat and mouse genes. The 93-nucleotide encodes a proline-rich region with unknown functions. The sizes of introns were generally smaller in the mouse compared to the human gene.

In the human, exon 8, contains nine base pairs (CAG GAT CAG) and encodes three amino acids (Gln-Asp-Gln) present in saposin B. An alternative splicing of exon 8 results in its exclusion from saposin B. In addition, another isoform of prosaposin containing the last two amino acids insertion may be generated via the use of an alternative acceptor site [198]. Synthetic peptides containing a putative α helix of saposin B without the Gln-Asp-Gln insertion encoded by exon 8 was shown to have different binding activities for G_{M1} ganglioside, sulfatide and sphingomyelin [226]. The insertion of the Gln-Asp-Gln sequence completely abolished the capacity of the peptide to bind to G_{M1} ganglioside, but its affinity for sulfatide and sphingomyelin was increased four-fold and two-fold, respectively. These results suggested that alternative splicing of exon 8 may change the binding specificites of saposin B presumably to adapt to the variable sphingolipid composition of tissues [226]. Alternative splicing or prosaposin in different tissues remains unknown, particularly in the mouse, due to the lack of information on the genomic structure of the prosaposin gene.

Our study revealed that the mouse gene also has an exon 8 consisting of the same nine base pairs CAG GAT CAG encoding the three amino acids within

saposin B. A close look of the intron-extron boundary of exon 8, revealed that CAGGATCAG is preceded by the intronic sequence gttcaacag (gttcaacagCAGGATCAG), which serves as the 3' acceptor splice site. Moreover, within the 9 bp exon the AG preceding the 6 bases GATCAG could also serve as an acceptor site to produce the isoform containing 6 bp, and the last AG in CAGGATCAG could equally serve as an acceptor splice site to produce the isoform lacking exon 8. In consequence, we decided to study the relative abundance of the different isoforms of alternatively spliced mRNA in various tissues using RT-PCR. Our data demonstrated that prosaposin mRNA of brain, heart and muscle contain mainly the isoform with the Gln-Asp-Gln insertion, whereas the transcripts from testis, lung, pancreas, spleen and kidney contain the smaller isoform without the Gln-Asp-Gln insertion. These results were confirmed by sequencing. The existence of the 6 bp isoform can not be ruled out considering the limitation of the gel resolution. It is tempting to speculate that alternative splicing of saposin B may alter its glycosphingolipid affinity in tissues basing on the abundance of a particular type of glycosphingolipid (e.g. sulfatide or GM1 ganglioside). However, a recent study suggested that the three human saposin B isoforms expressed in baby-hamster kidney cells are equally stable and have the same sphingolipid activator function [227]. On the other hand, Madar-Shapiro et al [221] cloned two isoforms of human prosaposin cDNAs, one with the 9 bp and one without the 9 bp, and using a T7/EMC/vaccinia virus-derived vector expressed them in human cells. The results indicated that prosaposin containing the three residues accumulated faster and in greater amounts in the medium,

whereas the prosaposin with no extra residues was mainly destined for lysosomes. The authors proposed that Gln-Asp-Gln may serve as a positive signal for secretion or as an inhibitory signal for lysosomal trafficking [221]. However, the association between alternative splicing and differential sorting of prosaposins requires experimental verification. Recently, the chicken prosaposin gene was identified and the three-amino-acid insertion of Lys-Asp-Gln was also found in saposin B domain. This isoform was found to be the most abundant [214]. Nevertheless, saposin B with three or two amino acid insertions has not been isolated from any mammalian tissues so far [228, 229]. Thus, further investigations are needed to clarify the role of exon 8. Although the mouse and human prosaposin genes have striking sequence similarity of the coding regions including the presence of exon 8, our results also showed some variations. An interesting difference between the human and mouse prosaposin genes was found in exon 11. In the mouse this exon consists of 279 nucleotide base pairs, whereas in the human gene 187 base pairs. The extra 93 nucleotide base pairs encoding 31 amino acids corresponds to a proline-rich region also found in rat prosaposin. This sequence was initially implicated in the secretory targeting of prosaposin [5, 138, 152]. However, recent findings demonstrated that the proline rich segment does not affect the routing of prosaposin to the lysosomes or to the extracellular space [11]. The proline-rich domain is perhaps the most significant difference between rodent and human prosaposin. Its role is still unknown, but the availability to these genomic clones may provide a starting point for further studies on the genetic role of this sequence.

4.1.2 Amino Acid Sequences Analysis of the Common Backbone Structures of Prosaposin among Different Species

Human and murine prosaposin cDNAs have been cloned in several laboratories [138, 152, 210, 230-232]. Although some interspecies heterogeneity exists among them, they exhibit high similarities. However, little information is available on the differences and similarities among mouse, rat and human prosaposin functional domains. In this study, we isolated the mouse and rat prosaposin cDNAs from two testicular libraries and compared to the human prosaposin cDNA sequence [210] chosen from NCBI Genebank. We decided to use our own rat and mouse cDNAs due to existing discrepancies reported by three different laboratories which could be the result of technical errors [215]. The entire amino acid residues of prosaposins, from the mouse, rat and human were aligned and compared. A pairwise comparison between the mouse and rat, the mouse and human and the rat and human was also conducted. In addition, the hydropathy profiles and their secondary structure predictions for each saposin among the three species studied were compared.

Our analysis showed functionally important amino acids, including cysteine and proline residues, and potential N-linked glycosylation sites are conserved in rodents and human. Six cysteine residues present in all four saposins are essential for building three disulfide bonds, which impart an unusual degree of stability to this molecule. Mutation of the N-linked glycosylation site in saposin B resulting in deficiency of saposin B suggested a role of the glycose

chain in protein folding and stability during biosynthesis [156]. Among the three species, saposin D displayed the highest degree of sequence identity, followed by the C-terminus, saposin A, saposin B, N-terminus and saposin C. Saposin C is the least conserved domain among the three species, but the similarity between the mouse and rat is still high (75%). The reason for the presence of a proline-rich segment (31 amino acids) in the mouse and rat but not in human was initially implicated in the secretory routing of this protein into the extracellular space [138]. However, human prosaposin is also found in various body fluids, such as human milk, seminal plasma, cerebrospinal fluids, and pancreatic juice in considerable concentrations. Therefore, it is tempting to speculate that this proline rich domain may act as a flexible hinge region linking the saposin C and D domain in rodents which permit the interaction of rodent's prosaposin with different glycosphingolipids.

Each saposin has a particularly high degree of interspecies similarity of hydrophobic amino acids. There are at least 15 hydrophobic amino acid residues in each saposin aligned in strictly conserved position among the three species. Together with this, our secondary structure predictions suggest that each saposin forms 4 amphipathic α helices and that those hydrophobic amino acids are located at the side chain of each folded helix structure, presumably facing a lipid interface. This configuration may explain the interaction of saposins with glycosphingolipid in vivo and in vitro. Interestingly, it has been noted that saposins have a remarkable structural similarity with other proteins, called SAPLIP (saposin-like proteins). All members of SAPLIP have six cysteines identical to saposins, a similar molecular

size and stability under extreme conditions. However, they do not always occur in tandem repeats as saposins. Individual saposin-like domains were found within the surfactant protein B (SP-B), *Entanmoeba hystolitica* pore-forming peptides, NK-lysin, acyloxyacyl hydrolase, acid sphingomyelinase and in a plant aspartic proteinase [177, 233]. A polypeptide motif characterized by the location of six cysteine residues and several hydrophobic residues found in saposins A-D and in the saposin-like domains of these proteins, has been linked to the affinity of this molecule for sphingolipids. No crystal structure of saposins has been determined so far, yet a NMR structure of NK-lysin [234] and a crystal structure of the plant aspartic proteinase [235] in the saposin-like proteins family, had been studied recently. Results are consistent with the present study demonstrating the characteristics of the high conservations of α-helical structure and the position of the hydrophobic amino acids.

The hydropathy profile is characteristically conserved among the same saposins. The profile of saposin B is nearly superimposable in all species except in the domain encoded by exon 8. The presence of the QDQ insertion increases dramatically the local hydrophilicity of the mouse and human prosaposin. As indicated above, alternative splicing of exon 8 may change the binding specificity of saposin B to adapt the function of this protein to the variable sphingolipid composition of different tissues. Thus, the change in hydrophilicity, as a result of the presence or absence of the QDQ insertion, may be important for the specific functions of saposin B.

Another significant difference in the hydropathy profile was noticed in

saposin C domain. An increase in its local hydrophilicity at the amino acid end of saposin C was also dramatic. This coincides with the location of a 12 amino acid which has been identified to have neurotrophic activity.

4.2 Study of the Mechanisms of Transport of Prosaposin to the Lysosomes

4.2.1 Identification of A Novel Sequence Involved in Lysosomal Targeting of Prosaposin

Lysosomes and as a 70 kDa secretory form that is secreted to the extracellular space [4, 153]. Time course experiments demonstrated that the 65 kDa form is derived from post-translational modification of a 53 kDa native protein and that precedes the 70 kDa secretory prosaposin [168]. Prosaposin is highly conserved from avian to mammals [214, 215]. Conserved regions of prosaposin include four saposin domains designated A, B, C, D [179] and its N- and C-termini. Little or no conservation exist among the linker regions found between domains A-B, B-C and C-D [214, 215]. In lysosomes, the 65 kDa protein is cleaved into four sphingolipid activator proteins termed saposins A-D which are essential cofactors for the hydrolysis of glycosphingolipids with short oligosaccharide chains by specific hydrolases [31, 236].

The dichotomy of prosaposin's lysosomal and secretory pathways raises a number of interesting questions such as how a fraction of the 65 kDa protein escape terminal glycosylation and what is the mechanism utilized by the lysosomal prosaposin to leave the Golgi apparatus.

Prosaposin, unlike most lysosomal hydrolases, is targeted to lysosomes

by a mannose 6-independent mechanism [11, 12]. The transport of soluble hydrolases to lysosomes depends on their mannose 6-phosphate residues that are recognized by the mannose 6-phosphate receptor in the trans-Golgi region [28, 43, 149]. The ligand-receptor complex is then carried to lysosomes via a clathrin-coated vesicle. The 65 kDa protein has been shown to be associated with Golgi membranes [11]. In vitro assays demonstrated that prosaposin and lysosomal saposins are capable of binding sphingolipids [165, 187, 237]. Incubation of cells with tunicamycin did not interfere with the transit of the nonglycosylated 53 kDa form of prosaposin from the ER to the Golgi apparatus nor with its association to Golgi membranes [11]. Moreover, as a result of tunicamycin treatment, the nonglycosylated prosaposin was transported to the lysosomes more efficiently [Igdoura, 1996 #46]. This suggested that the sorting and targeting of the 65 kDa prosaposin within the Golgi apparatus might be dependent on a protein-protein or protein-lipid interaction. To test this hypothesis and to determine whether or not a specific domain of prosaposin is involved in this process, a wild type prosaposin cDNA and several truncated constructs were subcloned into a mammalian expression vector and transfected into COS-7 cells. The recombinant constructs contained a myc epitope tag that allowed their identification from endogenous prosaposin during the course of our immunochemical studies. The lysosomal marker LysoTraker was also used to identify lysosomes by confocal microscopy. Confocal immunofluorescence demonstrated that deletion of individual domains encoding saposin A, B, C, D or the N-terminus did not interfere with the targeting of prosaposin to the lysosomal

compartment. On the other hand, deletion of the C-terminus abolished the targeting of prosaposin to lysosomes. To check if these deletions caused retention of mutated prosaposin in the ER, COS-7 cells were metabolically labeled with Trans^{35}S-label (methionine/cystine) and chased. Cell lysates and culture medium were immunoprecipitated and fluorographed. The results demonstrated the presence of the equivalent 65 kDa and 70 kDa proteins of prosaposin in the cell lysates and of the 70 kDa secretory protein in the medium. In summary, our results clearly indicated that deletions of the ΔA, ΔB, ΔC, ΔD, ΔN-term and ΔC-term did not cause retention of prosaposin in the ER and that the presence of the C-terminus of prosaposin was essential for the sorting and targeting of prosaposin to the lysosomes.

To verify if the C-terminus alone was sufficient for driving prosaposin to the lysosomes, a chimeric fusion protein between albumin and the C-terminus of prosaposin was expressed in COS-7 cells using the same vector. A vector containing the cDNA of albumin alone was used as a control. As expected for a secretory protein, wild type albumin was detected in the culture medium. However, chimeric albumin fused with the C-terminus of prosaposin was not found within lysosomes. Instead, it was secreted into the culture medium.

We rationalized then that truncated constructs ΔA, ΔB, ΔC, ΔD and ΔN-term, which were targeted to lysosomes contained the C-terminus and at least three saposins. Since saposins display, among themselves, similar structure and play similar roles in vivo and in vitro, we decided to test the hypothesis that at least one or more saposin domains plus the C-terminus are required for the

transport of prosaposin to lysosomes. Thus, two new fusion plasmids were made. The first one was composed of albumin plus domain D and the C-terminus of prosaposin. The second construct was made of albumin plus domains C, D and the C-terminus of prosaposin. As predicted, confocal immunostaining demonstrated that albumin was routed to the lysosomal compartment when it was connected to one saposin domain plus the C-terminus of prosaposin.

Each saposin has a high degree of interspecies similarity of hydrophobic amino acids [214, 215]. The percentage of hydrophobic amino acids is 36% in saposin A, 37% in B, 28% in C and 39% in D [214]. This high degree of conservation of hydrophobic residues and their alignment occupying equivalent positions with their side chains buried in the folded structure [215] underlines the capacity of saposins to interact with lipids. In fact, the interaction between prosaposin and its derived saposins with sphingolipids has been extensively documented. Saposins C and D have also been shown to exhibit a high affinity for phospholipids. Furthermore, the presence of acidic phospholipids such as phosphatidylserine (PS) in membrane bilayers greatly favour their binding to saposin D [238]. The interaction with phospholipids is a characteristic of several other saposin like proteins (SAPLIPs) [177], such as, surfactant protein B (SP-B)[239]. Others members of SAPLIPs family include the pore-forming peptide of Entamoeba hystolytica [240, 241], NK-lysin [242], acid sphingomyelinase [243] acyloxylacyl hydrolase [244] and plant aspartic proteinases [233, 245]. SAPLIPs differ widely in function, but the activity of most of them is mediated via lipid

interactions. Interestingly, the saposin like domain within aspartic proteinase has been implicated in the vacuolar targeting of this protein by means of its interaction with membrane phospholipids [245].

Lysosomal prosaposin was initially found to be targeted to lysosomes in a mannose 6-phosphate-independent manner [11, 12, 44]. When isolated Golgi fractions were permeabilized with a mild detergent [11], lysosomal prosaposin remained associated to the membrane while secretory prosaposin (70 kDa) was released into the incubation medium. This suggests that the interaction of lysosomal prosaposin with phospholipid or sphingolipids may play a role in sorting and targeting this protein to the lysosomes. Recently, sphingomyelin a membrane sphingolipid manufactured in the cis/medial region of the Golgi apparatus [246], was demonstrated to be involved in the transport of prosaposin to lysosomes [247]. Cultured cells incubated with fumonisin B1, an inhibitor of sphingolipid synthesis which competes with sphinganine as a substrate of ceramide synthase [248], produced a dramatic decrease in the immunogold labeling of lysosomes with anti-prosaposin antibody. To examine if the mannose 6-phosphate receptor mediated pathway was affected by this treatment, cells treated or not with fumonisin B1 were labeled with anti-cathepsin A antibody. The results showed no significant differences in the immunogold labeling of the lysosomal compartment of the treated and nontreated cells indicating that the effect of fumonisin B1 on the transport of prosaposin to the lysosomes was specific. The effect of DL-threo-1-phenyl-2-decanoyl-amino-3-morpholino-1-propanol-HCL (PDMP), a compound that selectively inhibits the synthesis of glycosphingolipids but not of

sphingomyelin and/or ceramide, and the effect of tricyclodecan-9-yl xanthate potassium (D609) which specifically blocks the formation of sphingomyelin [249] was also examined. The results showed that only D609 blocked the transport of prosaposin to the lysosomes, suggesting that sphingomyelin was the main sphingolipid implicated in the association with prosaposin to the lysosomes [247].

4.2.2 Site of Sorting of the 65 kDa Lysosomal Prosaposin

During the course of this investigation we showed that the 65 kDa lysosomal prosaposin is endo H sensitive whereas the 70 kDa secretory form is endo H resistant. Since the processing pathway within the Golgi apparatus is highly ordered, the treatment with this enzyme was used to distinguish complex from high mannose oligosaccharide linked to prosaposin [43, 250]. Glycoproteins are modified in successive stages as they move through the Golgi processing compartment. Thus, a significant fraction of the 65 kDa form must escape from the Golgi apparatus before it reaches the distal stacks where it becomes fully glycosylated and endo H resistant. This notion was confirmed in cells transfected with the wild type prosaposin after incubation in BFA. BFA is a fungal antibacterial drug which causes rapid redistribution of proteins located in the Golgi apparatus but not of proteins residing in a post-Golgi compartment. Our results showed an intracellular retention of the 65 kDa protein, indicating that the lysosomal form only reaches the cis/medial region of the Golgi apparatus before sorting. The presence of negligible amounts of the 70 kDa protein in the medium represented secretory prosaposin that already passed the distal region of the

Golgi prior to the addition of BFA.

4.2.3 Proposed Model for the Targeting of Prosaposin

Based on this evidence, a model (Figure 4-4), in which the interaction of prosaposin with phopholipids and/or sphingolipids may play an important role in bringing prosaposin close to the Golgi membrane near a "receptor protein", was proposed. According to this model, the C-terminus of prosaposin may contain the binding site for this receptor protein, creating a receptor-ligand-like complex, which is then packed into cargo vesicles and transported to the endosomes, MVBs and/or lysosomes. Interestingly, the C-terminus of prosaposin is significantly similar (66%) to the N-terminus of SP-B which has been implicated in the targeting of this protein to the lamellar bodies in pneumocyte type II [216]. Similar to prosaposin, which requires the C-terminus and at least one saposin domain, SP-B also requires the presence of the N-terminal region and a yet not identified sequence within the backbone of this protein that contains a saposin like domain. Taken together, all these results indicate that an alternative mechanism of sorting and transport of prosaposin between the Golgi apparatus and the lysosomes may exist. In conclusion, we demonstrated that the C-terminus and at least one saposin domain may be sufficient for the lysosomal sorting and targeting of this sphingolipid activator protein.

Figure 4-1: A working model on lysosomal targeting of the 65 kDa form of prosaposin was proposed. One of the saposin domains may recognize glycosphingolipids in the inner leaflet of the Golgi membrane and the C-terminus binds to a "docking protein"(in red) involved in the sorting and routing of prosaposin to the lysosomes via cargo vesicles. Small yellow squares represent carbohydrate chains.

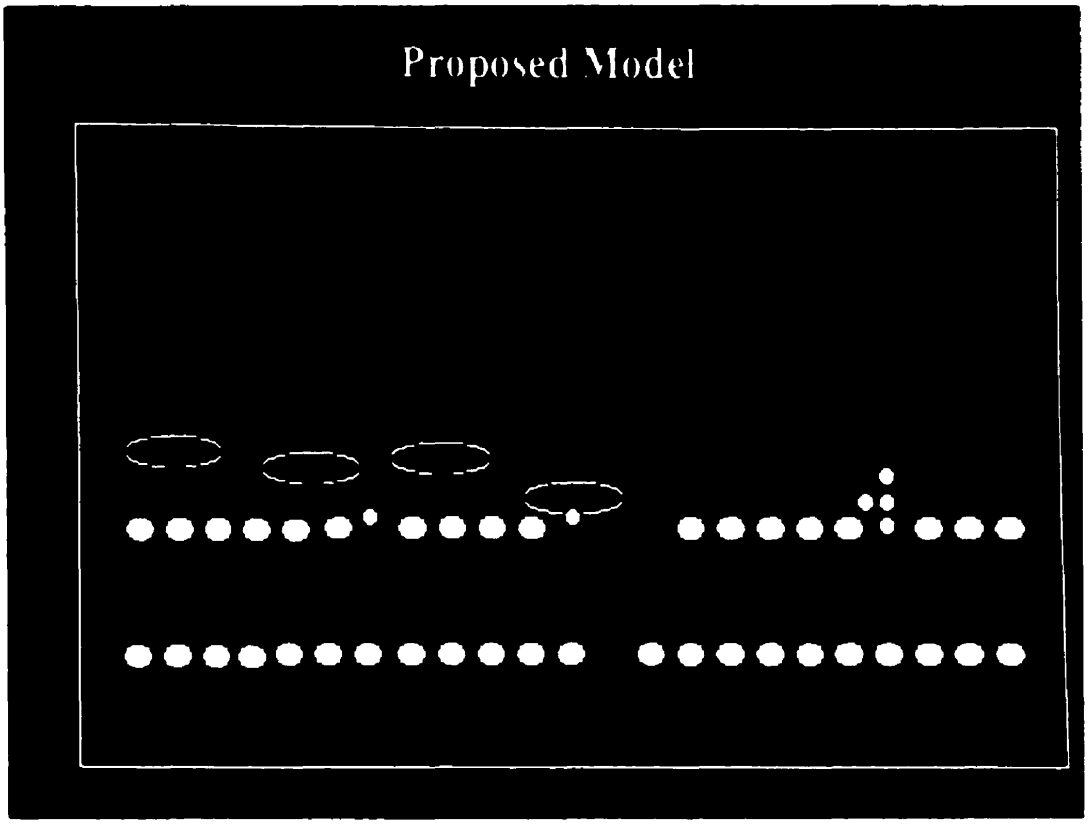
Proposed Model

4.3 Role of Prosaposin in the Male Reproductive System

4.3.1 Targeted Disruption of the Mouse Prosaposin Gene Affects the Development of the Prostate Gland and Other Male Reproductive System

Besides the well-documented role of prosaposin in the catabolism of glycosphingolipids (GLS), secreted prosaposin has been reported to present neurotrophic activity [3, 159]. Prosaposin is abundant in cerebrospinal fluid, stimulates neurite outgrowth in murine cells and choline acetyltransferase (ChAT) activity in human neuroblastoma cells. In addition, prosaposin appears to protect hippocampal neurons form ischemic damage and to prevent apoptosis of cerebellar granule neurons in culture submitted to paclitaxol toxicity [13, 14]

Interestingly, a sequence of 12 amino acids in the amino terminal end of saposin C binds to a putative receptor in Schwann cells and activates the mitogen activator protein kinase (MAPK) pathway by a G protein dependent mechanism. Furthermore, a 12-mer peptide representing this region of saposin C activates the MAPK extracellular signal regulated kinase-1 (ERK-1/p44) and -2 (ERK-2/p42).

Secreted prosaposin can be removed from the extracellular space by the mannose 6-phosphate receptor, the mannose receptor and the low-density lipoprotein receptor-related protein (LRP). The existence of such receptor-clearing events points to the importance of these mechanisms in the modulation of prosaposin signaling.

The recent development of a prosaposin -/- mouse model has provided an opportunity to investigate the mode of action of prosaposin in different tissues [10]. Inactivation of the prosaposin gene causes accumulation of

lactosylceramide, glucosylceramide, digalactosyl ceramide, sulfatide, ceramide and globotriaosylceramide in lysosomes of affected cells. Ultrastructural analysis of these cells shows an accumulation of undigested membranes in multivesicular bodies. These animals die at day 35-40 after birth due to neurological defects.

A morphometric analysis of the organs of the male reproductive system in 37-day-old mice reveals that disruption of the prosaposin gene produces a various degree of reduction in sizes and weights of the testes, the epididymis, the seminal vesicles and the prostate gland. Small-sized testes from homozygous mutant mice appear to be associated with reduced spermiogenesis, particularly late spermatids. The underdevelopment of the prostate gland of the prosaposin homozygous mice (-/-) is demonstrated from the considerably reduced diameter of the tubuloalveolar glands with no secretions in the lumen, the extremely increased and disorganized interstitial connective tissues and much shorter prostatic epithelial cells compared with control mice. Seminal vesicles, epididymis, and efferent ducts are also affected in the prosaposin homozygous mice (-/-). The phenotype is characterized by the underdevelopment of these organs, suggesting that prosaposin play a role in the growth of the male reproductive organs and also in the regulation of spermiogenesis.

In relation to our results on the involution of the prostate gland, it is important to emphasize that prostatic cancer is currently the most commonly diagnosed neoplasm in men and ranks second to lung cancer as a cause of cancer death [251]. The prostate gland is formed during late gestation as a consequence of signaling events between the urogenital sinus epithelium and

urogenital sinus mesenchyme (UGM). In rodents, the prostatic bud is formed during embryonic life, while the full ductal branching occurs postnatally. Androgens are known to be involved in all aspects of prostate development [252]. In fact, androgen-dependent signaling events in the UGM give rise to paracrine factors that act on local epithelial cells to induce morphogenesis and ductal branching [252]. During puberty and in adults, androgen-dependent signaling events are required for full cytodifferentiation and production of secretory proteins by the prostatic epithelium [252]. In adults, the prostate is subject to two primary age-related dieases, prostate cancer and benign prostatic hyperplasia. Prostatic cancer follows a generalized progression from an early, organ-defined disease, which may be clinically asymptomatic and is readily treatable by prostatectomy or androgen ablation therapy, to a highly invasive, androgen-independent, metastatic disease for which there is no current effective therapy or cure [253].

Growth factors are also responsible for mediating mesenchymal and epithelial interactions during prostate development. Although no single growth factor has been shown to have a direct role in prostate cancer, their expressions are altered during prostatic carcinogenesis. Experimental evidences indicate that androgen directly influence the expression of several growth factors [188, 254]. Following androgen withdrawal, the production of stimulatory growth factors, such as, the EGF, IGF and FGF secreted by prostate cells decreased whereas there is an increase in the expression of TGFβ-1 and TGFβ-2 receptors [255, 256] [257]. The net effect of these growth factors alterations is prostatic involution. Androgen replacement restores normal EGF, IGF and FGF levels and the prostate recovers

its original size [258].

Radioimmunoassay of blood samples from homozygous mutant, heterozygous and control mice (n=6) reveals that blood testosterone levels are normal or higher in mice with the inactivated prosaposin gene. Moreover, the immunostaining of prostate sections with an anti-androgen receptor antibody indicates that the epithelial cells lining the alveoli express androgen receptor in both the heterozygous and homozygous tissues. Thus, involution of the prostate gland and other male reproductive organs appears to be independent from androgen levels and androgen receptor. In addition, inactivation of the prosaposin gene seems to interfere with the proliferative activities of prostatic epithelial cells since apoptosis is not readily observed in the epithelium lining the tubuloalveolar glands.

Due to the dual roles of prosaposin as a lysosomal activator of hydrolases and a trophic factor, it is unclear what is the determining cause for the lack of development of the prostate. Inactivation of the gene not only causes the loss of prosaposin trophic activity but also affects the lysosomal degradation of sphingolipids which may alters the distribution lipophilic second messangers such as ceramide in the plasma membrane. In fact, catabolism of plasma membrane sphingolipids generates lipophilic intermediates which are involved in the transmission of extracellular signals to intracellular regulatory system [259]. For example, hydrolysis of sphingomyelin to ceramide can be induced by certain ligands and receptors in various cell types. In general, ceramide appears to mediate cell differentiation and apoptosis [260]. The identity of the cellular targets

of ceramide and other molecules downstream the signal flow is not fully known [260], but a strong body of evidence indicates that ceramide is also involved in the activation of the mitogen-activated kinase (MAPK) pathway [261] [262].

Mitogen-activated kinase is a general name for a family of serine/threonine kinases that play an important role in cell signaling through a variety of ligands and receptors including receptor tyrosine kinases [263] and G-protein-coupled receptors [264, 265]. The extracellular signal-regulated protein kinases ERK1 and ERK2 make up a part of the extracellular signal-regulated kinase (MAKP) family: p44 MAPK, ERK1 and p42 MAPK, ERK2. Activation of ERKs have traditionally been thought to be a result of a linear signaling cascade from growth factor receptors, SH2/SH3 adator proteins, guanine nucleotide exchange factors, p21 Ras, Raf-1, and MAPK-activated kinase such as MAP kinase kinase (MEK). However, there is emerging data indicating that signaling proteins such as phosphatidylinositol-3-kinase (PI3K) and protein kinase C (PKC) can also phophorylate MEK and ERKs independent of the Ras pathway [266, 267]. In many cellular systems, activation of the MAPK pathway by trophic factors has been implicated in the regulation of gene transcription [268] associated with proliferation and differentiation [269].

In summary, prosaposin may be involved directly, in signal transduction by transmission of extracellular signals to intracellular regulatory systems or indirectly, by regulating the levels of lipophilic intermediates of sphingolipid catabolism. However, in both cases the inactivation of the prosaposin gene could result in the inactivation of the MAPK pathway. To examine if this was the case,

prostate sections from homozygous and heterozygous mice were immunostained with two monoclonal antibodies which recognize the phosphorylated ERK1/2 and nonphosphorylated forms of ERK1/2. Sections immunostained with the antibody to the nonphosphorylated form of ERK1/2 reacted with all epithelial cells in heterozygous and homozygous prostates (Figure 3-35). Sections immunostained with the antibody to the phosphorylated ERK1/2 strongly reacted with tall prostatic secretory cells in prostate from heterozygous mouse (Figure 3-35). On the other hand, the epithelial cells in the homozygous prostate remained unstained (Figure 3-35).

In conclusion, the present observation demonstrated that inactivation of the prosaposin gene affects the development of the reproductive organs including the prostate gland. The mice described here should be useful to examine the following questions: 1) How does prosaposin affect the development of prostate gland? 2) Is it directly through its trophic activity, i.e., by binding to cell surface receptors and activating second messengers? 3) Is it indirectly, by regulating sphingolipid catabolism and production of lipophilic intermediates involved in signal transduction (i.e. ceramide, sphingosine and sphingosine 1-phosphate)?

Thus these mice should be useful to determine how prosaposin affects the proliferation of human prostate cells and to permit the development of a novel therapeutic strategy for the treatment of prostate cancer.

CHAPTER FIVE

Contributions to Original Knowledge

1. The cloning and the structural organization of the mouse prosaposin gene was characterized for the first time. The entire gene spans over 20 kb in length. The gene consists of 15 exons and 14 introns. Saposin A is encoded by exons 3, 4 and 5; saposin B is encoded by exons 6, 7, 8 and 9; saposin C is encoded by exons 10 and 11 and saposin D is encoded by exons 12, 13 and 14 (NCBI Genbank accession number: U57999). Exon 8 is the smallest exon of the prosaposin gene and consists of 9 nucleotide base pairs (CATGATCAT). Exon 8 is alternatively spliced in a tissue specific manner including or excluding the three encoded amino acids (QDQ). The abundance of prosaposin transcripts with the QDQ insertion is found in brain, heart and skeletal muscle and without the QDQ insertion in kidney, spleen, pancreas, lung and testis.
2. Two new mouse and rat prosaposin cDNAs were cloned from testicular libraries. They display a 94% similarity (88% identity). The average similarity between rodents and human prosaposin is 76% (65% identity). The overall similarity between the three sequences is 74% (62% identity). Saposin D and the C-terminus of prosaposin are the most conserved region among the three species, while saposin C is the least conserved domain among them. Secondary structure predictions indicated that there are three α helices in saposin A, B and D and four α helices in saposin C with an extended helix at the end. 15 conserved amino acids aligned in the same position of each saposin are occupied by bulky hydrophobic amino acids (Val, Ile, Leu, Met, Phe, or Tyr) illustrating a common framework of amino acids forming amphiphatic helices with an internal hydrophobic core that may interact with

lipids. The QDQ insertion increases the local hydrophilic profile of saposin B. An increase in local hydrophilicity at the amino terminal end of human saposin C, which is absent in the mouse and rat sequences, was also noted.

3. We determined that the C-terminus of prosaposin is required for its lysosomal targeting and that the C-terminus plus at least one saposin domain are sufficient for its lysosomal targeting.
4. We presented experimental evidence that the 65 kDa lysosomal prosaposin contains mainly high mannose sugar residues and that this form of the protein may exit from the proximal compartment of the Golgi apparatus. On the other hand, we found that the 70 kDa secretory prosaposin is glycosylated with complex/hybrid sugar residues and that it appears to exit from the distal region of the Golgi apparatus.
5. Inactivation of the prosaposin gene affects the development of testis, efferent ducts, epididymis, seminal vesicles and prostate gland. The secretory form of prosaposin appears to have a trophic activity on the development of the prostate gland via the activation of the MAKP pathway.

CHAPTER SIX

References

1. Morales CR, el-Alfy M, Zhao Q, Igdoura S. (1995) Molecular role of sulfated glycoprotein-1 (SGP-1/prosaposin) in Sertoli cells. Histol Histopathol, 10, 1023-34.

2. Kondoh K, Hineno T, Sano A, Kakimoto Y. (1991) Isolation and characterization of prosaposin from human milk. Biochem Biophys Res Commun, 181, 286-92.

3. O'Brien JS, Carson GS, Seo HC, Hiraiwa M, Kishimoto Y. (1994) Identification of prosaposin as a neurotrophic factor. Proc Natl Acad Sci U S A, 91, 9593-6.

4. Igdoura SA, Morales CR. (1995) Role of sulfated glycoprotein-1 (SGP-1) in the disposal of residual bodies by Sertoli cells of the rat. Mol Reprod Dev, 40, 91-102.

5. Morales CR, El-Alfy M, Zhao Q, Igdoura SA. (1996) Expression and tissue distribution of rat sulfated glycoprotein-1 (prosaposin). J Histochem Cytochem, 44, 327-37.

6. Kretz KA, Carson GS, Morimoto S, Kishimoto Y, Fluharty AL, O'Brien JS. (1990) Characterization of a mutation in a family with saposin B deficiency: a glycosylation site defect. Proc Natl Acad Sci U S A, 87, 2541-4.

7. Christomanou H, Aignesberger A, Linke RP. (1986) Immunochemical characterization of two activator proteins stimulating enzymic sphingomyelin degradation in vitro. Absence of one of them in a human Gaucher disease variant. Biol Chem Hoppe Seyler, 367, 879-90.

8. Stevens RL, Fluharty AL, Kihara H, Kaback MM, Shapiro LJ, Marsh B, Sandhoff K, Fischer G. (1981) Cerebroside sulfatase activator deficiency induced metachromatic leukodystrophy. Am J Hum Genet, 33, 900-6.

9. Bradova V, Smid F, Ulrich-Bott B, Roggendorf W, Paton BC, Harzer K. (1993) Prosaposin deficiency: further characterization of the sphingolipid activator protein-deficient sibs. Multiple glycolipid elevations (including lactosylceramidosis), partial enzyme deficiencies and ultrastructure of the skin in this generalized sphingolipid storage disease. Hum Genet, 92, 143-52.

10. Fujita N, Suzuki K, Vanier MT, Popko B, Maeda N, Klein A, Henseler M, Sandhoff K, Nakayasu H. (1996) Targeted disruption of the mouse sphingolipid activator protein gene: a complex phenotype, including severe leukodystrophy and wide-spread storage of multiple sphingolipids. Hum Mol Genet, 5, 711-25.

11. Igdoura SA, Rasky A, Morales CR. (1996) Trafficking of sulfated glycoprotein-1 (prosaposin) to lysosomes or to the extracellular space in rat Sertoli cells. Cell Tissue Res, 283, 385-94.

12. Vielhaber G, Hurwitz R, Sandhoff K. (1996) Biosynthesis, processing, and targeting of sphingolipid activator protein (SAP)precursor in cultured human fibroblasts. Mannose 6- phosphate receptor-independent endocytosis of SAP precursor. J Biol Chem, 271, 32438-46.

13. Sano A, Matsuda S, Wen TC, Kotani Y, Kondoh K, Ueno S, Kakimoto Y, Yoshimura H, Sakanaka M. (1994) Protection by prosaposin against ischemia-induced learning disability and neuronal loss. Biochem Biophys Res

Commun, 204, 994-1000.

14. Campana WM, Hiraiwa M, O'Brien JS. (1998) Prosaptide activates the MAPK pathway by a G-protein-dependent mechanism essential for enhanced sulfatide synthesis by Schwann cells. Faseb J, 12, 307-14.

15. Steinman RM, Mellman IS, Muller WA, Cohn ZA. (1983) Endocytosis and the recycling of plasma membrane. J Cell Biol, 96, 1-27.

16. Hermo L, Clermont Y, Morales C. (1985) Fluid-phase and adsorptive endocytosis in ciliated epithelial cells of the rat ductuli efferentes. Anat Rec, 211, 285-94.

17. Suzuki Y. (1995) [Lysosomal enzymes, sphingolipid activator proteins, and protective protein]. Nippon Rinsho, 53, 2887-91.

18. Marks MS, Roche PA, van Donselaar E, Woodruff L, Peters PJ, Bonifacino JS. (1995) A lysosomal targeting signal in the cytoplasmic tail of the beta chain directs HLA-DM to MHC class II compartments. J Cell Biol, 131, 351-69.

19. Marks SC, Jr. (1989) Osteoclast biology: lessons from mammalian mutations. Am J Med Genet, 34, 43-54.

20. Renfrew CA, Hubbard AL. (1991) Degradation of epidermal growth factor receptor in rat liver. Membrane topology through the lysosomal pathway. J Biol Chem, 266, 21265-73.

21. Morales C, Clermont Y, Nadler NJ. (1986) Cyclic endocytic activity and kinetics of lysosomes in Sertoli cells of the rat: a morphometric analysis. Biol Reprod, 34, 207-18.

22. Geuze HJ, Slot JW, Strous GJ, Schwartz AL. (1983) The pathway of the asialoglycoprotein-ligand during receptor-mediated endocytosis: a morphological study with colloidal gold/ligand in the human hepatoma cell line, Hep G2. Eur J Cell Biol, 32, 38-44.

23. Clermont Y, Morales C, Hermo L. (1987) Endocytic activities of Sertoli cells in the rat. Ann N Y Acad Sci, 513, 1-15.

24. Tang XM, Clermont Y, Hermo L. (1988) Origin and fate of autophagosomes in Leydig cells of normal adult rats. J Androl, 9, 284-93.

25. Stevens TH, Forgac M. (1997) Structure, function and regulation of the vacuolar (H+)-ATPase. Annu Rev Cell Dev Biol, 13, 779-808.

26. Fambrough DM, Takeyasu K, Lippincott-Schwarz J, Siegel NR. (1988) Structure of LEP100, a glycoprotein that shuttles between lysosomes and the plasma membrane, deduced from the nucleotide sequence of the encoding cDNA. J Cell Biol, 106, 61-7.

27. Ogata S, Fukuda M. (1994) Lysosomal targeting of Limp II membrane glycoprotein requires a novel Leu-Ile motif at a particular position in its cytoplasmic tail. J Biol Chem, 269, 5210-7.

28. Rohrer J, Schweizer A, Russell D, Kornfeld S. (1996) The targeting of Lamp1 to lysosomes is dependent on the spacing of its cytoplasmic tail tyrosine sorting motif relative to the membrane. J Cell Biol, 132, 565-76.

29. Braun M, Waheed A, von Figura K. (1989) Lysosomal acid phosphatase is transported to lysosomes via the cell surface. Embo J, 8, 3633-40.

30. O'Brien JS, Kishimoto Y. (1991) Saposin proteins: structure, function, and role in human lysosomal storage disorders. Faseb J, 5, 301-8.

31. Sandhoff K, Kolter T. (1997) Biochemistry of glycosphingolipid degradation. Clin Chim Acta, 266, 51-61.

32. Ehrenreich BA, Cohn ZA. (1969) The fate of peptides pinocytosed by macrophages in vitro. J Exp Med, 129, 227-45.

33. Schneider JA, Jonas AJ, Smith ML, Greene AA. (1984) Lysosomal transport of cystine and other small molecules. Biochem Soc Trans, 12, 908-10.

34. Bernar J, Tietze F, Kohn LD, Bernardini I, Harper GS, Grollman EF, Gahl WA. (1986) Characteristics of a lysosomal membrane transport system for tyrosine and other neutral amino acids in rat thyroid cells. J Biol Chem, 261, 17107-12.

35. Renlund M, Kovanen PT, Raivio KO, Aula P, Gahmberg CG, Ehnholm C. (1986) Studies on the defect underlying the lysosomal storage of sialic acid in Salla disease. Lysosomal accumulation of sialic acid formed from N-acetyl-mannosamine or derived from low density lipoprotein in cultured mutant fibroblasts. J Clin Invest, 77, 568-74.

36. Maxfield FR. (1982) Weak bases and ionophores rapidly and reversibly raise the pH of endocytic vesicles in cultured mouse fibroblasts. J Cell Biol, 95, 676-81.

37. De Duve C, Wattiaux R. (1966) Functions of lysosomes. Annu Rev Physiol, 28, 435-92.

38. Bainton DF. (1981) The discovery of lysosomes. J Cell Biol, 91,

66s-76s.

39. Posner BI, Khan MN, Bergeron JJ. (1982) Endocytosis of peptide hormones and other ligands. Endocr Rev, 3, 280-98.

40. Pohlmann R, Krentler C, Schmidt B, Schroder W, Lorkowski G, Culley J, Mersmann G, Geier C, Waheed A, Gottschalk S, et al. (1988) Human lysosomal acid phosphatase: cloning, expression and chromosomal assignment. Embo J, 7, 2343-50.

41. Dean RT, Jessup W, Roberts CR. (1984) Effects of exogenous amines on mammalian cells, with particular reference to membrane flow. Biochem J, 217, 27-40.

42. Kirschke H, Langner J, Wiederanders B, Ansorge S, Bohley P, Broghammer U. (1976) [Intracellular protein breakdown. VII. Cathepsin L and H; two new proteinases from rat liver lysosomes]. Acta Biol Med Ger, 35, 285-99.

43. von Figura K, Hasilik A. (1986) Lysosomal enzymes and their receptors. Annu Rev Biochem, 55, 167-93.

44. Rijnboutt S, Kal AJ, Geuze HJ, Aerts H, Strous GJ. (1991) Mannose 6-phosphate-independent targeting of cathepsin D to lysosomes in HepG2 cells. J Biol Chem, 266, 23586-92.

45. Campbell CH, Fine RE, Squicciarini J, Rome LH. (1983) Coated vesicles from rat liver and calf brain contain cryptic mannose 6- phosphate receptors. J Biol Chem, 258, 2628-33.

46. Geuze HJ, Slot JW, Strous GJ, Hasilik A, von Figura K. (1985) Possible pathways for lysosomal enzyme delivery. J Cell Biol, 101, 2253-62.

47. Schulze-Lohoff E, Hasilik A, von Figura K. (1985) Cathepsin D precursors in clathrin-coated organelles from human fibroblasts. J Cell Biol, 101, 824-9.

48. Lemansky P, Hasilik A, von Figura K, Helmy S, Fishman J, Fine RE, Kedersha NL, Rome LH. (1987) Lysosomal enzyme precursors in coated vesicles derived from the exocytic and endocytic pathways. J Cell Biol, 104, 1743-8.

49. Park JE, Draper RK, Brown WJ. (1991) Biosynthesis of lysosomal enzymes in cells of the End3 complementation group conditionally defective in endosomal acidification. Somat Cell Mol Genet, 17, 137-50.

50. Neufeld EF. (1991) Lysosomal storage diseases. Annu Rev Biochem, 60, 257-80.

51. Maillet CM, Shur BD. (1993) Uvomorulin, LAMP-1, and laminin are substrates for cell surface beta- 1,4-galactosyltransferase on F9 embryonal carcinoma cells: comparisons between wild-type and mutant 5.51 att- cells. Exp Cell Res, 208, 282-95.

52. Aerts JM, Schram AW, Strijland A, van Weely S, Jonsson LM, Tager JM, Sorrell SH, Ginns EI, Barranger JA, Murray GJ. (1988) Glucocerebrosidase, a lysosomal enzyme that does not undergo oligosaccharide phosphorylation. Biochim Biophys Acta, 964, 303-8.

53. Miller AL, Kress BC, Stein R, Kinnon C, Kern H, Schneider JA, Harms E. (1981) Properties of N-acetyl-beta-D-hexosaminidase from isolated normal and I- cell lysosomes. J Biol Chem, 256, 9352-62.

54. Lazzarino D, Gabel CA. (1990) Protein determinants impair recognition of procathepsin L phosphorylated oligosaccharides by the cation-independent mannose 6- phosphate receptor. J Biol Chem, 265, 11864-71.

55. Sahagian GG, Gottesman MM. (1982) The predominant secreted protein of transformed murine fibroblasts carries the lysosomal mannose 6-phosphate recognition marker. J Biol Chem, 257, 11145-50.

56. Zhu Y, Conner GE. (1994) Intermolecular association of lysosomal protein precursors during biosynthesis. J Biol Chem, 269, 3846-51.

57. Glickman JN, Kornfeld S. (1993) Mannose 6-phosphate-independent targeting of lysosomal enzymes in I-cell disease B lymphoblasts. J Cell Biol, 123, 99-108.

58. Dittmer F, Ulbrich EJ, Hafner A, Schmahl W, Meister T, Pohlmann R, von Figura K. (1999) Alternative mechanisms for trafficking of lysosomal enzymes in mannose 6-phosphate receptor-deficient mice are cell type-specific. J Cell Sci, 112, 1591-7.

59. Sahagian GG, Distler J, Jourdian GW. (1981) Characterization of a membrane-associated receptor from bovine liver that binds phosphomannosyl residues of bovine testicular beta- galactosidase. Proc Natl Acad Sci U S A, 78, 4289-93.

60. Hoflack B, Kornfeld S. (1985) Purification and characterization of a cation-dependent mannose 6- phosphate receptor from murine P388D1 macrophages and bovine liver. J Biol Chem, 260, 12008-14.

61. Dahms NM, Wick DA, Brzycki-Wessell MA. (1994) The bovine

mannose 6-phosphate/insulin-like growth factor II receptor. Localization of the insulin-like growth factor II binding site to domains 5-11. J Biol Chem, 269, 3802-9.

62. Garmroudi F, MacDonald RG. (1994) Localization of the insulin-like growth factor II (IGF-II) binding/cross-linking site of the IGF-II/mannose 6-phosphate receptor to extracellular repeats 10-11. J Biol Chem, 269, 26944-52.

63. Schmidt B, Kiecke-Siemsen C, Waheed A, Braulke T, von Figura K. (1995) Localization of the insulin-like growth factor II binding site to amino acids 1508-1566 in repeat 11 of the mannose 6-phosphate/insulin-like growth factor II receptor. J Biol Chem, 270, 14975-82.

64. Kornfeld S. (1992) Structure and function of the mannose 6-phosphate/insulinlike growth factor II receptors. Annu Rev Biochem, 61, 307-30.

65. Gabel CA, Goldberg DE, Kornfeld S. (1983) Identification and characterization of cells deficient in the mannose 6- phosphate receptor: evidence for an alternate pathway for lysosomal enzyme targeting. Proc Natl Acad Sci U S A, 80, 775-9.

66. Kyle JW, Nolan CM, Oshima A, Sly WS. (1988) Expression of human cation-independent mannose 6-phosphate receptor cDNA in receptor-negative mouse P388D1 cells following gene transfer. J Biol Chem, 263, 16230-5.

67. Lobel P, Fujimoto K, Ye RD, Griffiths G, Kornfeld S. (1989) Mutations in the cytoplasmic domain of the 275 kd mannose 6-phosphate receptor differentially alter lysosomal enzyme sorting and endocytosis. Cell, 57,

787-96.

68. Nolan CM, Kyle JW, Watanabe H, Sly WS. (1990) Binding of insulin-like growth factor II (IGF-II) by human cation- independent mannose 6-phosphate receptor/IGF-II receptor expressed in receptor-deficient mouse L cells. Cell Regul, 1, 197-213.

69. Watanabe H, Grubb JH, Sly WS. (1990) The overexpressed human 46-kDa mannose 6-phosphate receptor mediates endocytosis and sorting of beta-glucuronidase. Proc Natl Acad Sci U S A, 87, 8036-40.

70. Ma ZM, Grubb JH, Sly WS. (1991) Cloning, sequencing, and functional characterization of the murine 46- kDa mannose 6-phosphate receptor. J Biol Chem, 266, 10589-95.

71. Johnson KF, Kornfeld S. (1992) A His-Leu-Leu sequence near the carboxyl terminus of the cytoplasmic domain of the cation-dependent mannose 6-phosphate receptor is necessary for the lysosomal enzyme sorting function. J Biol Chem, 267, 17110-5.

72. Gartung C, Braulke T, Hasilik A, von Figura K. (1985) Internalization of blocking antibodies against mannose-6-phosphate specific receptors. Embo J, 4, 1725-30.

73. Stein M, Zijderhand-Bleekemolen JE, Geuze H, Hasilik A, von Figura K. (1987) Mr 46,000 mannose 6-phosphate specific receptor: its role in targeting of lysosomal enzymes. Embo J, 6, 2677-81.

74. Koster A, Saftig P, Matzner U, von Figura K, Peters C, Pohlmann R. (1993) Targeted disruption of the M(r) 46,000 mannose 6-phosphate receptor

gene in mice results in misrouting of lysosomal proteins. Embo J, 12, 5219-23.

75. Ludwig T, Ovitt CE, Bauer U, Hollinshead M, Remmler J, Lobel P, Ruther U, Hoflack B. (1993) Targeted disruption of the mouse cation-dependent mannose 6-phosphate receptor results in partial missorting of multiple lysosomal enzymes. Embo J, 12, 5225-35.

76. Barlow DP, Stoger R, Herrmann BG, Saito K, Schweifer N. (1991) The mouse insulin-like growth factor type-2 receptor is imprinted and closely linked to the Tme locus. Nature, 349, 84-7.

77. Dittmer F, Hafner A, Ulbrich EJ, Moritz JD, Schmidt P, Schmahl W, Pohlmann R, Figura KV. (1998) I-cell disease-like phenotype in mice deficient in mannose 6-phosphate receptors. Transgenic Res, 7, 473-83.

78. Kasper D, Dittmer F, von Figura K, Pohlmann R. (1996) Neither type of mannose 6-phosphate receptor is sufficient for targeting of lysosomal enzymes along intracellular routes. J Cell Biol, 134, 615-23.

79. Stein M, Braulke T, Krentler C, Hasilik A, von Figura K. (1987) 46-kDa mannose 6-phosphate-specific receptor: biosynthesis, processing, subcellular location and topology. Biol Chem Hoppe Seyler, 368, 937-47.

80. Duncan JR, Kornfeld S. (1988) Intracellular movement of two mannose 6-phosphate receptors: return to the Golgi apparatus. J Cell Biol, 106, 617-28.

81. Klumperman J, Hille A, Veenendaal T, Oorschot V, Stoorvogel W, von Figura K, Geuze HJ. (1993) Differences in the endosomal distributions of the two mannose 6- phosphate receptors. J Cell Biol, 121, 997-1010.

82. Koster A, von Figura K, Pohlmann R. (1994) Mistargeting of lysosomal enzymes in M(r) 46,000 mannose 6-phosphate receptor-deficient mice is compensated by carbohydrate-specific endocytotic receptors. Eur J Biochem, 224, 685-9.

83. Chao HH, Waheed A, Pohlmann R, Hille A, von Figura K. (1990) Mannose 6-phosphate receptor dependent secretion of lysosomal enzymes. Embo J, 9, 3507-13.

84. Ullrich K, Mersmann G, Fleischer M, von Figura K. (1978) Epithelial rat liver cells have cell surface receptors recognizing a phosphorylated carbohydrate on lysosomal enzymes. Hoppe Seylers Z Physiol Chem, 359, 1591-8.

85. Ullrich K, Gieselmann V, Mersmann G, Von Figura K. (1979) Endocytosis of lysosomal enzymes by non-parenchymal rat liver cells. Comparative study of lysosomal-enzyme uptake by hepatocytes and non-parenchymal liver cells. Biochem J, 182, 329-35.

86. Kovacina KS, Steele-Perkins G, Purchio AF, Lioubin M, Miyazono K, Heldin CH, Roth RA. (1989) Interactions of recombinant and platelet transforming growth factor- beta 1 precursor with the insulin-like growth factor II/mannose 6- phosphate receptor. Biochem Biophys Res Commun, 160, 393-403.

87. Dennis PA, Rifkin DB. (1991) Cellular activation of latent transforming growth factor beta requires binding to the cation-independent mannose 6-phosphate/insulin-like growth factor type II receptor. Proc Natl Acad

Sci U S A, 88, 580-4.

88. Lioubin MN, Madisen L, Marquardt H, Roth R, Kovacina KS, Purchio AF. (1991) Characterization of latent recombinant TGF-beta 2 produced by Chinese hamster ovary cells. J Cell Biochem, 45, 112-21.

89. Herzog V, Neumuller W, Holzmann B. (1987) Thyroglobulin, the major and obligatory exportable protein of thyroid follicle cells, carries the lysosomal recognition marker mannose-6- phosphate. Embo J, 6, 555-60.

90. Lemansky P, Herzog V. (1992) Endocytosis of thyroglobulin is not mediated by mannose-6-phosphate receptors in thyrocytes. Evidence for low-affinity-binding sites operating in the uptake of thyroglobulin. Eur J Biochem, 209, 111-9.

91. Herzog V. (1992) Regulation of the cellular transport and compactation of thyroglobulin. Exp Clin Endocrinol, 100, 12-3.

92. Brunetti CR, Burke RL, Kornfeld S, Gregory W, Masiarz FR, Dingwell KS, Johnson DC. (1994) Herpes simplex virus glycoprotein D acquires mannose 6-phosphate residues and binds to mannose 6-phosphate receptors. J Biol Chem, 269, 17067-74.

93. Kornfeld S, Sly WS. (1985) Lysosomal storage defects. Hosp Pract (Off Ed), 20, 71-5, 78-82.

94. Diment S, Leech MS, Stahl PD. (1988) Cathepsin D is membrane-associated in macrophage endosomes. J Biol Chem, 263, 6901-7.

95. McIntyre GF, Erickson AH. (1991) Procathepsins L and D are membrane-bound in acidic microsomal vesicles. J Biol Chem, 266, 15438-45.

96. Sloane BF, Moin K, Sameni M, Tait LR, Rozhin J, Ziegler G. (1994) Membrane association of cathepsin B can be induced by transfection of human breast epithelial cells with c-Ha-ras oncogene. J Cell Sci, 107, 373-84.

97. Valls LA, Winther JR, Stevens TH. (1990) Yeast carboxypeptidase Y vacuolar targeting signal is defined by four propeptide amino acids. J Cell Biol, 111, 361-8.

98. Klionsky DJ, Banta LM, Emr SD. (1988) Intracellular sorting and processing of a yeast vacuolar hydrolase: proteinase A propeptide contains vacuolar targeting information. Mol Cell Biol, 8, 2105-16.

99. Mattei MG, Matterson J, Chen JW, Williams MA, Fukuda M. (1990) Two human lysosomal membrane glycoproteins, h-lamp-1 and h-lamp-2, are encoded by genes localized to chromosome 13q34 and chromosome Xq24-25, respectively. J Biol Chem, 265, 7548-51.

100. Gough NR, Hatem CL, Fambrough DM. (1995) The family of LAMP-2 proteins arises by alternative splicing from a single gene: characterization of the avian LAMP-2 gene and identification of mammalian homologs of LAMP-2b and LAMP-2c. DNA Cell Biol, 14, 863-7.

101. Hatem CL, Gough NR, Fambrough DM. (1995) Multiple mRNAs encode the avian lysosomal membrane protein LAMP-2, resulting in alternative transmembrane and cytoplasmic domains. J Cell Sci, 108, 2093-100.

102. Harter C, Mellman I. (1992) Transport of the lysosomal membrane glycoprotein lgp120 (lgp-A) to lysosomes does not require appearance on the plasma membrane. J Cell Biol, 117, 311-25.

103. Honing S, Hunziker W. (1995) Cytoplasmic determinants involved in direct lysosomal sorting, endocytosis, and basolateral targeting of rat lgp120 (lamp-I) in MDCK cells. J Cell Biol, 128, 321-32.

104. Guarnieri FG, Arterburn LM, Penno MB, Cha Y, August JT. (1993) The motif Tyr-X-X-hydrophobic residue mediates lysosomal membrane targeting of lysosome-associated membrane protein 1. J Biol Chem, 268, 1941-6.

105. Hunziker W, Whitney JA, Mellman I. (1991) Selective inhibition of transcytosis by brefeldin A in MDCK cells. Cell, 67, 617-27.

106. Peters C, Braun M, Weber B, Wendland M, Schmidt B, Pohlmann R, Waheed A, von Figura K. (1990) Targeting of a lysosomal membrane protein: a tyrosine-containing endocytosis signal in the cytoplasmic tail of lysosomal acid phosphatase is necessary and sufficient for targeting to lysosomes. Embo J, 9, 3497-506.

107. Barriocanal JG, Bonifacino JS, Yuan L, Sandoval IV. (1986) Biosynthesis, glycosylation, movement through the Golgi system, and transport to lysosomes by an N-linked carbohydrate-independent mechanism of three lysosomal integral membrane proteins. J Biol Chem, 261, 16755-63.

108. Vega MA, Rodriguez F, Segui B, Cales C, Alcalde J, Sandoval IV. (1991) Targeting of lysosomal integral membrane protein LIMP II. The tyrosine-lacking carboxyl cytoplasmic tail of LIMP II is sufficient for direct targeting to lysosomes. J Biol Chem, 266, 16269-72.

109. Lehmann LE, Eberle W, Krull S, Prill V, Schmidt B, Sander C, von Figura K, Peters C. (1992) The internalization signal in the cytoplasmic tail of

lysosomal acid phosphatase consists of the hexapeptide PGYRHV. Embo J, 11, 4391-9.

110. D'Souza MP, August JT. (1986) A kinetic analysis of biosynthesis and localization of a lysosome- associated membrane glycoprotein. Arch Biochem Biophys, 249, 522-32.

111. Green SA, Zimmer KP, Griffiths G, Mellman I. (1987) Kinetics of intracellular transport and sorting of lysosomal membrane and plasma membrane proteins. J Cell Biol, 105, 1227-40.

112. Sandoval IV, Arredondo JJ, Alcalde J, Gonzalez Noriega A, Vandekerckhove J, Jimenez MA, Rico M. (1994) The residues Leu(Ile)475-Ile(Leu, Val, Ala)476, contained in the extended carboxyl cytoplasmic tail, are critical for targeting of the resident lysosomal membrane protein LIMP II to lysosomes. J Biol Chem, 269, 6622-31.

113. Marcusson EG, Horazdovsky BF, Cereghino JL, Gharakhanian E, Emr SD. (1994) The sorting receptor for yeast vacuolar carboxypeptidase Y is encoded by the VPS10 gene. Cell, 77, 579-86.

114. Rothman JH, Raymond CK, Gilbert T, O'Hara PJ, Stevens TH. (1990) A putative GTP binding protein homologous to interferon-inducible Mx proteins performs an essential function in yeast protein sorting. Cell, 61, 1063-74.

115. Horazdovsky BF, Busch GR, Emr SD. (1994) VPS21 encodes a rab5-like GTP binding protein that is required for the sorting of yeast vacuolar proteins. Embo J, 13, 1297-309.

116. Stack JH, Herman PK, Schu PV, Emr SD. (1993) A membrane-

associated complex containing the Vps15 protein kinase and the Vps34 PI 3-kinase is essential for protein sorting to the yeast lysosome-like vacuole. Embo J, 12, 2195-204.

117. Hakomori S. (1981) Glycosphingolipids in cellular interaction, differentiation, and oncogenesis. Annu Rev Biochem, 50, 733-64.

118. Rademacher TW, Parekh RB, Dwek RA. (1988) Glycobiology. Annu Rev Biochem, 57, 785-838.

119. Hakomori S. (1993) Structure and function of sphingoglycolipids in transmembrane signalling and cell-cell interactions. Biochem Soc Trans, 21, 583-95.

120. Ando A, Ando I, Hiraki T, Takeshita M, Hisada K. (1983) Mechanism of tumor and liver concentration of 67Ga: 67Ga binding substances in tumor tissues and liver. Int J Nucl Med Biol, 10, 1-9.

121. Symington FW, Murray WA, Bearman SI, Hakomori S. (1987) Intracellular localization of lactosylceramide, the major human neutrophil glycosphingolipid. J Biol Chem, 262, 11356-63.

122. Gillard BK, Thurmon LT, Marcus DM. (1993) Variable subcellular localization of glycosphingolipids. Glycobiology, 3, 57-67.

123. Rock P, Allietta M, Young WW, Jr., Thompson TE, Tillack TW. (1990) Organization of glycosphingolipids in phosphatidylcholine bilayers: use of antibody molecules and Fab fragments as morphologic markers. Biochemistry, 29, 8484-90.

124. Schnaar RL. (1991) Glycosphingolipids in cell surface recognition.

Glycobiology, 1, 477-85.

125. Griffiths G, Hoflack B, Simons K, Mellman I, Kornfeld S. (1988) The mannose 6-phosphate receptor and the biogenesis of lysosomes. Cell, 52, 329-41.

126. Wessling-Resnick M, Braell WA. (1990) Characterization of the mechanism of endocytic vesicle fusion in vitro. J Biol Chem, 265, 16751-9.

127. Sandhoff K, van Echten G, Schroder M, Schnabel D, Suzuki K. (1992) Metabolism of glycolipids: the role of glycolipid-binding proteins in the function and pathobiochemistry of lysosomes. Biochem Soc Trans, 20, 695-9.

128. Furst W, Sandhoff K. (1992) Activator proteins and topology of lysosomal sphingolipid catabolism. Biochim Biophys Acta, 1126, 1-16.

129. Sandhoff K, Klein A. (1994) Intracellular trafficking of glycosphingolipids: role of sphingolipid activator proteins in the topology of endocytosis and lysosomal digestion. FEBS Lett, 346, 103-7.

130. Hopkins CR, Gibson A, Shipman M, Miller K. (1990) Movement of internalized ligand-receptor complexes along a continuous endosomal reticulum [see comments]. Nature, 346, 335-9.

131. Harzer K, Paton BC, Poulos A, Kustermann-Kuhn B, Roggendorf W, Grisar T, Popp M. (1989) Sphingolipid activator protein deficiency in a 16-week-old atypical Gaucher disease patient and his fetal sibling: biochemical signs of combined sphingolipidoses. Eur J Pediatr, 149, 31-9.

132. Schnabel D, Schroder M, Furst W, Klein A, Hurwitz R, Zenk T, Weber J, Harzer K, Paton BC, Poulos A, et al. (1992) Simultaneous deficiency of

sphingolipid activator proteins 1 and 2 is caused by a mutation in the initiation codon of their common gene. J Biol Chem, 267, 3312-5.

133. Mehl E, Jatzkewitz H. (1964) [A cerebrosidesulfatase from swine kidney]. Hoppe Seylers Z Physiol Chem, 339, 260-76.

134. Kishimoto Y, Hiraiwa M, O'Brien JS. (1992) Saposins: structure, function, distribution, and molecular genetics. J Lipid Res, 33, 1255-67.

135. Conzelmann E, Sandhoff K. (1978) AB variant of infantile GM2 gangliosidosis: deficiency of a factor necessary for stimulation of hexosaminidase A-catalyzed degradation of ganglioside GM2 and glycolipid GA2. Proc Natl Acad Sci U S A, 75, 3979-83.

136. Nakai H, Byers MG, Nowak NJ, Shows TB. (1991) Assignment of beta-hexosaminidase A alpha-subunit to human chromosomal region 15q23----q24. Cytogenet Cell Genet, 56, 164.

137. Bikker H, Meyer MF, Merk AC, de Vijlder JJ, Bolhuis PA. (1988) XmnI RFLP at 5q13 detected by a 0.49 kb Xmn I fragment of human hexosaminidase (HEXB) cDNA. Nucleic Acids Res, 16, 8198.

138. O'Brien JS, Kretz KA, Dewji N, Wenger DA, Esch F, Fluharty AL. (1988) Coding of two sphingolipid activator proteins (SAP-1 and SAP-2) by same genetic locus. Science, 241, 1098-101.

139. Hiraiwa M, Martin BM, Kishimoto Y, Conner GE, Tsuji S, O'Brien JS. (1997) Lysosomal proteolysis of prosaposin, the precursor of saposins (sphingolipid activator proteins): its mechanism and inhibition by ganglioside. Arch Biochem Biophys, 341, 17-24.

140. Heng HH, Xie B, Shi XM, Tsui LC, Mahuran DJ. (1993) Refined mapping of the GM2 activator protein (GM2A) locus to 5q31.3- q33.1, distal to the spinal muscular atrophy locus. Genomics, 18, 429-31.

141. Vogel A, Schwarzmann G, Sandhoff K. (1991) Glycosphingolipid specificity of the human sulfatide activator protein. Eur J Biochem, 200, 591-7.

142. Hama Y, Li YT, Li SC. (1997) Interaction of GM2 activator protein with glycosphingolipids. J Biol Chem, 272, 2828-33.

143. Kytzia HJ, Sandhoff K. (1985) Evidence for two different active sites on human beta-hexosaminidase A. Interaction of GM2 activator protein with beta-hexosaminidase A. J Biol Chem, 260, 7568-72.

144. Burg J, Conzelmann E, Sandhoff K, Solomon E, Swallow DM. (1985) Mapping of the gene coding for the human GM2 activator protein to chromosome 5. Ann Hum Genet, 49, 41-5.

145. Conzelmann E, Burg J, Stephan G, Sandhoff K. (1982) Complexing of glycolipids and their transfer between membranes by the activator protein for degradation of lysosomal ganglioside GM2. Eur J Biochem, 123, 455-64.

146. Li SC, Sonnino S, Tettamanti G, Li YT. (1988) Characterization of a nonspecific activator protein for the enzymatic hydrolysis of glycolipids. J Biol Chem, 263, 6588-91.

147. Schlote W, Harzer K, Christomanou H, Paton BC, Kustermann-Kuhn B, Schmid B, Seeger J, Beudt U, Schuster I, Langenbeck U. (1991) Sphingolipid activator protein 1 deficiency in metachromatic leucodystrophy with normal arylsulphatase A activity. A clinical, morphological, biochemical, and

immunological study. Eur J Pediatr, 150, 584-91.

148. Rose JK, Doms RW. (1988) Regulation of protein export from the endoplasmic reticulum. Annu Rev Cell Biol, 4, 257-88.

149. Kornfeld R, Kornfeld S. (1985) Assembly of asparagine-linked oligosaccharides. Annu Rev Biochem, 54, 631-64.

150. Fu Q, Carson GS, Hiraiwa M, Grafe M, Kishimoto Y, O'Brien JS. (1994) Occurrence of prosaposin as a neuronal surface membrane component. J Mol Neurosci, 5, 59-67.

151. Kondoh K, Sano A, Kakimoto Y, Matsuda S, Sakanaka M. (1993) Distribution of prosaposin-like immunoreactivity in rat brain. J Comp Neurol, 334, 590-602.

152. Collard MW, Sylvester SR, Tsuruta JK, Griswold MD. (1988) Biosynthesis and molecular cloning of sulfated glycoprotein 1 secreted by rat Sertoli cells: sequence similarity with the 70-kilodalton precursor to sulfatide/GM1 activator. Biochemistry, 27, 4557-64.

153. Sylvester SR, Morales C, Oko R, Griswold MD. (1989) Sulfated glycoprotein-1 (saposin precursor) in the reproductive tract of the male rat. Biol Reprod, 41, 941-8.

154. Hermo L, Morales C, Oko R. (1992) Immunocytochemical localization of sulfated glycoprotein-1 (SGP-1) and identification of its transcripts in epithelial cells of the extratesticular duct system of the rat. Anat Rec, 232, 401-22.

155. Fujibayashi S, Wenger DA. (1986) Synthesis and processing of

sphingolipid activator protein-2 (SAP-2) in cultured human fibroblasts. J Biol Chem, 261, 15339-43.

156. Hiraiwa M, O'Brien JS, Kishimoto Y, Galdzicka M, Fluharty AL, Ginns EI, Martin BM. (1993) Isolation, characterization, and proteolysis of human prosaposin, the precursor of saposins (sphingolipid activator proteins). Arch Biochem Biophys, 304, 110-6.

157. Levy H, Or A, Eyal N, Wilder S, Widgerson M, Kolodny EH, Zimran A, Horowitz M. (1991) Molecular aspects of Gaucher disease. Dev Neurosci, 13, 352-62.

158. Qi X, Qin W, Sun Y, Kondoh K, Grabowski GA. (1996) Functional organization of saposin C. Definition of the neurotrophic and acid beta-glucosidase activation regions. J Biol Chem, 271, 6874-80.

159. O'Brien JS, Carson GS, Seo HC, Hiraiwa M, Weiler S, Tomich JM, Barranger JA, Kahn M, Azuma N, Kishimoto Y. (1995) Identification of the neurotrophic factor sequence of prosaposin. Faseb J, 9, 681-5.

160. Hiraiwa M, Campana WM, Martin BM, O'Brien JS. (1997) Prosaposin receptor: evidence for a G-protein-associated receptor. Biochem Biophys Res Commun, 240, 415-8.

161. Hiraiwa M, Taylor EM, Campana WM, Darin SJ, O'Brien JS. (1997) Cell death prevention, mitogen-activated protein kinase stimulation, and increased sulfatide concentrations in Schwann cells and oligodendrocytes by prosaposin and prosaptides. Proc Natl Acad Sci U S A, 94, 4778-81.

162. Campana WM, Hiraiwa M, Addison KC, O'Brien JS. (1996)

Induction of MAPK phosphorylation by prosaposin and prosaptide in PC12 cells. Biochem Biophys Res Commun, 229, 706-12.

163. Campana WM, Darin SJ, O'Brien JS. (1999) Phosphatidylinositol 3-kinase and Akt protein kinase mediate IGF-I- and prosaptide-induced survival in Schwann cells. J Neurosci Res, 57, 332-41.

164. Misasi R, Sorice M, Garofalo T, Griggi T, Campana WM, Giammatteo M, Pavan A, Hiraiwa M, Pontieri GM, O'Brien JS. (1998) Colocalization and complex formation between prosaposin and monosialoganglioside GM3 in neural cells. J Neurochem, 71, 2313-21.

165. Hiraiwa M, Soeda S, Kishimoto Y, O'Brien JS. (1992) Binding and transport of gangliosides by prosaposin. Proc Natl Acad Sci U S A, 89, 11254-8.

166. Kuwana T, Mullock BM, Luzio JP. (1995) Identification of a lysosomal protein causing lipid transfer, using a fluorescence assay designed to monitor membrane fusion between rat liver endosomes and lysosomes. Biochem J, 308, 937-46.

167. Ziemer MA, Swain WF, Rutter WJ, Clements S, Ann DK, Carlson DM. (1984) Nucleotide sequence analysis of a proline-rich protein cDNA and peptide homologies of rat and human proline-rich proteins. J Biol Chem, 259, 10475-80.

168. Igdoura SA, Hermo L, Rosenthal A, Morales CR. (1993) Nonciliated cells of the rat efferent ducts endocytose testicular sulfated glycoprotein-1 (SGP-1) and synthesize SGP-1 derived saposins. Anat Rec, 235, 411-24.

169. Griswold MD, Roberts K, Bishop P. (1986) Purification and

characterization of a sulfated glycoprotein secreted by Sertoli cells. Biochemistry, 25, 7265-70.

170. Marchase RB. (1977) Biochemical investigations of retinotectal adhesive specificity. J Cell Biol, 75, 237-57.

171. Wenger DA, DeGala G, Williams C, Taylor HA, Stevenson RE, Pruitt JR, Miller J, Garen PD, Balentine JD. (1989) Clinical, pathological, and biochemical studies on an infantile case of sulfatide/GM1 activator protein deficiency. Am J Med Genet, 33, 255-65.

172. O'Brien ET, Yeoman WB, Hobby JA. (1971) Hepatorenal damage from toluene in a "glue sniffer". Br Med J, 2, 29-30.

173. Morimoto S, Kishimoto Y, Tomich J, Weiler S, Ohashi T, Barranger JA, Kretz KA, O'Brien JS. (1990) Interaction of saposins, acidic lipids, and glucosylceramidase. J Biol Chem, 265, 1933-7.

174. Glew RH, Basu A, LaMarco KL, Prence EM. (1988) Mammalian glucocerebrosidase: implications for Gaucher's disease. Lab Invest, 58, 5-25.

175. Holtschmidt H, Sandhoff K, Furst W, Kwon HY, Schnabel D, Suzuki K. (1991) The organization of the gene for the human cerebroside sulfate activator protein. FEBS Lett, 280, 267-70.

176. Rorman EG, Scheinker V, Grabowski GA. (1992) Structure and evolution of the human prosaposin chromosomal gene. Genomics, 13, 312-8.

177. Munford RS, Sheppard PO, O'Hara PJ. (1995) Saposin-like proteins (SAPLIP) carry out diverse functions on a common backbone structure. J Lipid Res, 36, 1653-63.

178. Chou PY, Fasman GD. (1978) Prediction of the secondary structure of proteins from their amino acid sequence. Adv Enzymol Relat Areas Mol Biol, 47, 45-148.

179. Morimoto S, Martin BM, Yamamoto Y, Kretz KA, O'Brien JS, Kishimoto Y. (1989) Saposin A: second cerebrosidase activator protein. Proc Natl Acad Sci U S A, 86, 3389-93.

180. Berent SL, Radin NS. (1981) Mechanism of activation of glucocerebrosidase by co-beta-glucosidase (glucosidase activator protein). Biochim Biophys Acta, 664, 572-82.

181. Fabbro D, Grabowski GA. (1991) Human acid beta-glucosidase. Use of inhibitory and activating monoclonal antibodies to investigate the enzyme's catalytic mechanism and saposin A and C binding sites. J Biol Chem, 266, 15021-7.

182. Qi X, Leonova T, Grabowski GA. (1994) Functional human saposins expressed in Escherichia coli. Evidence for binding and activation properties of saposins C with acid beta- glucosidase. J Biol Chem, 269, 16746-53.

183. Vogel A, Furst W, Abo-Hashish MA, Lee-Vaupel M, Conzelmann E, Sandhoff K. (1987) Identity of the activator proteins for the enzymatic hydrolysis of sulfatide, ganglioside GM1, and globotriaosylceramide. Arch Biochem Biophys, 259, 627-38.

184. Peters SP, Coffee CJ, Glew RH, Lee RE, Wenger DA, Li SC, Li YT. (1977) Isolation of heat-stable glucocerebrosidase activators from the spleens of

three variants of Gaucher's disease. Arch Biochem Biophys, 183, 290-7.

185. Aerts JM, Donker-Koopman WE, van Laar C, Brul S, Murray GJ, Wenger DA, Barranger JA, Tager JM, Schram AW. (1987) Relationship between the two immunologically distinguishable forms of glucocerebrosidase in tissue extracts. Eur J Biochem, 163, 583-9.

186. Morimoto S, Martin BM, Kishimoto Y, O'Brien JS. (1988) Saposin D: a sphingomyelinase activator. Biochem Biophys Res Commun, 156, 403-10.

187. Azuma N, O'Brien JS, Moser HW, Kishimoto Y. (1994) Stimulation of acid ceramidase activity by saposin D. Arch Biochem Biophys, 311, 354-7.

188. Klein A, Henseler M, Klein C, Suzuki K, Harzer K, Sandhoff K. (1994) Sphingolipid activator protein D (sap-D) stimulates the lysosomal degradation of ceramide in vivo. Biochem Biophys Res Commun, 200, 1440-8.

189. Tatti M, Salvioli R, Ciaffoni F, Pucci P, Andolfo A, Amoresano A, Vaccaro AM. (1999) Structural and membrane-binding properties of saposin D. Eur J Biochem, 263, 486-94.

190. Wynn CH. (1986) A triple-binding-domain model explains the specificity of the interaction of a sphingolipid activator protein (SAP-1) with sulphatide, GM1-ganglioside and globotriaosylceramide. Biochem J, 240, 921-4.

191. Sandhoff K, Kolter T. (1995) [Glycolipids of the cell surface--biochemistry of their decomposition]. Naturwissenschaften, 82, 403-13.

192. Suzuki Y. (1995) [Disorders of sphingolipid activator proteins]. Nippon Rinsho, 53, 3025-7.

193. Vaccaro AM, Tatti M, Ciaffoni F, Salvioli R, Roncaioli P. (1992)

Reconstitution of glucosylceramidase on binding to acidic phospholipid-containing vesicles. Biochim Biophys Acta, 1119, 239-46.

194. Vaccaro AM, Tatti M, Ciaffoni F, Salvioli R, Maras B, Barca A. (1993) Function of saposin C in the reconstitution of glucosylceramidase by phosphatidylserine liposomes. FEBS Lett, 336, 159-62.

195. Vaccaro AM, Salvioli R, Barca A, Tatti M, Ciaffoni F, Maras B, Siciliano R, Zappacosta F, Amoresano A, Pucci P. (1995) Structural analysis of saposin C and B. Complete localization of disulfide bridges. J Biol Chem, 270, 9953-60.

196. Rafi MA, Zhang XL, DeGala G, Wenger DA. (1990) Detection of a point mutation in sphingolipid activator protein-1 mRNA in patients with a variant form of metachromatic leukodystrophy. Biochem Biophys Res Commun, 166, 1017-23.

197. Zhang XL, Rafi MA, DeGala G, Wenger DA. (1990) Insertion in the mRNA of a metachromatic leukodystrophy patient with sphingolipid activator protein-1 deficiency. Proc Natl Acad Sci U S A, 87, 1426-30.

198. Holtschmidt H, Sandhoff K, Kwon HY, Harzer K, Nakano T, Suzuki K. (1991) Sulfatide activator protein. Alternative splicing that generates three mRNAs and a newly found mutation responsible for a clinical disease. J Biol Chem, 266, 7556-60.

199. Schnabel D, Schroder M, Sandhoff K. (1991) Mutation in the sphingolipid activator protein 2 in a patient with a variant of Gaucher disease. FEBS Lett, 284, 57-9.

200. Rafi MA, de Gala G, Zhang XL, Wenger DA. (1993) Mutational analysis in a patient with a variant form of Gaucher disease caused by SAP-2 deficiency. Somat Cell Mol Genet, 19, 1-7.

201. Sanger F, Nicklen S, Coulson AR. (1977) DNA sequencing with chain-terminating inhibitors. Proc Natl Acad Sci U S A, 74, 5463-7.

202. Chomczynski P, Sacchi N. (1987) Single-step method of RNA isolation by acid guanidinium thiocyanate- phenol-chloroform extraction. Anal Biochem, 162, 156-9.

203. Molkentin JD, Black BL, Martin JF, Olson EN. (1995) Cooperative activation of muscle gene expression by MEF2 and myogenic bHLH proteins. Cell, 83, 1125-36.

204. Schagger H, von Jagow G. (1987) Tricine-sodium dodecyl sulfate-polyacrylamide gel electrophoresis for the separation of proteins in the range from 1 to 100 kDa. Anal Biochem, 166, 368-79.

205. Rost B, Sander C. (1993) Secondary structure prediction of all-helical proteins in two states. Protein Eng, 6, 831-6.

206. Sander C, Schneider R. (1991) Database of homology-derived protein structures and the structural meaning of sequence alignment. Proteins, 9, 56-68.

207. Kyte J, Doolittle RF. (1982) A simple method for displaying the hydropathic character of a protein. J Mol Biol, 157, 105-32.

208. Hermo L, Oko R, Hecht NB. (1991) Differential post-translational modifications of microtubules in cells of the seminiferous epithelium of the rat: a

light and electron microscope immunocytochemical study. Anat Rec, 229, 31-50.

209. Altschul SF, Lipman DJ. (1990) Protein database searches for multiple alignments. Proc Natl Acad Sci U S A, 87, 5509-13.

210. Dewji NN, Wenger DA, O'Brien JS. (1987) Nucleotide sequence of cloned cDNA for human sphingolipid activator protein 1 precursor. Proc Natl Acad Sci U S A, 84, 8652-6.

211. Williams MA, Fukuda M. (1990) Accumulation of membrane glycoproteins in lysosomes requires a tyrosine residue at a particular position in the cytoplasmic tail. J Cell Biol, 111, 955-66.

212. Honing S, Griffith J, Geuze HJ, Hunziker W. (1996) The tyrosine-based lysosomal targeting signal in lamp-1 mediates sorting into Golgi-derived clathrin-coated vesicles. Embo J, 15, 5230-9.

213. Rosenthal AL, Igdoura SA, Morales CR, Hermo L. (1995) Hormonal regulation of sulfated glycoprotein-1 synthesis by nonciliated cells of the efferent ducts of adult rats. Mol Reprod Dev, 40, 69-83.

214. Azuma N, Seo HC, Lie O, Fu Q, Gould RM, Hiraiwa M, Burt DW, Paton IR, Morrice DR, O'Brien JS, Kishimoto Y. (1998) Cloning, expression and map assignment of chicken prosaposin. Biochem J, 330, 321-7.

215. Zhao Q, Bell AW, El-Alfy M, Morales CR. (1998) Mouse testicular sulfated glycoprotein-1: sequence analysis of the common backbone structure of prosaposins. J Androl, 19, 165-74.

216. Lin S, Akinbi HT, Breslin JS, Weaver TE. (1996) Structural requirements for targeting of surfactant protein B (SP-B) to secretory granules in

vitro and in vivo. J Biol Chem, 271, 19689-95.

217. Hook GE, Gilmore LB. (1982) Hydrolases of pulmonary lysosomes and lamellar bodies. J Biol Chem, 257, 9211-20.

218. Voorhout WF, Veenendaal T, Haagsman HP, Weaver TE, Whitsett JA, van Golde LM, Geuze HJ. (1992) Intracellular processing of pulmonary surfactant protein B in an endosomal/lysosomal compartment. Am J Physiol, 263, L479-86.

219. Misumi Y, Miki K, Takatsuki A, Tamura G, Ikehara Y. (1986) Novel blockade by brefeldin A of intracellular transport of secretory proteins in cultured rat hepatocytes. J Biol Chem, 261, 11398-403.

220. Lippincott-Schwartz J, Yuan LC, Bonifacino JS, Klausner RD. (1989) Rapid redistribution of Golgi proteins into the ER in cells treated with brefeldin A: evidence for membrane cycling from Golgi to ER. Cell, 56, 801-13.

221. Madar-Shapiro L, Pasmanik-Chor M, Vaccaro AM, Dinur T, Dagan A, Gatt S, Horowitz M. (1999) Importance of splicing for prosaposin sorting. Biochem J, 337, 433-43.

222. Kotani Y, Matsuda S, Sakanaka M, Kondoh K, Ueno S, Sano A. (1996) Prosaposin facilitates sciatic nerve regeneration in vivo. J Neurochem, 66, 2019-25.

223. Sprecher-Levy H, Orr-Urtreger A, Lonai P, Horowitz M. (1993) Murine prosaposin: expression in the reproductive system of a gene implicated in human genetic diseases [published erratum appears in Cell Mol Biol (Noisy-le-grand) 1994 Mar;40(2):233]. Cell Mol Biol (Noisy-le-grand), 39, 287-99.

224. Bruns G, Stroh H, Veldman GM, Latt SA, Floros J. (1987) The 35 kd pulmonary surfactant-associated protein is encoded on chromosome 10. Hum Genet, 76, 58-62.

225. Kozak CA, Adamson MC, Horowitz M. (1994) Genetic mapping of the mouse prosaposin gene (Psap) to mouse chromosome 10. Genomics, 23, 508-10.

226. Lamontagne S, Potier M. (1994) Modulation of human saposin B sphingolipid-binding specificity by alternative splicing. A study with saposin B-derived synthetic peptides. J Biol Chem, 269, 20528-32.

227. Henseler M, Klein A, Glombitza GJ, Suziki K, Sandhoff K. (1996) Expression of the three alternative forms of the sphingolipid activator protein precursor in baby hamster kidney cells and functional assays in a cell culture system. J Biol Chem, 271, 8416-23.

228. Fluharty AL, Katona Z, Meek WE, Frei K, Fowler AV. (1992) The cerebroside sulfate activator from pig kidney: purification and molecular structure. Biochem Med Metab Biol, 47, 66-85.

229. Furst W, Schubert J, Machleidt W, Meyer HE, Sandhoff K. (1990) The complete amino-acid sequences of human ganglioside GM2 activator protein and cerebroside sulfate activator protein. Eur J Biochem, 192, 709-14.

230. Nakano T, Sandhoff K, Stumper J, Christomanou H, Suzuki K. (1989) Structure of full-length cDNA coding for sulfatide activator, a Co-beta-glucosidase and two other homologous proteins: two alternate forms of the sulfatide activator. J Biochem (Tokyo), 105, 152-4.

231. Rorman EG, Grabowski GA. (1989) Molecular cloning of a human co-beta-glucosidase cDNA: evidence that four sphingolipid hydrolase activator proteins are encoded by single genes in humans and rats. Genomics, 5, 486-92.

232. Reiner O, Dagan O, Horowitz M. (1989) Human sphingolipid activator protein-1 and sphingolipid activator protein-2 are encoded by the same gene. J Mol Neurosci, 1, 225-33.

233. Ponting CP, Russell RB. (1995) Swaposins: circular permutations within genes encoding saposin homologues [letter] [see comments]. Trends Biochem Sci, 20, 179-80.

234. Liepinsh E, Andersson M, Ruysschaert JM, Otting G. (1997) Saposin fold revealed by the NMR structure of NK-lysin [letter]. Nat Struct Biol, 4, 793-5.

235. Kervinen J, Tobin GJ, Costa J, Waugh DS, Wlodawer A, Zdanov A. (1999) Crystal structure of plant aspartic proteinase prophytepsin: inactivation and vacuolar targeting. Embo J, 18, 3947-55.

236. Kolter T, Sandhoff K. (1998) Recent advances in the biochemistry of sphingolipidoses. Brain Pathol, 8, 79-100.

237. Potier M, Lamontagne S, Michaud L, Tranchemontagne J. (1990) Human neuraminidase is a 60 kDa-processing product of prosaposin. Biochem Biophys Res Commun, 173, 449-56.

238. Vaccaro AM, Salvioli R, Tatti M, Ciaffoni F. (1999) Saposins and their interaction with lipids. Neurochem Res, 24, 307-14.

239. Johansson J, Curstedt T, Jornvall H. (1991) Surfactant protein B:

disulfide bridges, structurai properties, and kringle similarities. Biochemistry, 30, 6917-21.

240. Leippe M, Tannich E, Nickel R, van der Goot G, Pattus F, Horstmann RD, Muller-Eberhard HJ. (1992) Primary and secondary structure of the pore-forming peptide of pathogenic Entamoeba histolytica. Embo J, 11, 3501-6.

241. Lynch EC, Rosenberg IM, Gitler C. (1982) An ion-channel forming protein produced by Entamoeba histolytica. Embo J, 1, 801-4.

242. Andersson M, Gunne H, Agerberth B, Boman A, Bergman T, Sillard R, Jornvall H, Mutt V, Olsson B, Wigzell H, et al. (1995) NK-lysin, a novel effector peptide of cytotoxic T and NK cells. Structure and cDNA cloning of the porcine form, induction by interleukin 2, antibacterial and antitumour activity. Embo J, 14, 1615-25.

243. Ponting CP. (1994) Acid sphingomyelinase possesses a domain homologous to its activator proteins: saposins B and D. Protein Sci, 3, 359-61.

244. Hagen FS, Grant FJ, Kuijper JL, Slaughter CA, Moomaw CR, Orth K, O'Hara PJ, Munford RS. (1991) Expression and characterization of recombinant human acyloxyacyl hydrolase, a leukocyte enzyme that deacylates bacterial lipopolysaccharides. Biochemistry, 30, 8415-23.

245. Guruprasad K, Tormakangas K, Kervinen J, Blundell TL. (1994) Comparative modelling of barley-grain aspartic proteinase: a structural rationale for observed hydrolytic specificity. FEBS Lett, 352, 131-6.

246. Futerman AH, Stieger B, Hubbard AL, Pagano RE. (1990)

Sphingomyelin synthesis in rat liver occurs predominantly at the cis and medial cisternae of the Golgi apparatus. J Biol Chem, 265, 8650-7.

247. Lefrancois S, Michaud L, Potier M, Igdoura S, Morales CR. (1999) Role of sphingolipids in the transport of prosaposin to the lysosomes. J Lipid Res, 40, 1593-603.

248. Mays RW, Siemers KA, Fritz BA, Lowe AW, van Meer G, Nelson WJ. (1995) Hierarchy of mechanisms involved in generating Na/K-ATPase polarity in MDCK epithelial cells. J Cell Biol, 130, 1105-15.

249. Luberto C, Hannun YA. (1998) Sphingomyelin synthase, a potential regulator of intracellular levels of ceramide and diacylglycerol during SV40 transformation. Does sphingomyelin synthase account for the putative phosphatidylcholine- specific phospholipase C? J Biol Chem, 273, 14550-9.

250. Kornfeld S, Mellman I. (1989) The biogenesis of lysosomes. Annu Rev Cell Biol, 5, 483-525.

251. Coffey DS. (1993) Prostate cancer. An overview of an increasing dilemma. Cancer, 71, 880-6.

252. Cunha GR. (1994) Role of mesenchymal-epithelial interactions in normal and abnormal development of the mammary gland and prostate. Cancer, 74, 1030-44.

253. Jatzkewitz H, Stinshoff K. (1973) An activator of cerebroside sulphatase in human normal liver and in cases of congenital metachromatic leukodystrophy. FEBS Lett, 32, 129-31.

254. Kappler J, Potter W, Gieselmann V, Kiessling W, Friedl W,

Propping P. (1991) Phenotypic consequences of low arylsulfatase A genotypes (ASAp/ASAp and ASA-/ASAp): does there exist an association with multiple sclerosis? Dev Neurosci, 13, 228-31.

255. Hiramatsu M, Kashimata M, Minami N, Sato A, Murayama M. (1988) Androgenic regulation of epidermal growth factor in the mouse ventral prostate. Biochem Int, 17, 311-7.

256. Katz AE, Benson MC, Wise GJ, Olsson CA, Bandyk MG, Sawczuk IS, Tomashefsky P, Buttyan R. (1989) Gene activity during the early phase of androgen-stimulated rat prostate regrowth. Cancer Res, 49, 5889-94.

257. McKeehan WL, Adams PS, Rosser MP. (1984) Direct mitogenic effects of insulin, epidermal growth factor, glucocorticoid, cholera toxin, unknown pituitary factors and possibly prolactin, but not androgen, on normal rat prostate epithelial cells in serum-free, primary cell culture. Cancer Res, 44, 1998-2010.

258. Steiner MS. (1995) Transforming growth factor-beta and prostate cancer. World J Urol, 13, 329-36.

259. Kolesnick R, Fuks Z. (1995) Ceramide: a signal for apoptosis or mitogenesis?[comment]. J Exp Med, 181, 1949-52.

260. Spiegel S, Foster D, Kolesnick R. (1996) Signal transduction through lipid second messengers. Curr Opin Cell Biol, 8, 159-67.

261. Garrington TP, Johnson GL. (1999) Organization and regulation of mitogen-activated protein kinase signaling pathways. Curr Opin Cell Biol, 11, 211-8.

262. Luttrell LM, Daaka Y, Lefkowitz RJ. (1999) Regulation of tyrosine

kinase cascades by G-protein-coupled receptors. Curr Opin Cell Biol, 11, 177-83.

263. Cobb MH, Goldsmith EJ. (1995) How MAP kinases are regulated. J Biol Chem, 270, 14843-6.

264. Lopez-Ilasaca M, Crespo P, Pellici PG, Gutkind JS, Wetzker R. (1997) Linkage of G protein-coupled receptors to the MAPK signaling pathway through PI 3-kinase gamma. Science, 275, 394-7.

265. Luttrell LM, van Biesen T, Hawes BE, Koch WJ, Touhara K, Lefkowitz RJ. (1995) G beta gamma subunits mediate mitogen-activated protein kinase activation by the tyrosine kinase insulin-like growth factor 1 receptor. J Biol Chem, 270, 16495-8.

266. Grammer TC, Blenis J. (1997) Evidence for MEK-independent pathways regulating the prolonged activation of the ERK-MAP kinases. Oncogene, 14, 1635-42.

267. Klingmuller U, Wu H, Hsiao JG, Toker A, Duckworth BC, Cantley LC, Lodish HF. (1997) Identification of a novel pathway important for proliferation and differentiation of primary erythroid progenitors. Proc Natl Acad Sci U S A, 94, 3016-21.

268. Treisman R. (1996) Regulation of transcription by MAP kinase cascades. Curr Opin Cell Biol, 8, 205-15.

269. Cowley S, Paterson H, Kemp P, Marshall CJ. (1994) Activation of MAP kinase kinase is necessary and sufficient for PC12 differentiation and for transformation of NIH 3T3 cells. Cell, 77, 841-52.